THE UNIVERSITY of ADELAIDE

Biogeographic and Biological Comparisons Between the Emu Bay Shale (Kangaroo Island, South Australia) and Other Cambrian Burgess Shale-Type Biotas

James Dougal Holmes

B.Sc B.Ec

Thesis submitted for the degree of

Master of Philosophy

School of Biological Sciences

Faculty of Sciences

University of Adelaide

October 2016

Contents

Figures and Tables

Chapter 2

Chapter 3

Chapter 4

Chapter 6

Abstract

Konservat-Lagerstätten, or fossil deposits exhibiting exceptional preservation of non-biomineralised material, are particularly prevalent in the Cambrian, and offer us great insight into the evolution and ecology of early animals and communities. The Emu Bay Shale (EBS) from the north coast of Kangaroo Island, South Australia, houses an early Cambrian (Series 3 – c. 514 Ma) Lagerstätte that contains over 50 species, including sponges, brachiopods, molluscs, annelids, priapulids, lobopodians, arthropods, vetulicolians, and several problematic taxa, making it the most diverse Burgess Shale-type (BST) biota in the southern hemisphere. While considerable work in describing taxa from the EBS Lagerstätte has been completed, less has been undertaken that focuses on the relationships between this and other Cambrian BST biotas. This project aims to examine some of the links between the EBS Lagerstätte and similar deposits from around the world, including the Burgess Shale (Canada), Chengjiang (China) and Sirius Passet (Greenland) biotas, amongst others. To this end, the project has two major parts.

The first section aims to examine the biogeographic relationships between major Cambrian BST biotas from a global perspective. A substantial database of generic occurrence was constructed from the published literature, and analysed using various multivariate techniques in order to examine the relationships between these exceptionally preserved assemblages. Results suggest that both geographic distance and differences in age have an effect on the composition of BST biotas, and that assemblage similarity appears to increase through the Cambrian. The EBS

biota is most closely related to other Gondwanan sites in South China, most likely reflecting a regional relationship.

The second section involves a more focused description and interpretation of a single element of the EBS biota, namely an examination of the moulting habits of two common trilobite species from the Emu Bay Shale, *Estaingia bilobata* Pocock, 1964 and *Redlichia takooensis* Lu, 1950, and how this compares with other BST assemblages. Specimens from the EBS were examined and arrangements of exoskeletal elements likely representing moult ensembles identified, from which moulting behaviour was then inferred and compared. Analysis reveals that the EBS preserves a record of trilobite moulting unparalleled within other exceptionally preserved assemblages, representing a range of trilobite moulting behaviours, likely due to minimal water movement and relatively rapid burial within the biota's unique inshore depositional setting.

The unusual depositional setting of the EBS Lagerstätte seems to have had a minimal effect on the types of organisms present with the assemblage compared to other BST biotas. In contrast, this setting seems to have facilitated the preservation of an exceptional moulting record not found at other sites, including BST deposits. This, coupled with the unique preservation of certain structures such as eyes, confirms that the EBS is of great importance in elucidating the evolution of early animals and communities.

Declaration

I, James Dougal Holmes, certify that this work contains no material which has been accepted for the award of any other degree or diploma in my name in any university or other tertiary institution and, to the best of my knowledge and belief, contains no material previously published or written by another person, except where due reference has been made in the text. In addition, I certify that no part of this work will, in the future, be used in a submission in my name for any other degree or diploma in any university or other tertiary institution without the prior approval of the University of Adelaide and where applicable, any partner institution responsible for the joint award of this degree.

I give consent to this copy of my thesis when deposited in the University Library, being made available for loan and photocopying, subject to the provisions of the Copyright Act 1968. The author acknowledges that copyright of published works contained within this thesis resides with the copyright holder(s) of those works.
I also give permission for the digital version of my thesis to be made available on the web, via the University's digital research repository, the Library Search and also through web search engines, unless permission has been granted by the University to restrict access for a period of time.

James Dougal Holmes

1st December 2016

Acknowledgements

I would like to thank my supervisors, Dr Diego García-Bellido, Prof Mike Lee and Prof Corey Bradshaw, for the time and effort they have invested in supporting me through my candidature.

Thanks to my collaborators Allison Daley and in particular Harriet Drage, for their efforts and patience in working with me on the Emu Bay Shale trilobites.

I would like to thank staff, students, volunteers and associates of the South Australian Museum, as well as the University of Adelaide, the University of South Australia, and the University of New England, for their invaluable assistance, collection of material, and for giving up their time to help me, in particular Ronda Atkinson, Mary-Anne Binnie, Felicity Coutts, Jim Gehling, Jim Jago, Katrina Kenny, Justin Payne, John Paterson and Natalie Schroeder.

I would like to thank Paul and Carmen Buck for generously allowing access to the Emu Bay Shale field site on their property.

Finally, thanks to my family - to my parents for always encouraging me, and in particular to my fiancé Lily Reid for her help, patience and unwavering support of me in everything I do.

Chapter 1 – Introduction

1.1 Contextual statement

This thesis examines some of the links between the Emu Bay Shale (EBS) biota and other Burgess Shale-type (BST) biotas from around the world. In doing so, it aims to better place this particular deposit within the context of the Cambrian world. With this in mind, the project involves, (a) gaining a greater understanding of the biogeographic relationships between BST biotas, and in particular how the Emu Bay Shale is related to other sites; and (b) investigating patterns in a uniquely rich trilobite moulting record within the EBS to determine how some of the earliest arthropods moulted, and the reasons behind the preservation of such a record at the EBS compared to other sites.

Chapter 2 provides an introduction to Konservat-Lagerstätten and Burgess Shale-type biotas in general, and an overview of the Emu Bay Shale Lagerstätte in particular, including history of investigations at Emu Bay, geological context, description of the biota, ecological characteristics and biogeographic relationships, as well as a brief introduction to moulting in the EBS trilobites as currently presented in the published literature. This provides the necessary background context for the following chapters. Chapter 3 examines the relationships between BST assemblages at a broad level based on presence/absence of genera using various statistical analyses. Chapter 4 examines the moulting record of EBS trilobites, including a discussion on how this compares with other sites. Chapter 5 provides a thesis summary, including findings of the individual papers and possible future directions of research.

Chapter 2 – Background

2.1 Konservat-Lagerstätten and Burgess Shale-type (BST) biotas

Konservat-Lagerstätte (pl. *Lagerstätten*, literally “conservation storage-place”) is a German term that has become a standard in scientific literature when referring to a fossil deposit exhibiting exceptional preservation of ‘soft parts’. In terms of the early Palaeozoic, this refers largely to the preservation of non-mineralised invertebrate structures such as cuticle, muscle, appendages and eyes, as well as internal organs such as those of the digestive and circulatory systems. Filaments of algae and cyanobacteria can also be preserved in such deposits, hence the preference for the term “biota” rather than “fauna”.

The beginning of the Cambrian Period (542 Ma) marks the start of a remarkable diversification event, in which almost all of the major animal body plans (>90% of phyla), and the majority of classes (~75%), appeared in what has been termed the Cambrian ‘explosion’ (Erwin et al., 2011). As such, the study of this transition is of the utmost importance in understanding the evolution of early animals. Cambrian Lagerstätten are particularly useful as they provide a more unbiased view into early animal communities just after this critical interval, compared to conventional fossil deposits that preserve only biomineralised material (Conway Morris, 1985).

It has been recognised for some time that Konservat-Lagerstätten are unusually common during the Cambrian (Allison & Briggs, 1993), and that many of the assemblages present within these deposits share common taxonomic and ecological characteristics (e.g. Conway Morris, 1989; Han et al., 2008). These assemblages have come to be known as Burgess Shale-type (BST) biotas, named

after the renowned middle Cambrian Burgess Shale from the Canadian Rocky Mountains, where fossils of this kind were first discovered by C. D. Walcott in 1909 (Walcott, 1911). BST biotas are known from most continents and are concentrated from the late-early through middle Cambrian (Series 2 through Series 3), although there are also examples from the late Cambrian and Ordovician. There are particular concentrations of BST biotas in China and North America, with other notable examples from Greenland, Siberia, Morocco and South Africa, as well as the Emu Bay Shale Lagerstätte from Australia.

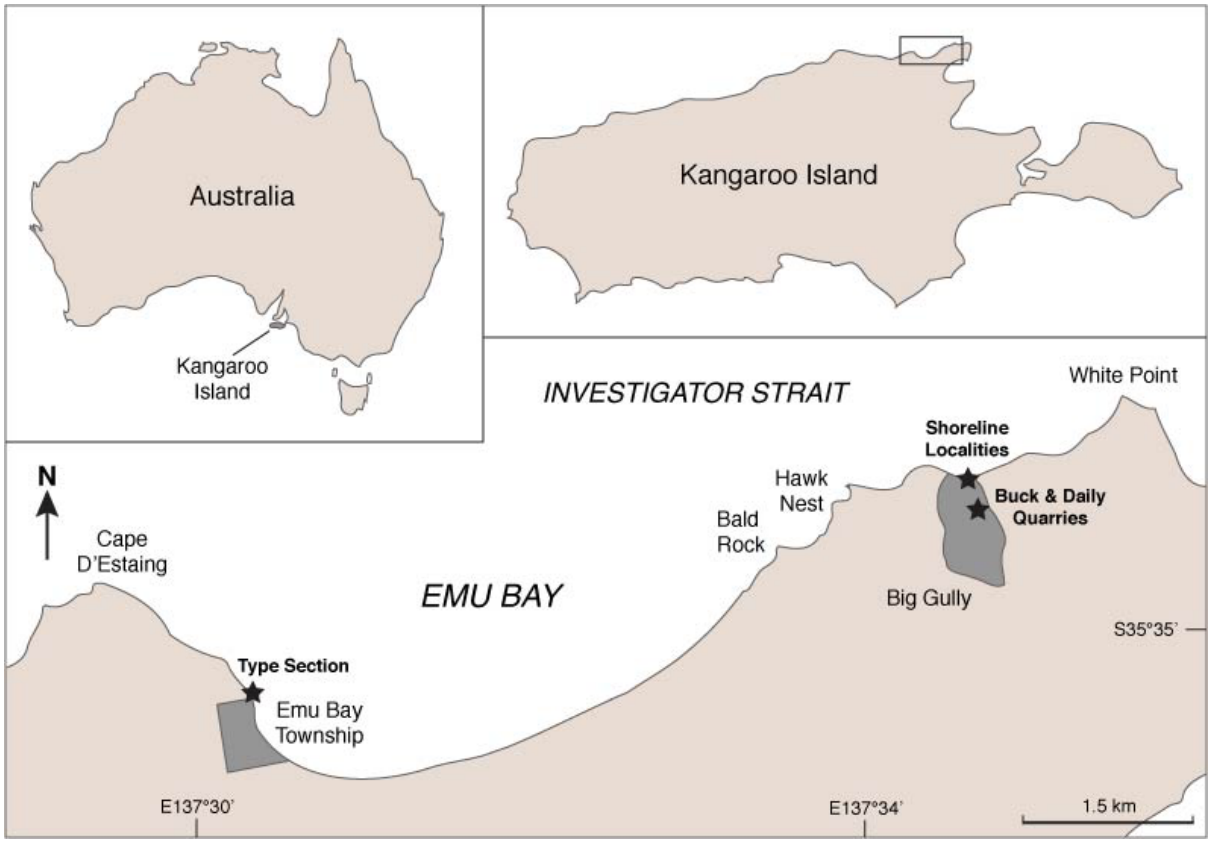

Figure 2.1: Map showing localities of the Emu Bay Shale (Kangaroo Island, South Australia).

2.2 History of the Emu Bay Shale

Fossils have been known from the Emu Bay Shale since 1952, when R. C. Sprigg, then a South Australian Geological Survey geologist, found trilobites in what is now the type section of the formation, approximately 200 m northwest of the Emu Bay jetty on the north coast of Kangaroo Island, South Australia (Sprigg, 1955). In late 1954, University of Adelaide PhD student B. Daily discovered what is now recognised as the Emu Bay Shale Lagerstätte, when he found trilobites and soft-bodied taxa, including the arthropod *Isoxys* and "an unidentified crustacean and annelid", in the cliff and wave-cut platform immediately east of the mouth of "Big Gully" (Daily, 1956; Jago & Cooper, 2011), approximately 7 km east of the Emu Bay township and 1.5 km west of White Point (Fig. 2.1). Pocock (1964) described the trilobite *Estaingia bilobata* from specimens collected from both localities, but for various reasons (see Jago & Cooper, 2011) the fauna at Big Gully was not fully reported on until Glaessner (1979) published descriptions of the "bivalved" arthropods *Isoxys communis* and *Tuzoia australis*, the vermiform *Palaeoscolex antiquus* (now *Wronascolex*), *Myoscolex ateles* and *Vetustovermis planus*, as well as noting the presence of the trilobites *E. bilobata* and a large species of *Redlichia*. Conway Morris and Jenkins (1985) described healed injuries in *Redlichia*, following which Jell in Bengtson et al. (1990) identified this species as *Redlichia takooensis*, previously described from the Early Cambrian of South China (Lu, 1950). In the nineties, McHenry and Yates (1993) identified the first specimens of the giant Cambrian predator *Anomalocaris* from Big Gully, and a PhD undertaken by C. Nedin at the University of Adelaide resulted in a number of papers examining various

aspects of the biota (Nedin, 1995, 1997, 1999; Briggs & Nedin, 1997; Nedin & Jenkins, 1999). A further three species of trilobite were identified by Paterson and Jago (2006).

Figure 2.2: Big Gully with Buck Quarry (bottom right) and Daily Quarry (centre).

In 2007, a new project commenced with the opening of a quarry approximately 400 m inland from the coastal exposures. “Buck Quarry” (named for landowners P. and C. Buck – see Fig. 2.2) as it is now known, has yielded a more diverse assemblage and higher quality preservation than previously seen at Big Gully, and has resulted in a series of publications and an increase in the diversity of the biota to over 50 species (Daley et al., 2013; Edgecombe et al., 2011; 2016; García-Bellido et al., 2009; 2013a; 2013b; 2014; Jago, et al., 2016; Lee et al., 2011;

Paterson et al., 2010; 2011; 2012; 2015). In recent years “Daily Quarry” (after EBS Lagerstätte discoverer B. Daily) has been opened slightly closer to shore and is also yielding high quality material.

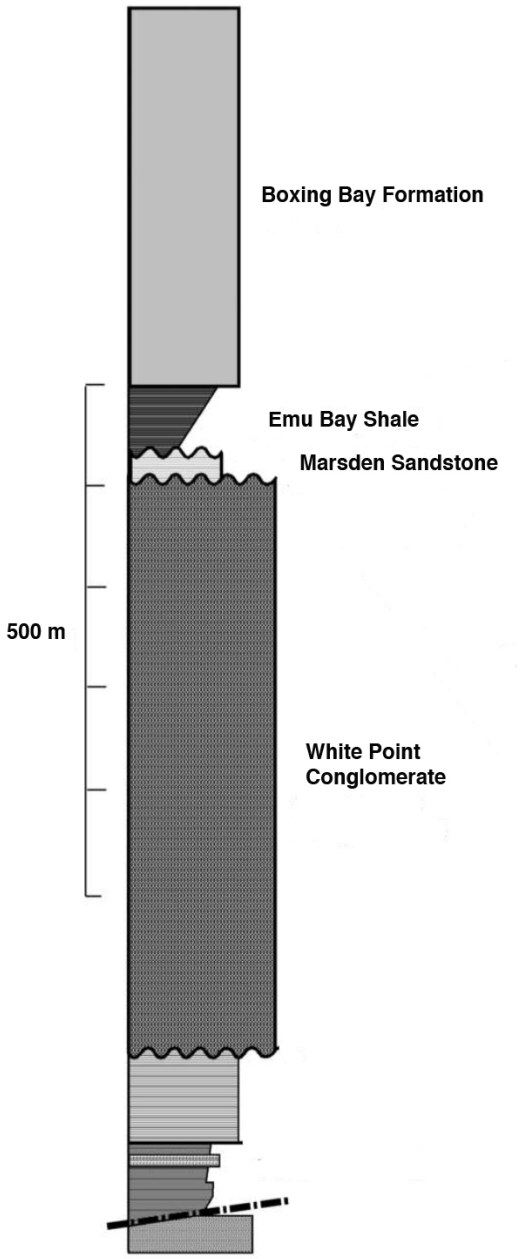

Figure 2.3: Generalised coastal section of the Cambrian succession near Big Gully (Kangaroo Island), after Daily et al., (1980) and based on Fig. 5 of Gehling et al., (2011).

2.3 Geology and environment

The Emu Bay Shale forms part of the Kangaroo Island Group (Daily, 1956), a platformal succession that outcrops on the north coast of Kangaroo Island, separated from the metamorphosed basinal sediments of the approximately coeval Kanmantoo Group to the south by the Kangaroo Island Shear Zone, a major zone of displacement during the Cambrian Delamerian Orogeny (Flöttmann et al., 1995). The Kanmantoo Group hosts granitic intrusions related to this orogenic event and extends to the Fleurieu Peninsula of the mainland, however, the Kangaroo Island Group is largely undeformed and restricted to the central northern section of the island between Stokes Bay and Point Marsden (Gehling et al., 2011).

In the vicinity of Emu Bay, the Cambrian succession (Fig. 2.3) begins with the White Point Conglomerate, which on the coast is generally a poorly-bedded, clast-to-matrix supported, cobble-to-boulder sized, polymict conglomerate, overlain by the fine-to-medium grained, red-brown feldspathic sandstones of the Marsden Sandstone (Gehling et al., 2011). The Rouge Mudstone Member of the Marsden Sandstone contains specimens of the trilobite *B. dailyi* and echinoderms. The Emu Bay Shale overlies the Marsden Sandstone, with the Lagerstätte preserved mostly within the lowest 10–12 m of the formation, within dark grey, micaceous, finely laminated mudstones, interspersed with silt and fine sand horizons interpreted as gravity flow or storm deposits (Gehling et al., 2011). Geochemical studies conducted by McKirdy et al. (2011) and Hall et al. (2011) suggest that the Lagerstätte was deposited beneath an oxic water column, with anoxic conditions prevailing below the sediment-water interface, possibly aided by the presence of microbial mats. This is

supported by the occurrence of diverse nekto-benthic and pelagic elements of the biota, a relatively limited diversity of fixo-sessile taxa, a lack of bioturbation, and the presence of sedimentary pyrite and pyritised soft tissues (Gehling et al., 2011; McKirdy et al., 2011; Paterson et al., 2016).

Conglomerate facies at the base and within the Emu Bay Shale that thin and lens out towards the south, as well as consistent soft-sediment deformation, suggest deposition adjacent to an active tectonic margin to the north, with the Lagerstätte-bearing mudstones likely deposited rapidly in a localised, relatively deep water mini-basin affected by syndepositional faulting and slumping, most likely in a fan delta setting (Gaines et al., 2016; Gehling et al., 2011; Paterson et al., 2016). This setting is very different from that interpreted for the majority of BST biotas, that are generally found in outer shelf settings (Gaines, 2014). The Emu Bay Shale shallows upwards with fine sandstone horizons increasing in frequency and thickness, and grades conformably on the coast (although channelled inland) into the subtidal sands of the Boxing Bay Formation, that contain abundant arthropod trackways (Daily et al., 1980; Gehling et al., 2011). The geological context of the Emu Bay Shale Lagerstätte is discussed in detail by Gehling et al. (2011).

The Emu Bay Shale has been correlated with the Cambrian Series 2 (Stage 4) *Pararaia janeae* zone of mainland South Australia, equivalent to the late Botoman of Siberia (Jell in Bengtson et al., 1990; Jago et al., 2006; Paterson & Brock, 2007), and is dated at approximately 514 Ma (Peng et al., 2012).

2.4 Preservation

Preservation of non-mineralised material within Cambrian Lagerstätten is usually represented by two-dimensional compression fossils composed of primary carbonaceous remains, a pathway termed “Burgess Shale-type preservation” (Gaines, 2014). The preservation at Big Gully seems to be somewhat different, with fossils exhibiting some three-dimensionality due to early-stage diagenetic mineralisation, including phosphatisation of internal structures such as muscle and gut tissue, phosphatisation and pyritisation of cuticular structures such as eyes, and late diagenetic replication of fossils by fibrous calcite (see Paterson et al., 2016 and references therein). It is possible that the presence of microbial mats may have helped facilitate exceptional preservation by inhibiting the decay of soft parts (McKirdy et al., 2011), possibly providing an alternative method of rapid “sealing” of the substrate than the early diagenetic precipitation of carbonate cements implicated in “standard” Burgess Shale-type preservation (Gaines et al., 2012; Paterson et al., 2016). This may explain some of the differences seen in preservation between the Emu Bay Shale and other Cambrian Lagerstätten.

2.5 Biota

The Emu Bay Shale houses a fairly typical BST biota. Like many such deposits the assemblage is dominated by panarthropods, but also comprises sponges, brachiopods, molluscs, palaeoscolecids, annelids, vetulicolians and a number of

problematic taxa (Paterson et al., 2016). Over 50 species are now recognised from the Lagerstätte.

Figure 2.4: Faunal slab from the EBS Lagerstätte (Buck Quarry). The large trilobite is *Redlichia takooensis* Lu, 1950 and the smaller specimens *Estaingia bilobata* Pocock, 1964.

Arthropods are overwhelmingly dominated by trilobites, and in particular *E. bilobata*, which is present on surfaces in densities up to 300 individuals per square metre (Paterson et al., 2016). *R. takooensis* is also abundant, although larger specimens (up to 25 cm) are less common (Fig. 2.3). Another three trilobite species are found within the Lagerstätte, *Megapharanaspis nedini*, *Balcoracania dailyi* and *Holyoakia simpsoni*, however, these are all extremely rare (Paterson & Jago, 2006). Other lamellipedian arthropods present in the biota include the nektaspids *Kangacaris zhangi* and *Emucaris fava* (Paterson et al., 2010), as well as

Australimicola spriggi (Paterson et al., 2012). The “bivalved” arthropod *Isoxys communis* is second only to *E. bilobata* in terms of abundance within Lagerstätte, although a second species of this cosmopolitan genus, *I. glaessneri*, is less common. Another genus of “bivalved” arthropod common to BST biotas, *Tuzoia*, is also represented by two species, *T. australis* and a larger species as yet to be named (García-Bellido et al., 2009). Other arthropods include artiopodan *Squamacula buckorum* (Paterson et al., 2012), aglaspidid-like *Eozetetes gemmelli* (Edgecombe et al., 2016), the chelicerate *Wisangocaris barbarahardyae* (Jago et al., 2016), and the “great appendage” arthropods *Oesterkerkus megacholix* (Edgecombe et al., 2011) and *Tanglangia rangatanga* (Paterson et al., 2015).

Two species of the giant Cambrian predator *Anomalocaris* are found within the Lagerstätte, *A. briggsi* and the more uncommon *A.* cf. *canadensis* (Daley et al., 2013; Nedin, 1995). Uniquely to the Emu Bay Shale, the disarticulated compound eyes of *Anomalocaris*, exhibiting up to 32,000 lenses, are also preserved (Paterson et al., 2011). A single specimen of an armoured lobopodian has been collected, and shows affinities with the ‘Collins’ Monster’ from the Burgess Shale (García-Bellido et al., 2013a).

Palaeoscolecid worms are represented by two species of *Wronascolex*, *W. antiquus*, as well as the smaller and rarer *W. iacoborum* (García-Bellido et al., 2013b). A single specimen of an undescribed polychaete annelid is also known from the Lagerstätte. *Vetustovermis planus* was originally described as an annelid by (Glaessner, 1979) based on a single specimen, but is now considered to be a possible nectocaridid, a group purported to have possible cephalopod affinities (Smith, 2013; Smith & Caron, 2010). The enigmatic *Myoscolex* has been interpreted

as both an annelid (Dzik, 2004; Glaessner, 1979) and an opabiniid (Briggs & Nedin, 1997), and is currently undergoing further revision.

Sponges are mostly of leptomitid affinities, but hamptoniids and choiids are also present, although none have been formally described (Paterson et al., 2016). Brachiopods are represented by rare linguliformeans, including a botsfordiid attributed to *Diandongia* (Paterson et al., 2016). Rare hyolith molluscs are also present. There are number of problematic taxa found within the Lagerstätte, including a chancelloriid attributed to *Chancelloria*, a strange "petalloid"-type organism, and eldoniids (Paterson et al., 2016). A single species of vetulicolian (tunicate-like early chordate), *Nesonektris aldredgei* is also known (García-Bellido et al., 2014).

2.6 Palaeogeography

Major tectonic events leading up to the Cambrian period centre on the assembly and breakup of the supercontinent Rodinia, and subsequent assembly of another supercontinent, Gondwana. It is generally accepted that Rodinia, comprised of all major continental landmasses at the time, came together between 1300–900 Ma, and started to break up at c. 750 Ma along what is now the western margin of Laurentia (Li et al., 2008). Under what is the most well-known hypothesis (SWEAT: southwest U.S. – East Antarctic), this margin was adjacent to eastern Australia and Antarctica (Goodge et al., 2008) – what would eventually become the East Gondwanan margin following assembly of that supercontinent. During the period in

question (c. 520–500 Ma) it is likely that Gondwana stretched from the south pole to the equator (Fig. 2.4), with Laurentia situated to the west and separated by various palaeocontinents including Siberia and Baltica (Alvaro et al., 2013; McKerrow et al., 1992; Torsvik & Cocks, 2013).

Figure 2.5: Cambrian continental reconstruction as at 510 Ma (based on Torsvik & Cocks, 2013; Fig. 2.8).

The Adelaide Rift Complex, within which the Neoproterozoic–Cambrian sediments that include the Emu Bay Shale were deposited, began to open during the breakup of Rodinia, with deposition continuing episodically until the onset of the contractional Delamerian Orogeny (c. 514–490 Ma; Foden et al., 2006), that resulted in compressional folding and faulting of the basin infill. It now forms a c. 700 km north-south trending, extremely thick accumulation of sediment, bound to the west by the Gawler Craton and the northeast by the Curnamona Province (Preiss, 2000). The Kangaroo Island Group, and the adjacent deeper-water Kanmantoo Group, form part of the southern extremity of this complex.

2.7 Biogeographic associations

Many of the taxa present within the EBS biota suggest biogeographic relationships with South China, which also constituted a part of (or was at least situated close to) Gondwana during the Cambrian (Fig. 2.4). The trilobite *Redlichia takooensis* was first described from South China (Lu, 1950), as was *Estaingia* (as *Lusatiops*; Chang, 1953). Both of these genera are also found in Antarctica, along with two other trilobites from the EBS biota, *Holyoakia* and *Balcoracania* (Palmer & Rowell, 1995; Paterson & Jago, 2006). The soft-bodied arthropods *Kangacaris*, *Squamacula* and *Tanglangia* are all shared by the EBS with the famous Chengjiang biota from South China (Paterson et al., 2015; Zhang et al., 2004; 2012). *Vetustovermis* is also shared with Chengjiang, however, recent studies have suggested that this genus is synonymous with *Nectocaris* from the Burgess Shale (Smith, 2013; Smith & Caron, 2010), although in this instance we consider them to be separate. *Wronascolex* is also shared with various Cambrian Lagerstätten in South China, as well as the Sinsk biota in Siberia, and there are also uncertain occurrences of this genus in Laurentia (see Supp. Tab. 6.1). Cosmopolitan taxa include the “bivalved” arthropods *Isoxys* and *Tuzoia*, the stem arthropod *Anomalocaris*, and the enigmatic, sponge-like, *Chancelloria*.

2.8 Moulting in Emu Bay Shale trilobites

As mentioned previously, the EBS biota is dominated by arthropods, in particular by two species of trilobite, *Estaingia bilobata* and *Redlichia takooensis*. Trilobites, as arthropods, are members of the Ecdysozoa, a clade of animals that grow by periodically moulting their exoskeleton (Telford et al., 2008). This means that trilobite specimens are represented within fossil deposits by both carcasses and moulted carapaces (exuviae). The moulting process (ecdysis) involves the separation of old exoskeletal cuticle from the epidermal cells, followed by the secretion of new, soft cuticle beneath this, after which the old exoskeleton separates along predetermined lines of weakness or "sutures" by body movement and/or an increase in internal pressure, allowing the egression of the animal followed by subsequent hardening of the new exoskeleton (Moussian, 2013).

Trilobites generally achieved ecdysis by the separation of the cephalon (head region – see Fig. 2.5) into various pieces along suture lines, allowing the trilobite to exit through an opening at the anterior, although there are exceptions to this (for a review of moulting in trilobites, see Daley & Drage, 2016). If undisturbed, these exuviae allow the recognition of moult configurations – repeated spatial arrangements of moulted pieces (sclerites) – which in turn allow the inference of moulting behaviour; one of the few instances in which animal behavioural patterns can be directly inferred from the early Phanerozoic. Unfortunately, in the majority of deposits, disturbance from animal activity (e.g. scavenging, burrowing), depositional processes (e.g. transport in flow deposits), or water movement due to currents or wave action, has resulted in the scattering of moulted sclerites, making it difficult to

infer behaviour. Transport would also have resulted in the mechanical breakage and disarticulation of carcasses, making them difficult to distinguish from moults.

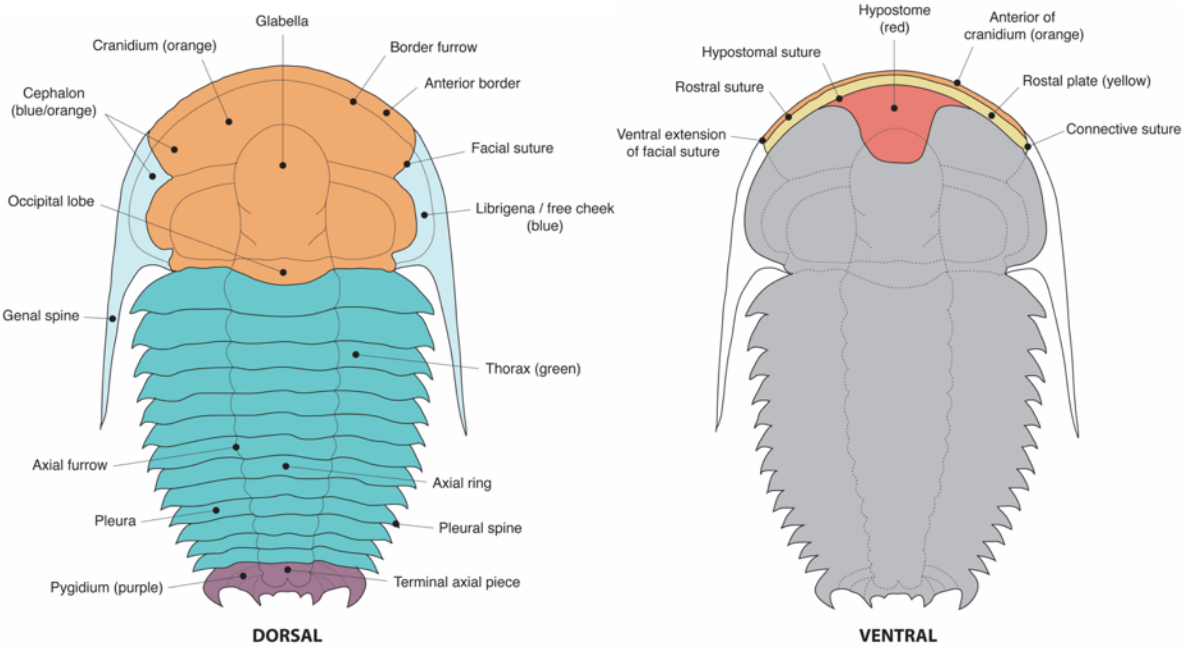

Figure 2.6: Simplified biomineralised anatomy of the trilobite *Estaingia bilobata*.

Although the majority of trilobite specimens within the EBS appear to be (mostly complete) carcasses (>90%; Gehling et al., 2011), moulted exoskeletons are common due to the abundance of the two aforementioned species. The conditions that led to the exceptional preservation at the EBS appear to have been particularly conducive to the preservation of intact moult ensembles, with the overwhelmingly majority represented by complete specimens. This suggests very little disturbance of any kind prior to burial, something that is not necessarily the case for other BST biotas. For example, the Wheeler Shale (Utah, USA) and the Mount Stephen Trilobite Beds (British Columbia, Canada) both contain large numbers of the trilobites, however, in both cases the majority of moulted exoskeletons are represented only by axial shields, without associated smaller sclerites, and therefore

preserve few details of moulting behaviour (see Chapter 3). The unique preservation within the Emu Bay Shale therefore provides a perfect opportunity to examine the moulting behaviours of early Cambrian trilobites that are not necessarily recorded in other deposits.

2.9 References

Allison, P. A., & Briggs, D. E. G. (1993). Exceptional fossil record: Distribution of soft-tissue preservation through the Phanerozoic. *Geology, 21*, 527-530.

Alvaro, J. J., Ahlberg, P., Babcock, L. E., Bordonaro, O. L., Choi, D. K., Cooper, R. A., . . . Zylinska, A. (2013). Global Cambrian trilobite palaeobiogeography assessed using parsimony analysis of endemicity. In D. A. T. Harper & T. Servais (Eds.), Early Palaeozoic Biogeography and Palaeogeography. *Geological Society, London, Memoirs, 38*, 273-296.

Bengtson, S., Conway Morris, S., Cooper, B. J., Jell, P. A., & Runnegar, B. N. (1990). Early Cambrian fossils from South Australia. *Memoirs of the Association of Australasian Palaeontologists, 9*, 1-364.

Briggs, D. E. G., & Nedin, C. (1997). The taphonomy and affinities of the problematic fossil *Myoscolex* from the Lower Cambrian Emu Bay Shale of South Australia. *Journal of Palaeontology, 71*, 22-32.

Chang, W. (1953). Some Lower Cambrian trilobites from western Hupei. *Acta Palaeontologica Sinica*, *1*, 121-149.

Conway Morris, S. (1985). Cambrian Lagerstätten: their distribution and significance. *Philosophical Transactions of the Royal Society B: Biological Sciences, 311*, 49-65.

Conway Morris, S. (1989). The persistence of Burgess Shale-type faunas: implications for the evolution of deeper-water faunas. *Earth and Environmental Science Transactions of the Royal Society of Edinburgh, 80*, 271-283.

Conway Morris, S. & Jenkins, R. J. F. (1985). Healed injuries in Early Cambrian trilobites from South Australia. *Alcheringa 9,* 167-177.

Daily, B. (1956). The Cambrian in South Australia. In J. Rodgers (Ed.), *El sistema Cámbrico, su palaeogeografía y el problema de su base* (pp. 91-147). Mexico, 1956: 20th International Geological Congress.

Daily, B., Moore, P. S., & Rust, B. R. (1980). Terrestrial-marine transition in the Cambrian rocks of Kangaroo Island, South Australia. *Sedimentology, 27*, 379-399.

Daley, A. C., & Drage, H. B. (2016). The fossil record of ecdysis, and trends in the moulting behaviour of trilobites. *Arthropod Structure & Development, 45*, 71-96.

Daley, A. C., Paterson, J. R., Edgecombe, G. D., García-Bellido, D. C., Jago, J. B., & Donoghue, P. (2013). New anatomical information on *Anomalocaris* from the Cambrian Emu Bay Shale of South Australia and a reassessment of its inferred predatory habits. *Palaeontology, 56*, 971-990.

Dzik, J. (2004). Anatomy and relationships of the Early Cambrian worm *Myoscolex*. *Zoologica Scripta, 33*, 57-69.

Edgecombe, G. D., García-Bellido, D. C., & Paterson, J. R. (2011). A New Leanchoiliid Megacheiran Arthropod from the lower Cambrian Emu Bay Shale, South Australia. *Acta Palaeontologica Polonica, 56*, 385-400.

Edgecombe, G. D., Paterson, J. R., & García-Bellido, D.C. (2016). A new aglaspidid-like euarthropod from the lower Cambrian Emu Bay Shale of South Australia. Geological Magazine.

Erwin, D. H., Laflamme, M., Tweedt, S. M., Sperling, E. A., Pisani, D., & Peterson, K. J. (2011). The Cambrian Conundrum: Early Divergence and Later Ecological Success in the Early History of Animals. *Science, 334*, 1091-1097.

Flöttmann, T., James, P., Menpes, R., Cesare, P., Twining, M., Fairclough, M., . . . Marshal, S. (1995). The structure of Kangaroo Island, South Australia: Strain and kinematic partitioning during Delamerian basin and platform reactivation. *Australian Journal of Earth Sciences, 42*, 35-49.

Foden, J., Elburg, M. A., Dougherty-Page, J., & Burtt, A. (2006). The Timing and Duration of the Delamerian Orogeny: Correlation with the Ross Orogen and Implications for Gondwana Assemby. *The Journal of Geology, 114*, 189-210.

Gaines, R. R. (2014). Burgess Shale-type preservation and its distribution in space and time. In M. Laflamme, J. D. Schiffbauer (Eds.), Reading and Writing of the Fossil Record: Preservational Pathways to Exceptional Fossilization. *The Paleontological Society Papers, 20*, 123-146.

Gaines, R. R., Hammarlund, E. U., Hou, X., Qi, C., Gabbott, S. E., Zhao, Y., . . . Canfield, D. E. (2012). Mechanism for Burgess Shale-type preservation. *Proceedings of the National Academy of Sciences of the USA, 109*, 5180-5184.

Gaines, R. R., Paterson, J. R., Jago, J. B., Gehling, J. G., & García-Bellido, D. (2016). Palaeoenvironmental and depositional setting of the Emu Bay Shale, a unique early Cambrian Lagerstätte, In J. R. Laurie, P. D. Kruse, D. C. García-Bellido & J. D. Holmes (Eds.), Palaeo Down Under 2, Adelaide, 11-15 July 2016. *Geological Society of Australia Abstracts, 117*.

García-Bellido, D. C., Edgecombe, G. D., Paterson, J. R., & Ma, X. (2013a). A 'Collins' monster'-type lobopodian from the Emu Bay Shale Konservat-Lagerstätte (Cambrian), South Australia. *Alcheringa, 37*, 474-478.

García-Bellido, D. C., Lee, M. S. Y., Edgecombe, G. D., Jago, J. B., Gehling, J. G., & Paterson, J. R. (2014). A new vetulicolian from Australia and its bearing on the chordate affinities of an enigmatic Cambrian group. *BMC Evolutionary Biology, 14*, 214.

García-Bellido, D. C., Paterson, J. R., & Edgecombe, G. D. (2013b). Cambrian palaeoscolecids (Cycloneuralia) from Gondwana and reappraisal of species assigned to *Palaeoscolex*. *Gondwana Research, 24*, 780-795.

García-Bellido, D. C., Paterson, J. R., Edgecombe, G. D., Jago, J. B., Gehling, J. G., & Lee, M. S. Y. (2009). The bivalved arthropods *Isoxys* and *Tuzoia* with soft-part preservation from the Lower Cambrian Emu Bay Shale Lagerstätte (Kangaroo Island, Australia). *Palaeontology, 52*, 1221-1241.

Gehling, J. G., Jago, J. B., Paterson, J. R., García-Bellido, D. C., & Edgecombe, G. D. (2011). The geological context of the Lower Cambrian (Series 2) Emu Bay Shale Lagerstätte and adjacent stratigraphic units, Kangaroo Island, South Australia. *Australian Journal of Earth Sciences, 58*, 243-257.

Glaessner, M. F. (1979). Lower Cambrian Crustacea and annelid worms from Kangaroo Island, South Australia. *Alcheringa, 3*, 21-31.

Goodge, J. W., Vervoort, J. D., Fanning, C. M., Brecke, D. M., Farmer, G. L., Williams, I. S., . . . DePaolo, D. J. (2008). A Positive Test of East Antarctica–Laurentia Juxtaposition Within the Rodinia Supercontinent. *Science, 321*, 235-240.

Hall, P. A., McKirdy, D. M., Halverson, G. P., Jago, J. B., & Gehling, J. G. (2011). Biomarker and isotopic signatures of an early Cambrian Lagerstätte in the Stansbury Basin, South Australia. *Organic Geochemistry, 42*, 1324-1330.

Han, J., Zhang, Z.-F., & Liu, J.-N. (2008). A preliminary note on the dispersal of the Cambrian Burgess Shale-type faunas. *Gondwana Research, 14*, 269-276.

Jago, J. B., & Cooper, B. J. (2011). The Emu Bay Shale Lagerstätte: a history of investigations. *Australian Journal of Earth Sciences, 58*, 235-241.

Jago, J. B., García-Bellido, D. C., & Gehling, J. G. (2016). An early Cambrian chelicerate from the Emu Bay Shale, South Australia. *Palaeontology, 59*, 549-562.

Jago, J. B., Zang, W.-L., Sun, X., Brock, G. A., Paterson, J. R., & Skovsted, C. B. (2006). A review of the Cambrian biostratigraphy of South Australia. *Palaeoworld, 15*, 406-423.

Lee, M. S. Y., Jago, J. B., García-Bellido, D. C., Edgecombe, G. D., Gehling, J. G., & Paterson, J. R. (2011). Modern optics in exceptionally preserved eyes of Early Cambrian arthropods from Australia. *Nature, 474*, 631-634.

Li, Z. X., Bogdanova, S. V., Collins, A. S., Davidson, A., De Waele, B., Ernst, R. E., . . . Vernikovsky, V. (2008). Assembly, configuration, and break-up history of Rodinia: A synthesis. *Precambrian Research, 160*(1-2), 179-210.

Lu, Y. H. (1950). On the genus *Redlichia* with description of its new species. *Geological Review, 15*, 157-170.

McHenry, B., & Yates, A. (1993). First report of the enigmatic metazoan *Anomalocaris* from the Southern Hemisphere and a trilobite with preserved appendages from the Early Cambrian of Kangaroo Island, South Australia. *Records of the South Australian Museum, 26*, 77-86.

McKerrow, W. S., Scotese, C. R., & Brasier, M. D. (1992). Early Cambrian continental reconstructions. *Journal of the Geological Society, London, 149*, 599-606.

McKirdy, D. M., Hall, P. A., Nedin, C., Halverson, G. P., Michaelsen, B. H., Jago, J. B., . . . Jenkins, R. J. F. (2011). Paleoredox status and thermal alteration of the lower Cambrian (Series 2) Emu Bay Shale Lagerstätte, South Australia. *Australian Journal of Earth Sciences, 58*, 259-272.

Moussian, B. (2013). The arthropod cuticle. In A. Minelli, G. Boxshall, G. Fusco, (Eds.), Arthropod Biology and Evolution: Molecules, Development, Morphology. Berlin Heidelberg: Springer-Verlag.

Nedin, C. (1995). The Emu Bay Shale, a Lower Cambrian fossil Lagerstätten, Kangaroo Island, South Australia. *Memoirs of the Association of Australasian Palaeontologists, 18*, 31-40.

Nedin, C. (1997). Taphonomy of the Early Cambrian Emu Bay Shale Lagerstätte, Kangaroo Island, South Australia. *Bulletin of National Museum of Natural Science, 10*, 133-141.

Nedin, C. (1999). *Anomalocaris* predation of nonmineralized and mineralized trilobites. *Geology, 27*, 987-990.

Nedin, C., & Jenkins, R. J. F. (1999). Heterochrony in the Cambrian trilobite *Hsuaspis*. *Alcheringa, 23*, 1-7.

Palmer, A. R., & Rowell, A. J. (1995). Early Cambrian Trilobites from the Shackleton Limestone of the Central Transantarctic Mountains. *Palaeontological Society Memoir, 45*.

Paterson, J. R., & Brock, G. A. (2007). Early Cambrian trilobites from Angorichina, Flinders Ranges, South Australia, with a new assemblage from the Pararaia bunyerooensis Zone. *Journal of Paleontology, 81*, 116-142.

Paterson, J. R., Edgecombe, G. D., GarcÍa-Bellido, D. C., Jago, J. B., & Gehling, J. G. (2010). Nektaspid arthropods from the Lower Cambrian Emu Bay Shale Lagerstätte, South Australia, with a reassessment of lamellipedian relationships. *Palaeontology, 53*, 377-402.

Paterson, J. R., Edgecombe, G. D., & Jago, J. B. (2015). The 'great appendage' arthropod *Tanglangia*: Biogeographic connections between early Cambrian biotas of Australia and South China. *Gondwana Research, 27*, 1667-1672.

Paterson, J. R., García-Bellido, D. C., & Edgecombe, G. D. (2012). New Artiopodan arthropods from the Early Cambrian Emu Bay Shale Konservat-Lagerstätte of South Australia. *Journal of Palaeontology, 86*, 340-357.

Paterson, J. R., García-Bellido, D. C., Jago, J. B., Gehling, J. G., Lee, M. S. Y., & Edgecombe, G. D. (2016). The Emu Bay Shale Konservat-Lagerstätte: a view of Cambrian life from East Gondwana. *Journal of the Geological Society, London, 173*, 1-11.

Paterson, J. R., García-Bellido, D. C., Lee, M. S. Y., Brock, G. A., Jago, J. B., & Edgecombe, G. D. (2011). Acute vision in the giant Cambrian predator *Anomalocaris* and the origin of compound eyes. *Nature, 480*, 237-240.

Paterson, J. R., & Jago, J. B. (2006). New trilobites from the Lower Cambrian Emu Bay Shale Lagerstätte at Big Gully, Kangaroo Island, South Australia. *Memoirs of the Association of Australasian Palaeontologists, 32*, 43-57.

Peng, S., Babcock, L. E., & Cooper, R. A. (2012). The Cambrian Period. In F. M. Gradstein, J. G. Ogg, M. D. Schmitz, & G. M. Ogg (Eds.), *The Geologic Time Scale 2012, Volume 2* (pp. 437-488). Oxford: Elsevier.

Pocock, K. J. (1964). *Estaingia*, a new trilobite genus from the Lower Cambrian of South Australia. *Palaeontology, 7*, 458-471.

Preiss, W. V. (2000). The Adelaide Geosyncline of South Australia and its significance in Neoproterozoic continental reconstruction. *Precambrian Research, 100*, 21-63.

Smith, M. R. (2013). Nectocaridid ecology, diversity and affinity: early origin of a cephalopod-like body plan. *Paleobiology, 39*(2), 297-321.

Smith, M. R., & Caron, J.-B. (2010). Primitive soft-bodied cephalopods from the Cambrian. *Nature, 465*, 469-472.

Sprigg, R. C. (1955). The Point Marsden Cambrian beds, Kangaroo Island, South Australia. *Transactions of the Royal Society of South Australia, 78*, 165-168.

Telford, M. J., Bourlat, S. J., Economou, A., Papillon, D., & Rota-Stabelli, O. (2008). The evolution of the Ecdysozoa. *Philosophical Transactions of the Royal Society B: Biological Sciences, 363*, 1529-1537.

Torsvik, T. H., & Cocks, L. R. M. (2013). New global palaeogeographical reconstructions for the Early Palaeozoic and their generation. In D. A. T. Harper & T. Servais (Eds.), Early Palaeozoic Biogeography and Palaeogeography. *Geological Society, London, Memoirs, 38*, 5-24.

Walcott, C. D. (1911). Middle Cambrian Merostomata. *Cambrian Geology and Palaeontology II: Smithsonian Miscellaneous Collections, 57*, 145-228.

Zhang, X. L., Fu, D. J., & Dai, T. (2012). A new species of Kangacaris (Arthropoda) from the Chengjiang lagerstätte, lower Cambrian, southwest China. *Alcheringa, 36*, 23-25.

Zhang, X. L., Han, J., Zhang, Z. F., Liu, H. Q., & Shu, D. G. (2004). Redescription of the Chengjiang arthropod *Squamacula clypeata* Hou and Bergström, from the Lower Cambrian, south-west China. *Palaeontology, 47*, 605-617.

Chapter 3 – Quantitative comparison of Cambrian *Lagerstätten* assemblages in space and time

J. D. Holmes, D. C. García-Bellido and M. S. Y. Lee

3.1 Abstract

Exceptional fossil deposits exhibiting soft-part preservation, or *Konservat-Lagerstätten* (literally 'conservation storage-places'), are particularly prevalent in Cambrian rocks and provide detailed information on fossil assemblages not available from conventional deposits. It has long been recognised that many of these assemblages exhibit certain taxonomic similarities, with many elements seemingly having cosmopolitan distributions. These types of assemblages, particularly those of Cambrian age, have become known as Burgess Shale-type (BST) biotas, named for the famous deposit in the Canadian Rocky Mountains where fossils preserved in this way were first discovered. This study provides the first broad-scale analysis of the biogeographic relationships between all major BST biotas. We compiled a database of the presences and absences of over 600 genera in 12 Lagerstätten from Laurentia, Siberia, South China and East Gondwana, ranging in age from Cambrian Series 2 through Series 3 (late-early to middle Cambrian; c. 518 – 502 Ma), and analysed this using a variety of quantitative methods in order to investigate the relationships between these sites. Mantel tests and Multiple Regression of Distance Matrices (MRM) were used to test the correlations between differences in assemblage, with differences in age and geographic distance between sites. Non-metric multidimensional scaling (NMDS) ordination, cluster analysis and Parsimony Analysis of Endemicity (PAE) were used to group localities and examine relationships. We also use Bayesian inference and illustrate the benefits of this approach to biogeographic studies. Results suggest that both space and time have important effects on the constitution of BST biotas, and that the similarity of these

assemblages appears to increase from Series 2 through Series 3, largely driven by a rise in shared cosmopolitan biomineralised taxa such as trilobites and brachiopods. There is also evidence of higher-level taxonomic turnover across this period. Based on our analyses, purported similarities between the BST biotas of Laurentia and South China are not apparent. Endemic taxa help amplify these patterns, despite their frequent exclusion from biogeographic analyses.

3.2 Introduction

3.2.1 Background

Cambrian *Konservat-Lagerstätten* – fossil deposits exhibiting exceptional preservation of soft parts – offer great insight into the diversity and ecology of early communities following the 'Cambrian explosion' (Conway Morris, 1985). As well as providing enhanced biological information about individual organisms, they also provide a more faithful representation of the full diversity and relative abundances of taxa present within these communities. This information should allow us not only to undertake more accurate and meaningful ecological analysis of these early communities, but also to examine their biogeographic relationships based on shared taxa. The former has been undertaken for several Cambrian Lagerstätten (e.g. Caron & Jackson, 2008; Conway Morris, 1986; Dornbos & Chen, 2008; Ivantsov et al., 2005; Zhao et al., 2010; 2014), however, the latter is yet to be pursued in any great detail.

It is well known that many Cambrian Lagerstätten share common faunal elements. A substantial number of genera found within these assemblages exhibit largely cosmopolitan distributions, e.g. the sponges *Choia*, *Hazelia*, *Leptomitus* and *Protospongia*, sponge-like *Chancelloria*, cnidarian *Byronia*, brachiopods *Lingulella* and *Nisusia*, molluscs *Haplophrentis* and *Wiwaxia*, anomalocaridid *Anomalocaris*, lobopodian *Hallucigenia*, the euarthropods *Canadaspis*, *Isoxys*, *Leanchoilia*, *Liangshanella*, *Naraoia* and *Tuzoia*, annelid *Selkirkia*, and the enigmatic taxa *Eldonia* and *Dinomischus*. It is likely that at least some of these had larval stages capable of

long distance dispersal via ocean currents (García-Bellido et al., 2007; Han et al., 2008; Zhao et al., 2011). These taxa are not particularly informative in a biogeographic sense, as their broad distributions provide little evidence when attempting to draw conclusions about relationships between localities; however, they do suggest that we are looking at similar types of communities. These have been termed Burgess Shale-type (BST) biotas, named after the famous Cambrian Series 3 deposit in the Canadian Rocky Mountains.

3.2.2 Previous work

Comparisons between BST biotas have been made by many authors; however, little quantitative analysis focusing on shared taxa between localities has been undertaken. Hendricks et al. (2008) used species occurrence data and continental reconstructions to examine the geographic and temporal distribution of Cambrian arthropods, and showed that soft-bodied species had wider geographic and stratigraphic ranges than contemporaneous trilobites. Hendricks (2013) conducted a similar analysis of a wider range of Cambrian metazoan phyla, as well as algae and cyanobacteria, and showed that patterns varied across different clades, and that geographic range of species (and genera) was positively correlated with temporal persistence. However, these studies focused on distributions of individual taxa rather than on assemblage similarity as a whole. One of the few dedicated studies to focus on assemblage similarity between Cambrian Lagerstätten on a broad scale was Han et al. (2008), who listed shared genera for a number of site comparisons as part of their analysis, in particular focusing on associations between sites in Laurentia and

South China. They suggested that the Chengjiang (Series 2) and Burgess Shale (Series 3) assemblages were closely related based on qualitative analysis of shared genera, and that the development of pelagic larvae may have resulted in the worldwide distribution of BST biotas. Similarities between the Chengjiang and Burgess Shale assemblages have also been mentioned by other authors (e.g. Babcock et al., 2001; Conway Morris, 1989; 1998). Common generic occurrences between the Kaili Biota (Series 3), and the Burgess Shale and Chengjiang Lagerstätten were discussed by (Zhao et al., 2005), who gave figures of 38 and 30 shared genera respectively, and suggested that the greater similarity with the Laurentian site was possibly due to elements of middle-to-outer shelf faunas becoming more stable and widespread by this time. It was suggested by (Zhao et al., 2011) that the similarity in age (as well as environment) between Kaili and the Laurentian Burgess Shale and Spence Shale (Utah, USA), may partially account for the similarity seen between these assemblages, and that perhaps age was a greater determinant of assemblage than geography during the late-early to middle Cambrian. Similar features between the Sinsk Biota of Siberia and the Burgess Shale assemblage (the Phyllopod Bed in particular) were noted by Ivantsov et al. (2005), including co-occurrence of a small number of genera. Numerous studies have acknowledged the existence of shared taxa (mostly at the genus level) between the Emu Bay Shale from South Australia, and other Cambrian Series 2 Lagerstätten in South China; this association has been strengthened in recent years with the discovery of new taxa from the EBS with Chinese representatives (Paterson et al., 2010; 2012; 2015; 2016; Paterson & Jago, 2006). A high level of similarity between certain Series 3 Laurentian sites was recognised by Hagadorn (2002), with

the Marjum and Wheeler formations from Utah and the Burgess Shale exhibiting a particularly high proportion of shared genera. Previous palaeoecological analyses have also compared the ecological attributes of BST biotas, e.g. patterns in species abundances, species diversity, phylum-level abundance, and so on (e.g. Caron & Jackson, 2008; Dornbos & Chen, 2008; Ivantsov et al., 2005; Zhao et al., 2014). Ecological comparison of different assemblages has also been undertaken between subsets of individual Lagerstätten, either temporally (e.g. the "bedding assemblages" from the Burgess Shale's Phyllopod Bed: Caron and Jackson (2008), or spatially (e.g. the comparison of individual localities of the Chengjiang Biota: (Zhao et al., 2012).

The majority of comments relating to taxonomic and biogeographic similarity between BST biotas have been made within studies mostly dedicated to other fields, e.g. palaeobiology and palaeoecology. The literature on the biogeography of these deposits is sparse, simply due to the fact that the paucity of data spread through space and time might make them seem poor candidates for biogeographic study when examined in isolation. It is important to note that within the biotas there are many different groups that may show completely different biogeographic patterns due to factors such as the history of individual lineages and their dispersal abilities. It has been shown, for example, that early Cambrian trilobite distributions are possibly a vicariant result of the breakup of the short-lived supercontinent Pannotia during the late Neoproterozoic (Lieberman, 2003; Meert & Lieberman, 2004), whereas the distribution of non-trilobite arachnomorph arthropods is more likely a result of other factors such as dispersal ability and sea level change (Hendricks & Lieberman, 2007). For traditional biogeographic purposes it is more sensible to focus on

mineralised groups that have wide distributions across space and time, such as trilobites (e.g. Alvaro et al., 2013; Hally & Paterson, 2014) and/or on clades with robust phylogenetic hypotheses (Hendricks & Lieberman, 2007; Lieberman, 2003). Despite this, Cambrian Lagerstätten still contain important biogeographic information that should be considered. The resolution with which we can view these exceptionally preserved assemblages, i.e. the fact that they provide a more faithful representation of taxa present than conventional fossil deposits, means that we can analyse taxonomic associations in greater detail, and then suggest what factors may be responsible for the relationships we see based on the characteristics of the sites in question.

This study undertakes the first quantitative analysis of the taxonomic relationships between all major BST biotas. The importance of these deposits to our understanding of early animal life and evolution has resulted in considerable scholarly attention, and the resulting literature has allowed for the compilation of a substantial database of generic occurrence to be constructed. We analyse this database using a variety of statistical methods to provide insights into how and why BST biotas are related.

3.2.3 Locations and relative ages

In this study we consider 12 BST biotas from East Gondwana (Emu Bay Shale), South China (Chengjiang, Kaili, Guanshan, Balang), Laurentia (Burgess, Wheeler, Marjum, Spence and Kinzers Shales, and Sirius Passet) and Siberia (Sinsk) (Fig. 3.1), and ranging in age from Series 2 through Series 3 (formerly late-early through middle Cambrian; Tab. 3.1). Absolute ages are estimated below for modelling

purposes and are based on correlation with the Cambrian timescale presented in Peng (2012, Fig. 19.3) unless otherwise stated.

Figure 3.1: Cambrian continental reconstruction (based on Torsvik & Cocks, 2013; Fig. 2.8) showing hypothesised locations of Cambrian Lagerstätten (as at 510 Ma). Note that all sites are located within approximately 20° of the equator.

The Chengjiang Biota occurs within the Maotianshan Shale – the middle member of the Yu'anshan Formation based on the organisation of MacKenzie et al. (2015) (as per Hu, 2005; Zhao et al., 2012), overlying the "Black Shale" and underlying the "Upper Siltstone" members. Fossils of the Chengjiang Biota occur primarily in the middle to upper part of the Maotianshan Shale member, essentially in the middle part of the Yu'anshan Formation (MacKenzie et al., 2015). This is consistent with a mid-late Atdabanian age (e.g. Steiner et al., 2007), or ~518 Ma based on correlation with Fig. 19.11 of Peng et al. (2012). The Sirius Passet Lagerstätte (lower Buen Formation) is stratigraphically poorly constrained and its position based mainly on the Nevadiid affinities of the trilobite *Buenellus* and

subsequent correlation with the *Nevadella* trilobite zone of Laurentia (Babcock & Peel, 2007), the middle of which is dated to around 517 Ma. Incidentally, this is the same age tentatively assigned to Sirius Passet by Budd (2011). Based on the presence of the Sinsk Biota within the *Bergeroniellus gurarii* zone (Astashkin et al., 1990) we estimate an age of 515 Ma. The age of the Balang Formation is approximately 514 Ma based on placement within the *Arthricocephalus chaveaui* zone (Yan et al., 2014). The Guanshan Biota (Wulongqing Formation) falls within the *Palaeolenus/ Megapalaeolenus* zone and is therefore approximately coeval with the Balang Formation (see Peng, 2009, Tab. 1), as is the Emu Bay Shale based on correlation with the *Pararaia janeae* zone of mainland South Australia (e.g. Paterson & Brock, 2007; Paterson et al., 2008). The Kinzers Lagerstätte is confined to the basal Emigsville Member of the Kinzers Formation, Olenellid trilobites from which suggest a Dyeran age; however, trilobites from higher levels suggest that the Series 2/3 boundary lies higher in the formation (Skinner, 2005) and, as such, we assign a late Dyeran age of 512 Ma (see Peng et al., 2012, Fig. 19.11). The Kaili Biota is found within the *Oryctocephalus indicus* zone and the lower part of *Peronopsis taijiangensis* zone within the Kaili Formation (Zhao et al., 2011), and is thus given an age of 508 Ma. The Spence Shale Member of the Langston Formation is found within the *Glossopleura* zone of Laurentia (Robison & Babcock, 2011) and dated at 506 Ma. The boundary between the *Glossopleura* and *Bathyuriscus-Elrathina* zones, which is equivalent to the base of the *Ehmaniella* zone (Peng et al., 2012), is found in the lower part of the Burgess Shale Formation between the Yoho River Limestone and Campsite Cliff Shale Members (Collom et al., 2009). Soft-bodied preservation within the Burgess Shale occurs at various stratigraphic levels above this and is

therefore approximately 505 Ma. The lower part of the Wheeler Shale is within the *Ptychagnostus gibbus* zone and the upper within the *P. atavus* zone (Robison & Babcock, 2011), and is thus given an age of 504 Ma. The centre of the Marjum Formation is within the *P. punctuosus* zone (Robison & Babcock, 2011) and dated at 502 Ma. A point to note from the above is that the majority of Series 3 sites are Laurentian and the Series 2 sites Gondwanan, although there are exceptions.

Table 3.1: Estimated age, location, number of genera, and number of shared/endemic genera (excluding questionable assignations) for each of the 12 Cambrian Lagerstätten considered in this study.

Locality	Age	Location	No. of genera	Shared / Endemic
Chengjiang	518	**Gondwana** (South China)	231	68/163
Sirius Passet	517	**Laurentia** (Greenland)	28	3/25
Sinsk	515	**Siberia**	45	13/32
Guanshan	514	**Gondwana** (South China)	55	34/21
Balang	514	**Gondwana** (South China)	34	20/14
Emu Bay Shale	514	**Gondwana** (East)	32	10/22
Kinzers	511	**Laurentia** (South)	28	15/13
Kaili	508	**Gondwana** (South China)	129	65/64
Spence	506	**Laurentia** (North)	69	48/21
Burgess Shale	505	**Laurentia** (North)	165	89/76
Wheeler	504	**Laurentia** (North)	87	57/30
Marjum	502	**Laurentia** (North)	78	45/33

The localities considered in this study are interpreted to have been deposited under a range of different environmental settings. Most were deposited in mixed siliciclastic-carbonate low-angle ramp settings seaward of carbonate platforms, such as those that surrounded Laurentia during the Cambrian (Gaines, 2014). The Utah Lagerstätten (the Spence, Wheeler and Marjum Shales), the Kinzers Shale, as well as the Kaili, Balang and Sinsk Formations, are examples of this (Brett et al., 2009; Gaines et al., 2011; Garson et al., 2012; Ivantsov et al., 2005; Peng et al., 2005; Skinner, 2005). The Burgess Shale Formation, while occupying a similar setting, was deposited directly adjacent to the (older) platformal carbonates of the Cathedral Formation, which provided a steep, local escarpment at the time of deposition (Collom et al., 2009; Fletcher & Collins, 1998). The Sirius Passet Lagerstätte is thought to have been deposited in a somewhat comparable environment (Ineson & Peel, 2011). The depositional setting of the Chengjiang Biota is quite different to that discussed above, and is interpreted as a shallow, gently sloping, siliciclastic shelf (Hu, 2005). The Guanshan Biota occupied a similar environment (Hu et al., 2010). Perhaps the most unique setting of any BST biota is that of the Emu Bay Shale, in that it was deposited in an inner-shelf, fan-delta setting adjacent to an active tectonic margin (Gaines et al., 2016; Gehling et al., 2011). Despite the evident differences in local environmental settings, BST biotas do have some similar characteristics, e.g. all are interpreted to involve rapid burial in fine sediment, at or below storm wave base. It should be noted that Gaines (2014) defined Burgess Shale-type *deposits* based on the standard mode of preservation for BST assemblages, which involves the preservation of primary carbonaceous films.

3.2.4 Considerations in comparing assemblages

Comparisons between BST biotas are complicated by the fact that these deposits are distributed somewhat unevenly through space (although relatively evenly through time), with potential local environmental and depositional conditions, as well as taphonomic and collection biases, also having an effect on assemblage compositions. As discussed above, the localities considered in this study are aged between c. 518–502 Ma (Cambrian Series 2 through Series 3); however, the earlier Series 2 sites are mostly confined to Gondwana, and the later Series 3 sites concentrated in Laurentia. The fact that these sites are spread across a substantial time period also makes it difficult to infer biogeographic relationships due to the fact that multiple dispersal events are likely to have occurred between areas during this period. Not only that, the Cambrian is considered to be a time of considerable tectonic change (e.g. Meert & Lieberman, 2004), and geographic relationships between areas themselves were not static. It is generally accepted, however, that at this time the supercontinent Gondwana occupied a position stretching from the south pole to the equator, and was separated from Laurentia to the west by the palaeocontinents of Siberia and Baltica, as well as various microcontinents (Alvaro et al., 2013; McKerrow et al., 1992; Torsvik & Cocks, 2013). The Iapetus Ocean separated Laurentia (comprising the majority of modern day North America and Greenland rotated approximately 90 degrees clockwise) from Gondwana to the west and south (Fig. 3.1). This general pattern is not considered to have changed substantially during the period in question.

The deposits themselves also show considerable variation. Quality and type of preservation, effects of weathering, density of specimens, stratigraphic continuity and geographic range all vary greatly between localities (e.g. Briggs et al., 1994; Gaines, 2014; Hou et al., 2004; Paterson et al., 2016; Peel & Ineson, 2011; Robison et al., 2015; Zhao et al., 2011). A three-tiered ranking system of Burgess Shale-type deposits was proposed by Gaines (2014) based on the number of soft-bodied taxa known (taxonomic richness) at each locality (>100 = Category 1; 10-100 = Category 2; <10 = Category 3), and the fact that fidelity of preservation is generally correlated with taxon counts; however, he noted that this system does not take into account differences in collection effort between sites, and that further developments could alter the current rating of a deposit. Our dataset contains representatives from each of these classes. Category 1 assemblages such as Chengjiang (231 total, 68 shared, 163 singleton genera) and the Burgess Shale (165, 89, 76) have been particularly well studied, with multiple sub-localities and long histories of collection. Category 2 assemblages are less diverse, e.g. the Guanshan Biota (55, 34, 21) and the Wheeler Shale (87, 57, 30). The Kinzers Lagerstätte (28, 15, 13) represents a Category 3 biota (see Tab. 3.1 for a full list of BST biotas considered here, including total, shared and singleton taxon counts).

Our analysis also includes two deposits specifically excluded from the list of Burgess Shale-type deposits by Gaines (2014) based on their anomalous preservation styles (Sirius Passet and the Emu Bay Shale). While these localities do not appear to be typical Burgess Shale-type deposits in a preservation sense, they do seem to house relatively typical Burgess Shale-type biotas, and were therefore included in our analysis. Cambrian Lagerstätten are also represented by a variety of

different environmental and depositional settings (Gaines, 2014). This is difficult to account for in a quantitative sense and we have not attempted to introduce this variable into our quantitative analysis at this stage, but we acknowledge this as a potential factor affecting assemblage composition.

Many of the issues mentioned above are inherent in the comparison of fossil assemblages, and must be addressed in palaeobiogeographic studies. One of the biggest problems is that of "double zero" matches, i.e. how can we tell if the absence of a taxon from a particular site reflects true absence from the original assemblage, or simply the fact that it has either (a) not been discovered yet, or (b) was not preserved due to taphonomic bias? This is compounded by the fact that, in many cases, levels of collection effort vary across sites, resulting in large differences in taxon counts (sample sizes).

Another issue is how best to account for endemic or 'singleton' taxa (i.e. those peculiar to a single site), and also the variation in relative proportions of 'singletons' between sites, a factor linked to biodiversity. Palaeobiogeographic studies that utilise presence/absence data often exclude singletons and focus only on taxa shared between localities. This may be appropriate in certain cases (e.g. when taxon counts and proportions of shared/singleton taxa are similar across sites), but we argue that this is not necessarily the case. Removing singletons increases the similarities between assemblages, and changes the ratios of shared/singleton taxa utilised in similarity and distance coefficients, which can result in assemblages being classified as very similar to each other despite large differences in their numbers of endemic taxa. This is of particular importance if certain localities are rich in endemics or sample size varies greatly. Conversely, in some cases it may be desirable to exclude

singletons, especially those that are represented by only a small number of specimens, particularly at sites with high levels of collection effort. It is important to consider these issues when deciding on what measures to use in a palaeobiogeographic analysis.

Given the difficulties mentioned above, the choice of an appropriate distance coefficient is extremely important when conducting multivariate analyses in palaeobiogeography, and can help to mitigate their effects. Our dataset is subject to a number of these issues, e.g. it contains sites with greatly differing taxon counts and varying levels of endemicity, largely due to the peculiarities of the individual sites; this "poor sampling" is essentially unavoidable in this instance. Shi (1993) compared 39 different binary similarity and distance coefficients based on a number of different criteria and concluded that Jaccard's coefficient of community (Jaccard, 1908) was the most informative (but see also Archer & Maples, 1987; Maples & Archer, 1988). The Jaccard coefficient, in a biogeographic sense, is the ratio of taxa shared between two localities, over the combined pool of taxa present in both localities; as such, it ignores shared absences of taxa, helping to mitigate the problem of double zeroes. The Jaccard coefficient, however, is not particularly suited to situations where there are large variations in sample size (i.e. taxon diversity). When comparing sites with disparate sample sizes, the Jaccard coefficient will always be relatively small (Hammer & Harper, 2006). Despite this, the Jaccard coefficient is considered a standard and is commonly used in palaeobiogeographic studies, and as such we have used both this and another of the coefficients recommended by Shi (1993), Ochiai's coefficient of closeness (Ochiai, 1957). The Ochiai coefficient was chosen due to the fact that, like the Jaccard coefficient, it discounts instances of

shared absence, but is defined as the ratio of shared taxa over the geometric mean of the two sample sizes, thus somewhat reducing the effect of disparate sample sizes. Comparisons between sites with similar sample sizes (taxon diversity) will have similar values under both the Jaccard and Ochiai coefficients, but as disparity between sites increases the value of the Jaccard will drop more steeply than that of the Ochiai coefficient. The latter is a desirable trait in a coefficient when analysing a database such as ours that contains sites with widely varying numbers of taxa, and is particularly important when sites contain large numbers of singletons, as the coefficient is less affected by these taxa.

3.3 Data and methodology

3.3.1 General considerations

The database constructed for this study contains presence/absence information for 605 genera (in 15 animal phyla, as well as algae and cyanobacteria) within the 12 deposits under consideration. Given the broad nature of this study, both in space and time, data from Lagerstätten with multiple localities were pooled. Relative coordinates of sites were obtained by plotting their positions on the 510 Ma reconstruction of Torsvik and Cocks (2013, Fig. 2.8), as well as the Series 2 reconstruction of McKerrow et al. (1992, Fig. 3) and the Cambrian reconstruction of Alvaro et al. (2013, Fig. 19.1) for comparison. It should be noted that these reconstructions are based at least partly on the distribution of shelly fossils; however,

they are currently the best estimates available of continental arrangements during the Cambrian. A matrix containing the presence/absence of taxa, relative geographic coordinates, and absolute age estimates was then prepared for analysis (Supp. Tab. 6.1). Questionably assigned genera (?, c.f., aff.) were conservatively coded as '?'. References pertaining to the generic presence/absence data are provided in Supp. Tab. 6.3.

3.3.2 Statistical modelling

We used Mantel tests (Mantel, 1967) and "Multiple Regression of Distance Matrices" (MRM; Legendre et al., 1994; Legendre & Legendre, 1998; Manly, 1986) to test the significance of the relationships between assemblage dissimilarity, and geographic distance and age difference between sites. These methods involve obtaining "distance matrices" for each variable, which provide distance measures between all possible pairs of sites. These are $n \times n$ matrices (in this case of sites) that are diagonally symmetrical. After one set of duplicate values and the main diagonal (i.e. self-distances) are removed we are left with $n(n-1)/2$ observations (Lichstein, 2007). Ochiai's coefficient of closeness (Ochiai, 1957) and Jaccard's coefficient of community (Jaccard, 1908) were used to generate "assemblage distance" matrices based on the generic level presence/absence data; these give a distance measure between 0 and 1 for all site pairings, with 0 reflecting identical and 1 reflecting entirely different assemblages. Assemblage distance matrices were produced both including and excluding singleton taxa. Missing values (uncertain taxa) were accommodated by pair-wise deletion. A matrix of geographic distances was

generated using the relative coordinates of sites for each of the reconstructions considered, with the “age distance” matrix reflecting the differences in age between assemblage pairs.

Initially, we used Mantel tests to test the linear correlation between distance matrices. This method involves unfolding the matrices into vectors and testing the correlation between corresponding pair-wise values. Like Pearson’s correlation coefficient, the standardised Mantel statistic gives the linear association between variables as a figure between -1 and 1; it should be noted that strongly non-linear relationships may not be identified by the Mantel test (Legendre & Legendre, 1998). Given the fact that pair-wise observations are not independent (i.e. in this instance changing the value of one site will alter the distances between that site and all others), tests for significance are undertaken by permutation. The rows of one of the original matrices (or distance matrices) are permuted and the distance matrices recalculated multiple times to provide a sampling distribution of the Mantel statistic under the null hypothesis, with which the observed value can be compared (Legendre & Legendre, 1998). The nature of our data suggested that log transformation of geographic distance may be appropriate; analyses were therefore performed on both raw and logged data (for the latter, we added 1 to all values to accommodate site pairings showing a geographic distance of 0).

MRM is an extension of the Mantel test and provides a framework for testing the effects of multiple explanatory variables. As with Mantel analysis, the distance matrices are first unfolded into vectors. The pair-wise values in the response vector are then regressed against their corresponding values in the explanatory vectors. The multiple regression framework provides a convenient way for us to

independently test the effects of multiple explanatory variables on a hypothesised response variable, and allows the use of non-linear and non-parametric models (Lichstein, 2007). As with the Mantel test, significance testing is carried out by permutation. Using assemblage distance as the response variable and geographic and age distances as explanatory variables, we tested a range of simple MRM models to see which best explained the variation we see between assemblages.

Analyses were carried out through the "R" statistical software environment (R Core Team, 2015) using the RStudio® interface (RStudio Team, 2015). Geographic distances were calculated using the "geosphere" package (Hijmans, 2015). Mantel tests were conducted using the "vegan" package (Oksanen et al., 2015). Multiple regression of distance matrices was carried out using the "ecodist" package (Goslee & Urban, 2007). Assemblage distance matrices using the Ochiai and Jaccard coefficients were produced in PAST Version 3.10 (PAlaeotological STasistics; Hammer et al., 2001) before importing to R in order to easily allow for pair-wise deletion of missing values. R-script files of all analyses are included in the electronic Supplementary Material.

3.3.3 Ordinations and cluster analysis

We analysed the presence/absence data using ordinations to help visualise the relationships between localities and cluster analysis to group sites based on assemblage composition. Using the Ochiai and Jaccard assemblage distance matrices discussed above, non-metric multidimensional mcaling (NMDS) ordination plots were produced, and cluster analysis was used to produce "Q-mode"

dendrograms based on the unweighted arithmetic average (UPGMA) algorithm. Ordination and cluster analysis was carried out using the “vegan” package for R (Oksanen et al., 2015). Dendrograms were produced using the “dendextend” package (Galili, 2015).

3.3.4 Parsimony and Bayesian analysis

Parsimony analysis of endemicity (PAE – Morrone, 2014; Rosen & Smith, 1988) was conducted based on the presence/absence data. PAE essentially constructs a cladogram of relationships between areas, using taxon occurrences as "characters”. While certain variations of this approach have been criticised in the past (for a review see Nihei, 2006), PAE provides an alternative way to assess biogeographic relationships from multivariate ordination and clustering methods; it clusters areas according to the inferred individual histories of taxa rather than overall faunal similarity. All PAE analysis used PAUP* (Swofford, 2001), with all characters in the matrix (i.e. presence/absence of genera) equally weighted, and branch-and-bound searches which guarantee to find all most-parsimonious trees. Support for groupings of areas was ascertained using bootstrapping (each replicate using branch-and-bound searches). Our analysis included singleton taxa, but as these are not parsimony-informative, their exclusion would not have any topological effect.

We also analysed the presence/absence matrix using Bayesian inference. The potential advantages and shortcomings of Bayesian phylogenetic methods are widely discussed elsewhere (e.g. O'Reilly et al., 2016). The most relevant differences in this context are as follows. (1) PAE typically weights all taxa equally,

but it might be expected that taxa with greater dispersal ability might exhibit less biogeographic signal (i.e. more "area homoplasy"). Bayesian methods can potentially identify and accommodate this, by allowing some taxa to "evolve" (i.e. change areas) rapidly and exhibit more expected incongruence with the overall area cladogram. (2) Unlike parsimony, Bayesian inference doesn't attempt to find a single "best" area cladogram. Rather, it integrates over all possible cladograms, weighted by their posterior probability (good topologies are weighted more highly). Thus, it might better estimate uncertainty in area relationships.

Bayesian inference was undertaken using MrBayes 3.2.5 (http://www.ncbi.nlm.nih.gov/pmc/articles/PMC3329765/). Variation in rates across taxa was accommodated using the gamma parameter; inclusion of this parameter was supported by Bayes Factors (=20), as calculated using stepping-stone sampling. Four replicate MCMC runs were performed to ensure convergence. Each run composed 4 incrementally heated (temperature 0.2) chains, run for 10 million generations with sampling every 10 000 generations, with the first 20% discarded as burnin. The majority-rule consensus tree, with posterior probabilities of all groupings of areas, was obtained from the concatenated post-burnin samples of all 4 runs.

Both parsimony and Bayesian methods essentially produce unrooted trees; we arbitrarily rooted the trees based on the rooting identified in the UPGMA analyses, for ease of topological comparison.

3.3.5 Phyla diversity

The number of genera (including singletons) within each major taxonomic group considered (mostly phyla) at each site were summed and proportions calculated; this information was then presented as a stacked histogram chart. Changes in certain groups were then examined further using biplots and regression analysis (conducted in PAST Version 3.10; Hammer et al., 2001). Note that we have separated trilobites from non-trilobite arthropods for this analysis, in order to examine suspected changes in relative abundances within the Arthropoda over the period in question.

3.4 Results

3.4.1 Statistical modelling

The Mantel tests show highly significant, positive correlations between assemblage and geographic distance (e.g. using the 510 Ma reconstruction of Torsvik and Cocks, 2013, the Ochiai coefficient, and including singleton taxa, Mantel $r = 0.39$, $p = 0.003$), and assemblage and age distance (Mantel $r = 0.37$, $p = 0.008$). Geographic and age distance were also positively correlated but to a lesser extent (Mantel $r = 0.32$, $p = 0.026$). Logging geographic distance values resulted in a marked increase in correlation with assemblage distance (Mantel $r = 0.58$, $p = 0.001$). Results utilising either the Ochiai or Jaccard coefficients, including or excluding singleton taxa, or

substituting coordinates from the different continental reconstructions, were comparable (Supp. Tab. 6.2).

The MRM models that best explained the observed variation between assemblages contained both age and geographic distance as explanatory variables. The best models produced R^2 values of around 0.40; however, the simplest to do so was [ass.dist ~ log(geo.dist + 1) + age.dist], i.e. assemblage differences were best explained as a function of the natural logarithm of geographic distance plus age distance. In contrast, models containing only one of the two explanatory variables produced much lower R^2 values, although taking the natural logarithm of geographic distance nearly doubled explanatory power over untransformed data. Based on examination of the data this suggests that geographic separation reduces assemblage similarity at a decreasing rate. As with the Mantel tests, model results utilising either the Ochiai or Jaccard coefficients, including or excluding singleton taxa, or substituting coordinates from the different continental reconstructions, were comparable (see Supp. Tab. 6.3 and the R script files provided in the electronic Supplementary Material).

3.4.2 Ordinations and cluster analysis

The NMDS ordinations and UPGMA cluster analyses were conducted on the presence/absence matrix using the Ochiai and Jaccard coefficients as distance measures, both with and without singleton taxa included. Stress levels are relatively high, but acceptable (0.11–0.13). The ordinations all show similar patterns (Fig. 3.2). The Series 3 “northern” Laurentian sites (Wheeler, Marjum, Spence and Burgess

Shale) and Kaili (South China) tend to group together; this is particularly evident in the Ochiai distance plot that includes singletons (Fig. 3.2A) where these sites form a tight cluster. The Series 2 South Chinese sites (Chengjiang, Guanshan and Balang)

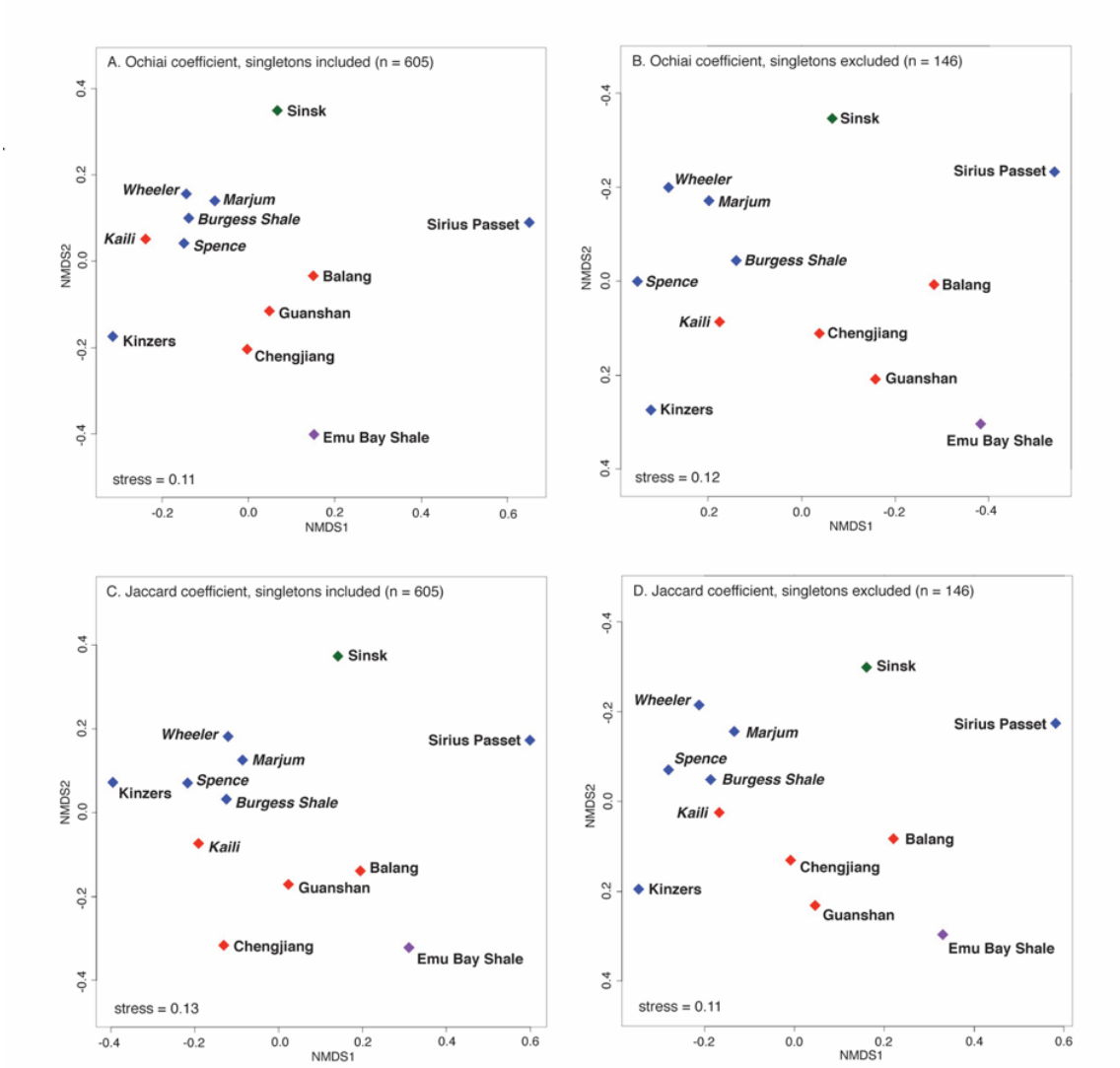

Figure 3.2: Non-metric multidimensional scaling (NMDS) ordination plots of major BST biotas based on presence/absence of genera. A, using the Ochiai coefficient with singletons included. B, Ochiai coefficient, singletons excluded. C, Jaccard coefficient, singletons included. D.Jaccard coefficient, singletons excluded. Sites in *italics* = Series 3. Point colours; red = South China, blue = Laurentia, purple = East Gondwana, green = Siberia. Note that polarity of axes is arbitrary and all plots are orientated to match 3.2A for ease of comparison.

tend to form a looser association adjacent to the cluster mentioned above. While Kaili seems to group more consistently with the Laurentian sites, in particular with the Burgess and Spence Shales, it is usually more closely associated with the South

Chinese sites than other members of the cluster. The late Series 2 Kinzers Shale seems to be more distantly related to both clusters, although in the Jaccard plot including singletons (Fig. 3.2C) it is more closely related to the Laurentian sites. The other three sites (Sirius Passet, Sinsk and Emu Bay Shale – all Series 2) are positioned more distantly to both the clusters mentioned above, and to each other. Sinsk appears to be more closely related to the northern Laurentian sites, and Emu Bay more closely to the South Chinese sites. Sirius Passet appears to be the most unique locality with no close associations. From a temporal perspective, the Series 3 sites (Burgess Shale, Kaili, Wheeler, Marjum and Spence) tend to be closely associated. The Series 2 sites by comparison are rather more scattered.

In general, the results of the UPGMA cluster analyses (Fig. 3.3) are consistent with the NMDS ordinations. The dendrograms based on analyses including singleton taxa group all Series 3 sites into a single cluster, with the stratigraphically continuous Marjum and Wheeler formations showing close affinity; however, the older Spence Shale groups with the more contemporaneous Burgess Shale. Kaili sits outside this western Laurentian group, with Kinzers the most basal. In the Ochiai plot (Fig. 3.3A) the Series 2 Gondwanan sites form a sister group to the Series 3 cluster. Within this, Guanshan and Balang are most closely related, with the Emu Bay Shale outside of this, and Chengjiang further outside again. Sinsk sits outside both of these larger groups with Sirius Passet the most basal. The Jaccard plot (Fig. 3.3C) shows the same arrangement except for Chengjiang, which swaps to sit outside the Series 3 cluster. The dendrograms based on analyses that exclude singleton taxa show a somewhat different arrangement, with the western Laurentian sites forming a sister group to a cluster containing the three most diverse sites from South China;

Chengjiang, Kaili and Guanshan. Kinzers sits outside this larger group. In the Ochiai dendrogram (Fig. 3.3B), Sinsk sits outside this again, with the Emu Bay Shale, Balang and Sirius Passet forming a separate group. The Jaccard dendrogram (Fig. 3.3D) is slightly different with Sinsk switching to form a group with the Balang and the Emu Bay Shale, and Sirius Passet sitting outside the two larger groups. The cophenetic correlations of the dendrograms vary somewhat, and are higher for those that include endemic taxa (suggesting greater tree-like structure), which could explain some of the variation in topology observed.

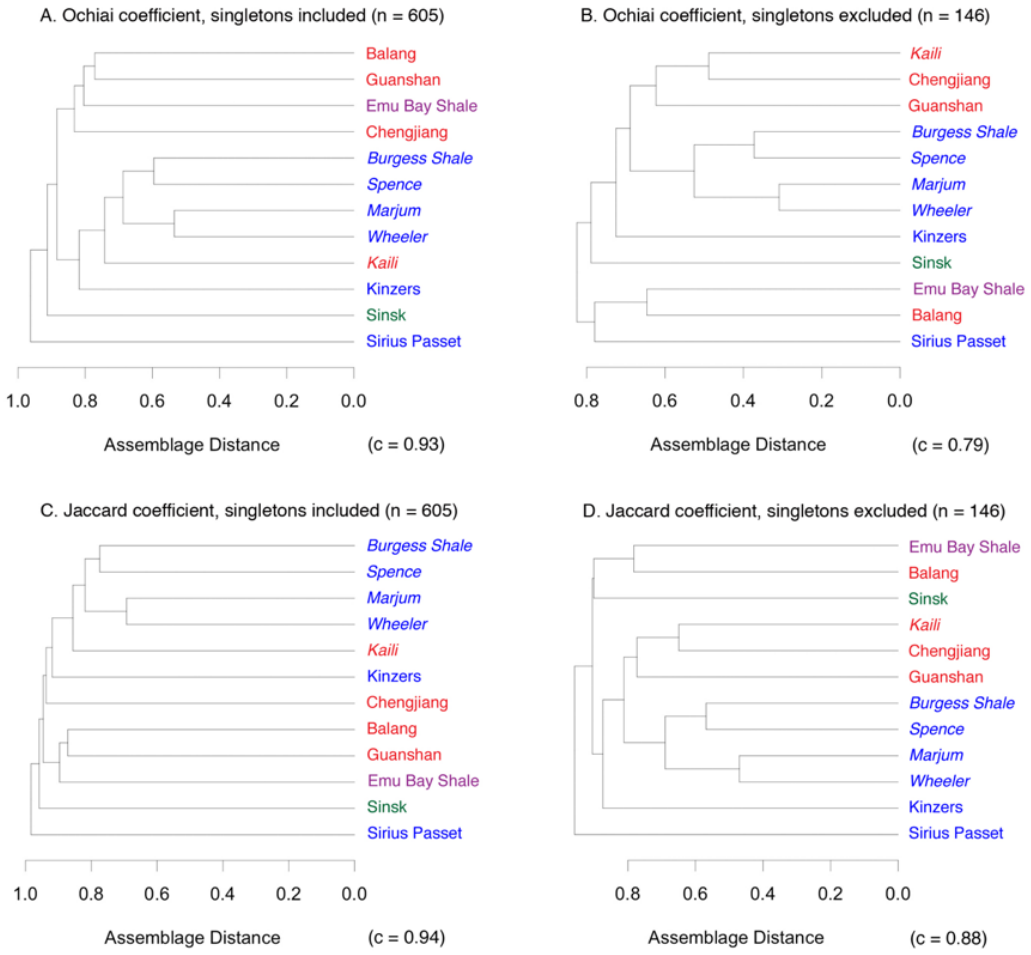

Figure 3.3: UPGMA cluster analysis dendrograms depicting assemblage distance between major BST biotas based on presence/absence of genera. A, using the Ochiai coefficient with singletons included. B, Ochiai coefficient, singletons excluded. C, Jaccard coefficient, singletons included. D.Jaccard coefficient, singletons excluded. Sites in *italics* = Series 3. Text colours; red = South China, blue = Laurentia, purple = East Gondwana, green = Siberia (c = cophenetic correlation).

3.4.3 PAE and Bayesian analysis

PAE produced a single best tree (752 steps; Fig. 3.4A) with topology very similar to the dendrograms produced by cluster analysis with singleton taxa included. The parsimony tree is strictly an unrooted network; however, for ease of comparison with the cluster analysis, we show it rooted at the same point (Sirius Passet vs all other sites; this also applies to the Bayesian inference results, discussed below). In this instance we have presented the results as a phylogram, meaning that branch length reflects the number of steps; therefore, terminal branch length reflects the number of singleton taxa within each of the assemblages considered. In this tree, all Series 3 sites group together, with Kinzers and Sinsk sitting immediately outside this grouping; the Series 2 Gondwanan sites form a sister group to this larger clade. The relationships within the larger groups do, however, differ from the dendrograms. Kaili is more deeply nested within the (otherwise Laurentian) Series 3 clade, as is Chengjiang within the Series 2 Gondwanan cluster. It should be noted that bootstrap values are relatively low in this instance and suggest that the majority of groupings are not well supported.

The topology of the majority-rule consensus tree produced by Bayesian inference was very similar to that produced by PAE, the only difference being that Kaili and Spence switched places within the Series 3 clade (Fig. 3.4B). Branch lengths in this instance reflect percentage divergence. In contrast to the bootstrap values of the PAE phylogram, groupings are generally well supported by posterior probabilities. The exception to this is the Sinsk Biota, which under both the PAE and

Bayesian analysis is tenuously placed at the base of the clade that contains the Series 3 sites and Kinzers.

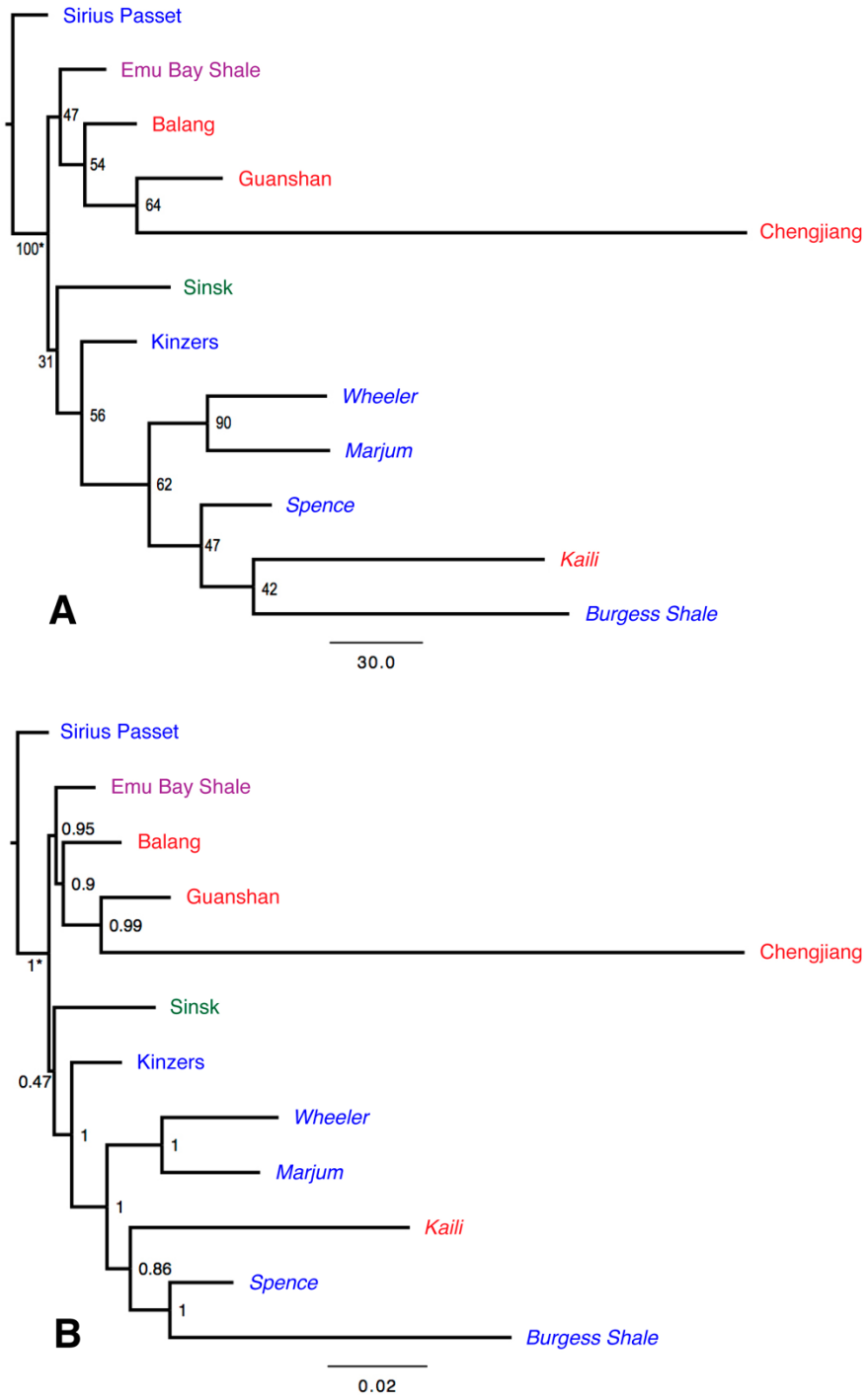

Figure 3.4: A. PAE phylogram (single shortest tree of 752 steps). Branch lengths reflect number of steps (scale bar = 30 steps), with terminal branch lengths reflecting number of singleton taxa within each assemblage; numbers refer to bootstrap values. B. Bayesian majority-rule consensus tree. Branch lengths are proportional to percentage divergence (scale bar = 2%); numbers refer to posterior probabilities. Sites in *italics* = Series 3. Text colours; red = South China, blue = Laurentia, purple = East Gondwana, green = Siberia.

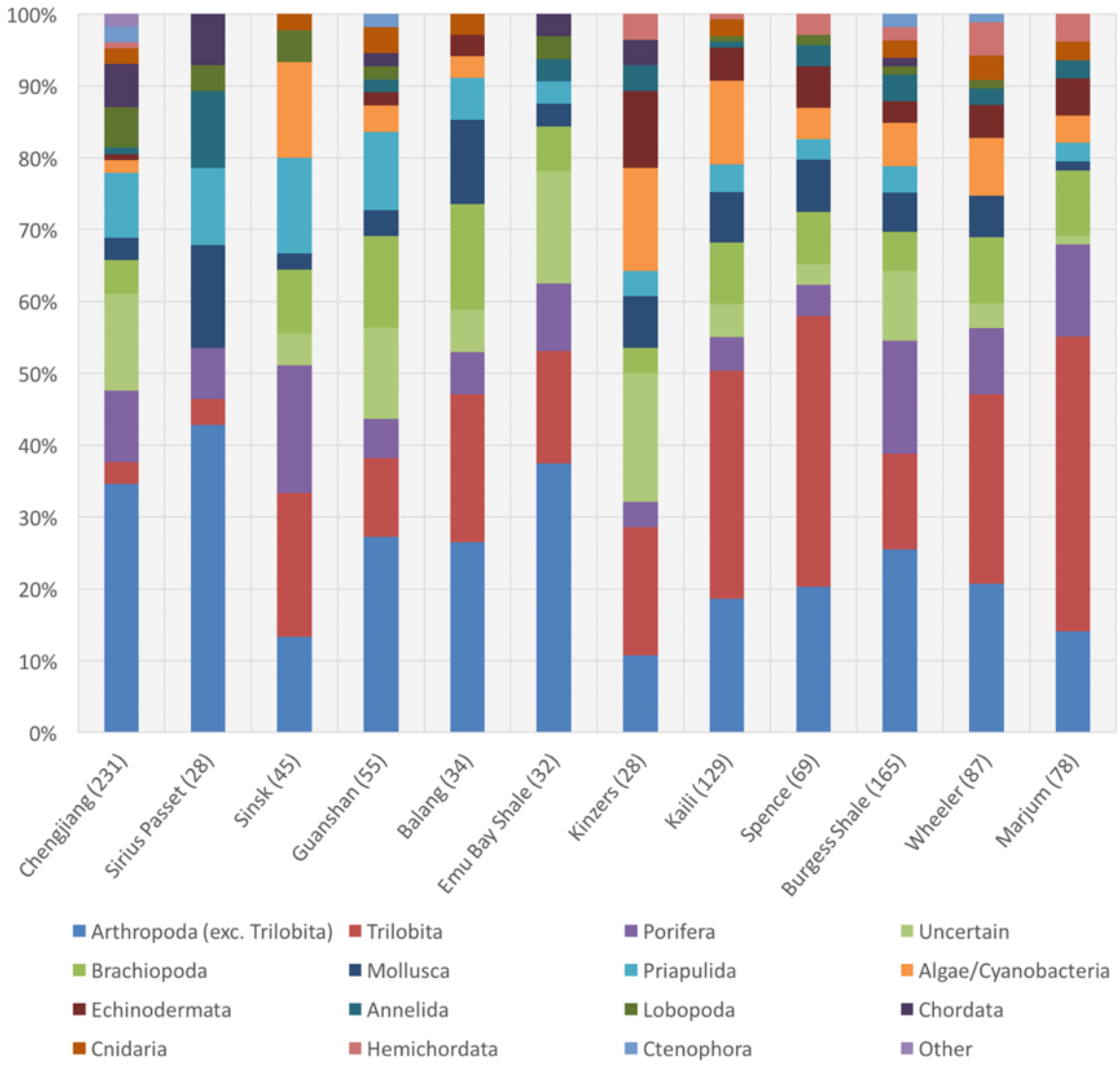

Figure 3.5: Composition of the 12 Cambrian Lagerstätten assemblages considered in this study in order of age, based on number of genera per phylum (or other high-level taxonomic group in the case of trilobites, algae/cyanobacteria, and *incertae sedis* taxa). Older sites generally exhibit low trilobite:non-trilobite arthropod ratios, low echinoderm and algal/cyanobacterial diversity, presence of "chordates" (including vetulicolians), and high proportions of *incertae sedis* taxa, with younger sites showing the reverse. Total number of genera at each locality is shown in parentheses.

3.4.4 Phyla diversity

Examination of the composition of assemblages through time reveals a number of patterns (Fig. 3.5). In general, older sites are characterised by low ratios of trilobite to

non-trilobite arthropods, low echinoderm and algal/cyanobacterial diversity, the presence of “chordates” (including vetulicolians after García-Bellido et al., 2014), and higher proportions of *incertae sedis* taxa. Conversely, the younger sites are generally characterised by high ratios of trilobite to non-trilobite arthropods, higher echinoderm and algal/cyanobacterial diversity, and a general lack of chordate and *incertae sedis* taxa. There are some exceptions to this, e.g. the Burgess Shale exhibits a lower relative proportion of trilobites, with the Sinsk Biota having an unusually high level of algal/cyanobacterial diversity.

3.5 Discussion

3.5.1 General palaeobiogeographic patterns

Our analyses indicate that both time and space have an important effect on the makeup of Cambrian Lagerstätten assemblages. Although it is difficult to accurately quantify the contribution of each variable due to their interdependence, the fact that the Mantel tests produced highly significant, positive correlations between assemblage and both geographic and age distance suggests that both variables are having an effect on assemblage composition (Supp. Tab. 6.2). Our best bivariate MRM models confirmed this by exhibiting much greater explanatory power than any single variable model (see Supp. Tab. 6.3 and the R script files provided in the electronic Supplementary Material).

The Series 3 Laurentian sites consistently group together in the dendrograms and cladograms produced by cluster (Fig. 3.3), parsimony (Fig. 3.4A) and Bayesian analysis (Fig. 3.4B), although their relationships to other Lagerstätten change substantially between analyses that include (Figs 3.3A, C) and exclude singleton taxa (Figs 3.3B, D). In the dendrograms that exclude singletons the most diverse sites form a single, larger clade. It is possible that this arrangement is at least partially influenced by the disparity in diversity between localities, and the tendency for lower diversity sites to sit further down the trees simply due to the lower probability of sharing taxa between sites with lower sampled taxonomic richness (and vice versa). This potential bias is reduced when singletons are included, as these taxa increase the uniqueness of well-sampled sites and offset any extra overlap with other localities caused by increased sampling alone. This is one potential reason why it may be beneficial to retain singleton taxa in an analysis, particularly when sample sizes vary greatly; at any rate, analyses including and excluding them might be advisable. This is perhaps the reason behind previous assertions of greater similarity between the Lagerstätten of Laurentia and South China (e.g. Han et al., 2008), i.e. these exhibit the highest sampled diversity and are therefore more likely to share taxa. These sites do tend to group together as a broader cluster within our various analyses, but only compared with the small number of other, much more singular sites, making it difficult to draw conclusions as to how closely related these two groups really are.

Interestingly, the results of the PAE (Fig. 3.4A), that implicitly excludes singleton taxa (as not parsimoniously informative), agrees much more closely with the dendrograms that include singletons (Figs 3.3A, B), as does the Bayesian

cladogram (Fig. 3.4B). Bayesian methods are of particular interest in this instance as they have characteristics that make them inherently suitable for comparing assemblages. Usually in presence/absence studies, co-occurrences of taxa are equally weighted. This is not necessarily the best approach given that taxa could be expected to show a range of biogeographic signal given variations in dispersal ability. It is therefore desirable that co-occurrence of cosmopolitan taxa should receive a lower weighting than taxa displaying more regional affiliations. Bayesian inference accommodates this by down-weighting 'characters' (in this case 'taxa') that display higher levels of 'area homoplasy', in a manner analogous to the treatments of homoplasious characters in a phylogenetic analysis.

Despite the variations in topology between singleton and non-singleton analyses, the relative positions of the sites between the various NMDS ordination plots do not change that much. This exposes a potential shortcoming of the dendrogram-based methods in that the algorithms impose a hierarchical pattern (groups within groups) on the dataset even if there is no such arrangement. In this case, therefore, relationships are probably best explained by the ordination plots, rather than the dendrograms. In terms of singleton taxa, we suggest that the best approach, at least in the case of our dataset, is to include endemic taxa but employ an appropriate similarity or distance measure (in this case we prefer the Ochiai coefficient); however, in reality it is possible that the true relationships will lie somewhere between the results produced by these two extremes.

In the NMDS ordination plots (Fig. 3.2), the Series 3 sites tend to group closely, particularly using our preferred combination of the Ochiai coefficient and including singleton taxa, whereas the Series 2 sites are much more disparate. This

could potentially be due to environmental differences, although it seems unlikely that the greater variation observed between these older sites can be completely explained by this (see discussion below). It is also illustrative that the Series 2 localities in South China tend to show greater dissimilarity amongst themselves than do the Series 3 sites of Laurentia, despite a smaller age range. This disparity between Series 2 assemblages (and particularly the oldest sites), in contrast with those from Series 3, suggests an increasing importance of age as a determinant of assemblage homogeneity through the period in question, and a decrease in provinciality (at least from a broad assemblage sense). This increase in similarity between Cambrian Lagerstätten assemblages through time has been noted before and has been linked to the advent and dispersal of pelagic larvae (Han et al., 2008; Zhao et al., 2005; 2011).

Unfortunately, the concentration of Series 2 sites in Gondwana and Series 3 sites in Laurentia makes it difficult to interpret the observed differences in assemblage compositions, however, there are exceptions from which some conclusions may be drawn.

3.5.2 Individual comparisons

The Kaili Formation contains the only Series 3 biota from South China in our database; all other Chinese sites are of Series 2 age. If we assume that both space and time have (similar) significant effects on composition, then we could predict that such a site should be positioned somewhere between the Series 3 sites (the rest of which are all Laurentian) and the Series 2 South Chinese sites in terms of

assemblage relationships. In fact, in the ordinations Kaili tends to group more closely with the Laurentian sites, and particularly it's closest contemporaries, the Burgess and Spence Shales. This is reflected in a greater number of shared taxa between Kaili and the Burgess Shale (42), than between Kaili and the Series 2 Chengjiang biota (34), while the Burgess Shale and Chengjiang share 33 genera. The fact that Kaili shares fewer genera with the older, but much closer Chengjiang biota, than it does with the Burgess Shale, a locality on a different palaeocontinent but of similar age, suggests that age rather than geographic distance is having a stronger effect on assemblage composition, as suggested by Zhao et al. (2011). As might be expected, however, Kaili tends to be the Series 3 site most closely associated with the Series 2 Chinese localities in the ordination plots. This is also reflected in the tree topologies in that Kaili groups with the other Series 3 sites in the cladograms, as well as the dendrograms including singletons, but with the more diverse Chinese sites in the dendrograms excluding singletons; although as discussed above this could be a result of overemphasising the similarities between assemblages.

Similarities between the Chengjiang (68 shared taxa/133 endemic taxa) and Burgess Shale assemblages (89/76) have been noted before (see Han et al., 2008), although it seems that a large number of their 33 shared genera are those with relatively cosmopolitan distributions as listed previously, e.g. *Selkirkia*, *Anomalocaris*, *Canadaspis*, *Isoxys*, *Leanchoilia*, *Liangshanella*, *Naraoia*, *Tuzoia*, *Lingulella*, *Yuknessia*, *Hallucigenia*, *Wiwaxia*, *Choia*, *Hazelia*, *Leptomitus*, *Protospongia*, *Dinomischus* and *Eldonia*. Presumably these were good dispersers, although it should be noted that the Lagerstätten considered here are spread through c. 16 million years, implying that these taxa are not only widespread, but

also long-lived in geologic time. In addition, the term ‘cosmopolitan’ is of some limited value in this instance given that the majority of Lagerstätten occur in Laurentia and South China, although many of these taxa also occur at one or more of the singular sites in Sinsk, Sirius Passet and the Emu Bay Shale.

Similarities in biomineralised taxa that are more dependent on age (i.e. have higher turnover) rather than soft-bodied elements of BST biotas that tend to persist through time, appear to be the major cause of Kaili tending to group with Laurentian sites of similar age. Firstly, these sites share a number of trilobite genera, namely *Burlingia*, *Kootenia*, *Olenoides*, *Oryctocephalus* and *Pagetia*. Kaili also shares all of these, as well as *Peronopsis* (although this is considered something of a ‘bucket’ taxon), with one or more of the Utah Lagerstätten. In contrast, Chengjiang shares no trilobites with Kaili or any of the sites in Utah simply due to the fact that trilobite genera do not persist across the time gaps seen between the Series 2 and 3 deposits. Kaili also shares the brachiopods *Lingulella*, *Linnarssonia*, *Micromitra*, *Nisusia* and *Paterina* with the Burgess Shale, as well as the majority of these plus *Acrothele* and *Dictyonina* with the Utah sites, whereas with Chengjiang it shares only *Kutorgina* and *Lingulella*. Other notable similarities include the cyanobacteria *Morania* and *Marpolia*, molluscs such as *Latouchella* and *Scenella*, and soft-bodied arthropods *Perspicaris*, *Mollisonia* and *Skania*.

The relationships between the Spence (c. 506 Ma), Wheeler (c. 504 Ma) and Marjum (c. 502 Ma) Shales of Utah, and the Burgess Shale (c. 505 Ma), are of particular interest, as they provide a ‘time series’ of well-sampled assemblages, present on the same palaeocontinent. It is clear that in this instance time is having the major effect on assemblage composition. The Spence Shale, the oldest of this

group of subsites, shares a higher number of genera with the Burgess Shale, than it does with the slightly younger Wheeler Shale, and less again with the (even younger) Marjum Formation. In fact, if we plot the number of shared genera against age difference for each site pairing within this group, there is a strong correlation in general between these variables, with sites closer in age clearly showing higher numbers of shared taxa (Fig. 3.6). The geographic distance between the Utah sites and the Burgess Shale (~1,500 km) seems to have little effect on this, with site pairings with similar age differences showing comparable amounts of assemblage distance, regardless of whether the Burgess Shale is under consideration. Moreover, the Spence Shale tends to group with the almost contemporaneous Burgess Shale in our various analyses, rather than with it's closest neighbors.

The Sirius Passet assemblage, despite its uniqueness (3/25), also gives us potential clues as to how the relationships between sites have changed through time. Sirius Passet shares only the annelid *Hyolithellus* (with the Wheeler and Marjum Formations), and the cosmopolitan *Isoxys* and *Choia* with a number of other sites, despite being thought to have occupied a setting very similar to that of the Burgess Shale, in relatively deep water immediately adjacent an escarpment representing the outer edge of the carbonate platform (Ineson & Peel, 2011; Peel & Ineson, 2011). It has recently been shown that microbial mats and silica 'death masks' may have played a role in the unique preservation observed at Sirius Passet (Strang et al., 2016). The assemblage (despite anomalous preservation style) also seems to house a relatively representative BST biota, suggesting that perhaps some other reason is responsible for the uniqueness of Sirius Passet. It is illustrative that this site is vastly different from other Series 2 sites of possibly very similar age (e.g. Chengjiang),

when Series 3 sites present on different palaeocontinents (e.g. Kaili and the Burgess and Spence Shales) are much more similar to one another, i.e. one might expect that Sirius Passet exhibit similarities to other Series 2 sites. Given that this is not the case, it is possible that at this time BST biotas were not yet stable and widespread (as per Zhao et al., 2005), but rather more peculiar and individual, perhaps due to more limited dispersal ability of constituent taxa.

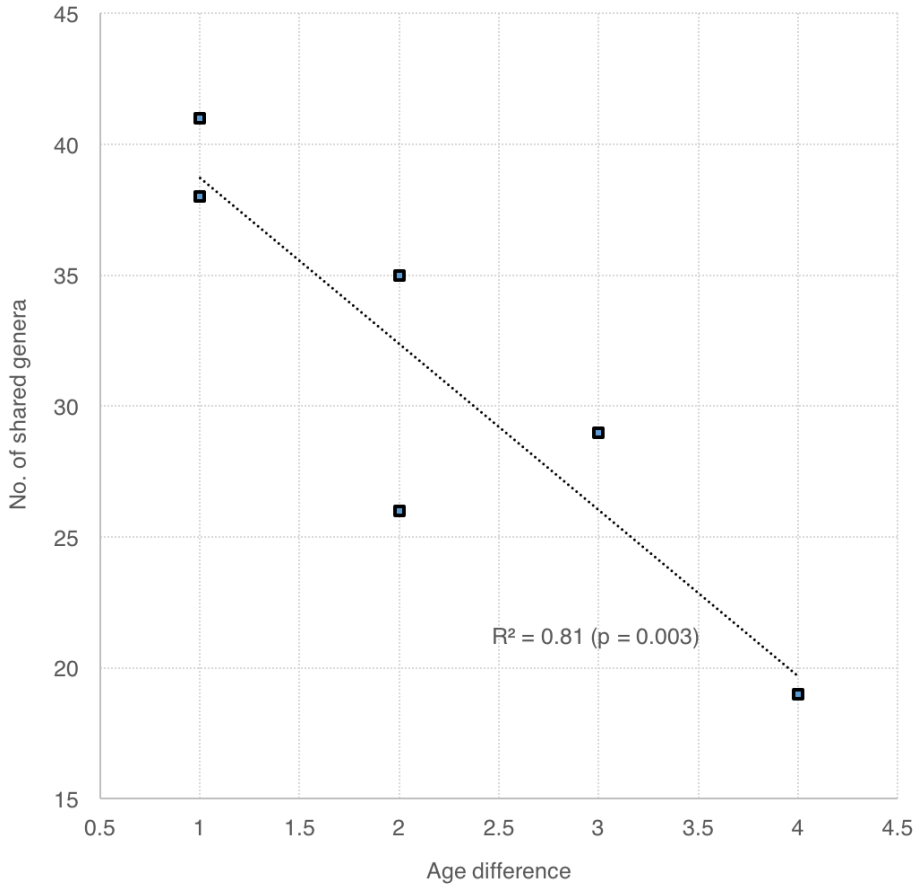

Figure 3.6: Biplot and linear regression of age difference vs shared genera between Laurentian Lagerstätten. There is a clear decrease in the number of shared genera with increasing age difference between these sites.

Despite the fact that the Emu Bay Shale assemblage (10/22) appears to be quite singular based on the ordination plots, it is consistently positioned closer to the

South Chinese Lagerstätten than to other sites, and groups with these in the cluster, parsimony and Bayesian analyses. This is reflected by a clear link between the EBS biota (East Gondwana) and the Series 2 South Chinese sites in terms of shared taxa. The EBS shares the trilobite *Redlichia* with the contemporaneous Balang and Guanshan Lagerstätten, and the arthropods *Kangacaris*, *Squamacula* and *Tanglangia* with Chengjiang, as well as the problematic *Vetustovermis* (although it is uncertain as to whether these represent the same taxon). A brachiopod assigned to *Diandongia* (Paterson et al., 2016) is shared with Chengjiang and Guanshan. The palaeoscolecid *Wronascolex* is shared with all three, as well as the Sinsk biota (it should be noted that there are also uncertain assignations of specimens to this genus from the Spence and Marjum Formations of Utah). In contrast, the EBS shares only the cosmopolitan *Anomalocaris*, *Isoxys* and *Tuzoia* with Laurentian localities (as well as with all of the South Chinese sites), suggesting sufficient separation of East Gondwana and Laurentia by this time to limit dispersal across the Iapetus Ocean. The uniqueness of the Emu Bay Shale is likely due to its relative isolation, and the similarities between this site and the BST biotas of South China also suggest a geographic relationship, however, it is not possible to discount similarity in age as a major factor. The unique inner-shelf depositional setting (Gehling et al., 2011), as well as preservation style (Gaines, 2014), of the Emu Bay Shale could also potentially explain why this assemblage is rather singular, although, as with Sirius Passet, the assemblage does seem to be relatively typical of BST biotas.

The Sinsk biota (13/32) is also similar to Sirius Passet and the Emu Bay Shale in that it appears to be quite distinct from sites of similar age. The biota

appears to show a mix of affinities, with certain taxa linked to Laurentia (e.g. *Cambrorhytium*, *Diagoniella*, *Laenigma*) and others more closely aligned with Gondwana (e.g. *Wronascolex*), although the majority of shared genera have representatives on both palaeocontinents, e.g. *Marpolia*, *Linnarssonia*, *Archiasterella*, as well as many of the cosmopolitan taxa mentioned above. On balance, Sinsk appears to be more closely related to the Laurentian Series 3 sites, which is possibly a geographic signal given that palaeogeographic reconstructions tend to place Siberia between Gondwana and Laurentia at this time, although more closely associated with the latter. The distinctiveness of the Sinsk biota could also be partly due to environmental differences between sites. The Lagerstätte occurs largely within a relatively thin (c. 0.5m) section of calcareous shale, within the clastic limestones of the Sinsk Formation (Ivantsov et al., 2005). Despite this slightly unusual depositional setting, other factors are consistent with typical BST deposits (i.e. fine sediment, rapidly deposited in an outer-shelf setting at or below storm wave base; Gaines, 2014).

The Kinzers Shale of southeastern Pennsylvania (USA) spans the Cambrian Series 2/Series 3 boundary. The basal Emigsville Member is of uppermost Series 2 age and contains a relatively low diversity (15/13) Lagerstätte, that in terms of age, links the Series 2 and Series 3 localities. In the NMDS ordinations (Fig. 3.2), Kinzers tends to group partway between the Series 3 cluster and the (more scattered) Gondwanan Series 2 sites, although slightly offset (possibly due to limited diversity or “sample size”). The cluster analyses corroborate this (Fig. 3.3), with Kinzers grouping as either the most basal of the otherwise Series 3 cluster (including endemics), or as an outgroup to the western Laurentian and high diversity South

Chinese sister groups (excluding endemics). Despite this, it seems clear that in terms of shared genera, Kinzers is more closely aligned with Laurentian/Series 3 sites, sharing *Dalyia*, *Metaspriggina* and *Tubulella* exclusively with the Burgess Shale, *Paterina* with the Burgess Shale and Kaili, *Pelagiella* with the Wheeler Shale, as well as *Morania* and *Yuknessia* with all of the Series 3 Lagerstätten. All other shared taxa are largely cosmopolitan, e.g. *Selkirkia*, *Anomalocaris*, *Tuzoia*, *Haplophrentis*, *Hazelia*, *Kootenia* and *Allonnia*. Assemblage relationships therefore seem to be a result of both geographic proximity to the other Laurentian sites, as well as similarities in age (e.g. with Kaili).

3.5.3 Phyla diversity

The analysis of generic diversity based on the number of genera per phylum (or other higher-level taxonomic group in the case of trilobites, algae/cyanobacteria, and *incertae sedis* taxa) shows a number of patterns. There is a large and statistically significant increase in the proportion of trilobites, whilst non-trilobite arthropods decrease (although less dramatically) through time. The total proportion of arthropods seems to increase slightly across the same period, although this change is not significant (Fig. 3.7). This trend is possibly a signal of the general success of trilobites due to the advantages of having evolved a mineralised exoskeleton for protection, at the expense of other arthropods with similar ecological characteristics. This increase reflects the trilobite fossil record in general, which shows a dramatic increase following their appearance in the early Cambrian through to the end of the period (Fortey & Owens, 1997). An exception to this trend in our dataset is the Sinsk

Biota, a possible cause for which was noted by Ivantsov et al. (2005) in that this Lagerstätte occurs predominantly in carbonate facies. This may have represented a more hospitable environment for trilobites (as predominantly benthic inhabitants) compared to the anoxic/dysoxic conditions inferred for many Lagerstätten. This suggests an increase in tolerance to low oxygen conditions as an alternative explanation for increasing trilobite proportions in BST biotas through time. The Burgess Shale is also something of an exception and tends to group with the older sites, in particular Chengjiang, Guanshan and the Emu Bay Shale, mainly based on a relatively low trilobite:non-trilobite arthropod ratio, and low relative arthropod diversity in general compared to other localities. This may simply be an artifact of the higher number of taxa known from this locality, essentially "diluting" the proportion of trilobites, although we also note that this may be a result of data bias due to relatively poor constraints on the sections that exhibit exceptional preservation within the other Series 3 formations.

There is an increase in the proportion of echinoderms across the period in question, which again mirrors the pattern suggested by the fossil record in general, which shows increasing diversity from an appearance in Stage 3 through Stage 5 (Zamora et al 2013). There is also decline in the proportion of chordates (driven largely by the pattern in vetulicolians), priapulids, and *incertae sedis* taxa, and an increase in the number of echinoderms through time, suggesting that this was a critical period where the rapid evolution of communities was occurring, and that the variable success of major lineages of animals was playing a significant role.

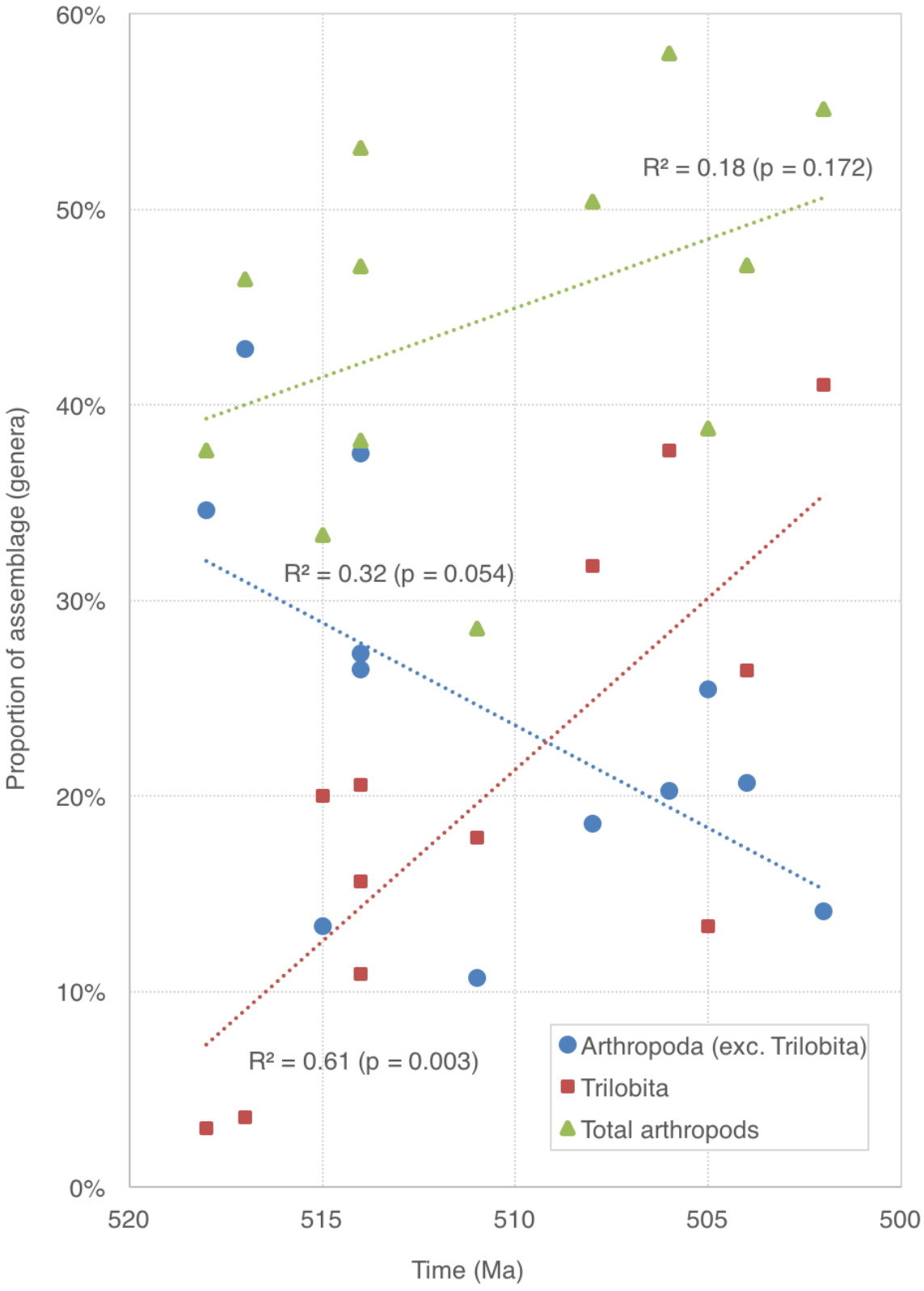

Figure 3.7: Relative proportions and linear regression trendlines for trilobites, non-trilobite arthropods, and total arthropods through time for the assemblages under consideration. There is a large increase in the proportion of trilobites and a smaller decrease in non-trilobite arthropods across the period.

A point of note is that on this index, the Burgess Shale tends to group with the older sites, in particular Chengjiang, Guanshan and the Emu Bay Shale, mainly based on a relatively low trilobite:non-trilobite arthropod ratio, and low relative arthropod diversity in general compared to other localities. This may simply be an artefact of the higher number of taxa known from this locality, essentially "diluting" the proportion of trilobites, although we also note that this may be a result of data bias due to relatively poor constraints on the sections that exhibit exceptional preservation within the other Series 3 formations.

3.6 Conclusions

Both space and time have important effects on the taxonomic composition of Cambrian Lagerstätten assemblages. Early Cambrian (Series 2) Lagerstätten from different geographic regions are highly distinct, but later (Series 3) localities appear to be more globally homogenous. This pattern seems to be driven largely by a general increase in the number of biomineralised taxa such as trilobites and brachiopods shared between sites, occurring against a backdrop of "cosmopolitan" taxa that are pervasive both in space and time. This pattern might be related to a general increase in dispersal ability, possibly linked to an increased development of pelagic larvae in certain groups. There is also evidence of higher-level taxonomic turnover through time, with certain groups (e.g. trilobites, echinoderms) becoming more prevalent, while others disappear (e.g. vetulicolians). The reduction in *incertae sedis* taxa through time is also illustrative, suggesting that more "recognisable" taxa

were emerging during this time, and that this was indeed an important period in the evolution of modern lineages and communities. The proposed link between the Cambrian Lagerstätten assemblages of Laurentia and South China (e.g. Chengjiang and Burgess Shale) is not particularly evident, partly because these relationships have been proposed mainly on the basis of large numbers of shared cosmopolitan taxa, and also due to a lack of context, i.e. there is a very limited number of other sites with which to make meaningful comparisons. The discovery of new deposits and further investigation of the lesser-known localities would help to resolve this. It should also be noted that the exclusion of endemic (singleton) taxa may not always be the best approach in biogeographic studies, particularly from a palaeontological perspective where sample sizes may vary greatly. Adopting metrics that better accommodate endemic taxa might be a more productive approach.

3.7 Acknowledgements

Funding for this project was provided by a Master of Philosophy scholarship to J. D. Holmes from the University of Adelaide, as well as Australian Research Council grants to D. C. García-Bellido (ARC FT130101329) and M. S. Y. Lee.

3.8 References

Alvaro, J. J., Ahlberg, P., Babcock, L. E., Bordonaro, O. L., Choi, D. K., Cooper, R. A., . . . Zylinska, A. (2013). Global Cambrian trilobite palaeobiogeography assessed using parsimony analysis of endemicity. In D. A. T. Harper & T. Servais (Eds.), Early Palaeozoic Biogeography and Palaeogeography. *Geological Society, London, Memoirs, 38*, 273-296.

Archer, A. W., & Maples, C. G. (1987). Monte Carlo Simulation of Selected Binomial Similarity Coefficients (I): Effect of Number of Variables. *Palaios, 2*, 609-617.

Astashkin, V. A., Varlamov, A. I., Esakova, N. V., Zhuravlev, A. Yu., Repina, L. N., Rozanov, A. Yu., . . . Shabanov, Yu. Ya. (1990). *Guidebook for excursion on the Aldan and Lena rivers. Siberian Platform. 3d Internat. Sym. Cambrian System*. Novosibirsk: IGIG.

Babcock, L. E., & Peel, J. S. (2007). Palaeobiology, taphonomy and stratigraphic significance of the trilobite *Buenellus* from the Sirius Passet Biota, Cambrian of North Greenland. *Memoirs of the Association of Australasian Palaeontologists, 34*, 401-418.

Babcock, L. E., Zhang, W. T., & Leslie, S. A. (2001). The Chengjiang Biota: Record of the Early Cambrian Diversification of Life and Clues to Exceptional Preservation of Fossils. *GSA Today, 5*, 4-9.

Brett, C. E., Allison, P. A., DeSantis, M. K., Liddell, W. D., & Kramer, A. (2009). Sequence stratigraphy, cyclic facies, and *lagerstätten* in the Middle Cambrian Wheeler and Marjum Formations, Great Basin, Utah. *Palaeogeography, Palaeoclimatology, Palaeoecology, 277*, 9-33.

Briggs, D. E. G., Erwin, D. H., & Collier, F. J. (1994). *The fossils of the Burgess Shale*. Washington: Smithsonian Institution Press.

Budd, G. E. (2011). *Campanamuta mantonae* gen. et. sp. nov., an exceptionally preserved arthropod from the Sirius Passet Fauna (Buen Formation, lower Cambrian, North Greenland). *Journal of Systematic Palaeontology, 9*, 217-260.

Caron, J.-B., & Jackson, D. A. (2008). Paleoecology of the Greater Phyllopod Bed community, Burgess Shale. *Palaeogeography, Palaeoclimatology, Palaeoecology, 258*, 222-256.

Collom, C. J., Johnston, P. A., & Powell, W. G. (2009). Reinterpretation of 'Middle' Cambrian stratigraphy of the rifted western Laurentian margin: Burgess Shale Formation and contiguous units (Sauk II megasequence), Rocky Mountains, Canada. *Palaeogeography, Palaeoclimatology, Palaeoecology, 277*, 63-85.

Conway Morris, S. (1985). Cambrian Lagerstätten: their distribution and significance. *Philosophical Transactions of the Royal Society B: Biological Sciences, 311*, 49-65.

Conway Morris, S. (1986). The community structure of the Middle Cambrian Phyllopod Bed (Burgess Shale). *Palaeontology, 29*, 423-467.

Conway Morris, S. (1989). Burgess Shale Faunas and the Cambrian Explosion. *Science, 246*, 339-346.

Conway Morris, S. (1998). *The Crucible of Creation: The Burgess Shale and the Rise of Animals*. New York: Oxford University Press.

Dornbos, S. Q., & Chen, J.-Y. (2008). Community palaeoecology of the early Cambrian Maotianshan Shale biota: Ecological dominance of priapulid worms. *Palaeogeography, Palaeoclimatology, Palaeoecology, 258*, 200-212.

Fletcher, T. P., & Collins, D. H. (1998). The Middle Cambrian Burgess Shale and its relationship to the Stephen Formation in the southern Canadian Rocky Mountains. *Canadian Journal of Earth Sciences, 35*, 413-436.

Fortey, R.A., & Owens, R.M. (1997). Evolutionary History, In R. L. Kaesler (Ed.), Treatise on Invertebrate Paleontology, Part O, Revised. Arthropoda 1, Trilobita 1, (Introduction, Order Agnostida, Order Redlichiida). Geological Society of America and University of Kansas Paleontological Institute, Boulder, Colorado and Lawrence, Kansas, pp. 249-287.

Gaines, R. R. (2014). Burgess Shale-type preservation and its distribution in space and time. In M. Laflamme, J. D. Schiffbauer (Eds.), Reading and Writing of the Fossil Record: Preservational Pathways to Exceptional Fossilization. *The Paleontological Society Papers, 20*, 123-146.

Gaines, R. R., Mering, J. A., Zhao, Y.-L., & Peng, J. (2011). Stratigraphic and microfacies analysis of the Kaili Formation, a candidate GSSP for the Cambrian Series 2-Series 3 boundary. *Palaeogeography, Palaeoclimatology, Palaeoecology, 311*, 171-183.

Gaines, R. R., Paterson, J. R., Jago, J. B., Gehling, J. G., & García-Bellido, D. (2016). Palaeoenvironmental and depositional setting of the Emu Bay Shale, a unique early Cambrian Lagerstätte, In J. R. Laurie, P. D. Kruse, D. C. García-Bellido & J. D. Holmes (Eds.), Palaeo Down Under 2, Adelaide, 11-15 July 2016. *Geological Society of Australia Abstracts, 117*.

Galili, T. (2015). dendextend: an R package for visualizing, adjusting, and comparing trees of hierarchical clustering. *Bioinformatics, 31*, 3718-3720.

García-Bellido, D. C., Gozalo, R., Chirivella Martorell, J. B., & Liñán, E. (2007). The demosponge genus *Leptomitus* and a new species from the Middle Cambrian of Spain. *Palaeontology, 50*, 467-478.

García-Bellido, D. C., Lee, M. S. Y., Edgecombe, G. D., Jago, J. B., Gehling, J. G., & Paterson, J. R. (2014). A new vetulicolian from Australia and its bearing on the chordate affinities of an enigmatic Cambrian group. *BMC Evolutionary Biology, 14*, 214.

Garson, D. E., Gaines, R. R., Droser, M. L., Liddell, W. D., & Sappenfield, A. (2012). Dynamic palaeoredox and exceptional preservation in the Cambrian Spence Shale of Utah. *Lethaia, 45*, 164-177.

Gehling, J. G., Jago, J. B., Paterson, J. R., García-Bellido, D. C., & Edgecombe, G. D. (2011). The geological context of the Lower Cambrian (Series 2) Emu Bay Shale Lagerstätte and adjacent stratigraphic units, Kangaroo Island, South Australia. *Australian Journal of Earth Sciences, 58*, 243-257.

Goslee, S. C., & Urban, D. L. (2007). The ecodist package for dissimilarity-based analysis of ecological data. *Journal of Statistical Software, 22*, 1-19.

Hagadorn, J. W. (2002). Burgess Shale-Type Localities: The Global Picture. In D. J. Bottjer, W. Etter, J. W. Hagadorn, & C. M. Tang (Eds.), Exceptional Fossil Preservation: A Unique View on the Evolution of Marine Life (pp. 35-60). New York: Columbia University Press.

Hally, L. A., & Paterson, J. R. (2014). Biodiversity, biofacies and biogeography of middle Cambrian (Series 3) arthropods (Trilobita and Agnostida) on the East Gondwana margin. *Gondwana Research, 26*, 654-674.

Hammer, Ø., & Harper, D. (2006). *Paleontological data analysis*. Oxford: Blackwell Publishing.

Hammer, Ø., Harper, D. A. T., & Ryan, P. D. (2001). PAST: Paleontological statistics software package for education and data analysis. *Palaeontologia Electronica, 4*, 9pp.

Han, J., Zhang, Z.-F., & Liu, J.-N. (2008). A preliminary note on the dispersal of the Cambrian Burgess Shale-type faunas. *Gondwana Research, 14*, 269-276.

Hendricks, J. R. (2013). Global distributional dynamics of Cambrian clades as revealed by Burgess Shale-type deposits. In D. A. T. Harper, T. Servais (Eds.) Early Palaeozoic Biogeography and Palaeogeography. *Geological Society, London, Memoirs 38,* 35-43.

Hendricks, J. R., & Lieberman, B. S. (2007). Biogeography and the Cambrian radiation of arachnomorph arthropods. *Memoirs of the Association of Australasian Palaeontologists, 34*, 461-471.

Hendricks, J. R. & Lieberman, B. S. (2008). New phylogenetic insights into the Cambrian radiation of arachnomorph arthropods. *Journal of Paleontology 82*, 585-594.

Hijmans, R. J. (2015). geosphere: Spherical Trigonometry. R package version 1.3-13 https://cran.r-project.org/package=geosphere

Hou, X. G., Aldridge, R. J., Bergström, J., Siveter, D. J., Siveter, D. J., & Feng, X. H. (2004). *The Cambrian Fossils of Chengjiang, China: The Flowering of Early Animal Life*. Oxford: Blackwell.

Hu, S. (2005). *Taphonomy and Palaeoecology of the Early Cambrian Chengjiang Biota from Eastern Yunnan, China.* (PhD), Freie Universität Berlin, Berlin.

Hu, S. X., Zhu, M. Y., Steiner, M., Luo, H. L., Zhao, F. C., & Liu, Q. (2010). Biodiversity and taphonomy of the Early Cambrian Guanshan biota, eastern Yunnan. *Science China Earth Sciences, 53*, 1765-1773.

Ineson, J. R., & Peel, J. S. (2011). Geological and depositional setting of the Sirius Passet Lagerstätte (Early Cambrian), North Greenland. *Canadian Journal of Earth Sciences, 48*, 1259-1281.

Ivantsov, A. Yu., Zhuravlev, A. Yu., Leguta, A. V., Krassilov, V. A., Melnikova, L. M., & Ushatinskaya, G. T. (2005). Palaeoecology of the Early Cambrian Sinsk biota from the Siberian Platform. *Palaeogeography, Palaeoclimatology, Palaeoecology, 220*, 69-88.

Jaccard, P. (1908). Nouvelles recherches sur la distribution florale. *Bulletin de la Societe Vaudoise des Sciences Naturelles, 44*, 223-270.

Legendre, P., Lapointe, F.-J., & Casgrain, P. (1994). Modeling Brain Evolution from Behavior: A Permutational Regression Approach. *Evolution, 48*, 1487-1499.

Legendre, P., & Legendre, L. (1998). *Numerical Ecology* (2nd English ed.). Amsterdam: Elsevier Science.

Lichstein, J. W. (2007). Multiple regression on distance matrices: a multivariate spatial analysis tool. *Plant Ecology, 188*, 117-131.

Lieberman, B. S. (2003). Taking the Pulse of the Cambrian Radiation. *Integrative and Comparative Biology, 43*, 229-237.

MacKenzie, L. A., Hofmann, M. H., Junyuan, C., & Hinman, N. W. (2015). Stratigraphic controls of soft-bodied fossil occurrences in the Cambrian Chengjiang Biota Lagerstätte, Maotianshan Shale, Yunnan Province, China. *Palaeogeography, Palaeoclimatology, Palaeoecology, 420*, 96-115.

Manly, B. F. J. (1986). Randomization and regression methods for testing for associations with geographical, environmental and biological distances between populations. *Researches on Population Ecology, 28*, 201-218.

Mantel, N. (1967). The Detection of Disease Clustering and a Generalized Regression Approach. *Cancer Research, 27*, 209-220.

Maples, C. G., & Archer, A. W. (1988). Monte Carlo Simulation of Selected Binomial Similarity Coefficients (II): Effect of Sparse Data. *Palaios, 3*, 95-103.

McKerrow, W. S., Scotese, C. R., & Brasier, M. D. (1992). Early Cambrian continental reconstructions. *Journal of the Geological Society, London, 149*, 599-606.

Meert, J. G., & Lieberman, B. S. (2004). A palaeomagnetic and palaeobiogeography perspective on the latest Neoproterozoic and early Cambrian tectonic events. *Journal of the Geological Society, London, 161*, 477-487.

Morrone, J. J. (2014). Parsimony analysis of endemicity (PAE) revisited. *Journal of Biogeography, 41*, 842-854.

Nihei, S. S. (2006). Misconceptions about parsimony analysis of endemicity. *Journal of Biogeography, 33*, 2099-2106.

O'Reilly, J. E., Puttick, M. N., Parry, L., Tanner, A. R., Tarver, J. E., Fleming, J., . . . Donoghue, P. C. J. (2016). Bayesian methods outperform parsimony but at the expense of precision in the estimation of phylogeny from discrete morphological data. *Biology Letters, 12*, 20160081.

Ochiai, A. (1957). Zoogeographic studies on the soleoid fishes found in Japan and its neighbouring regions. *Bulletin of the Japanese Society of Scientific Fisheries, 22*, 526-530.

Oksanen, J., Blanchet, F. G., Kindt, R., Legendre, P., Minchin, P. R., O'Hara, R. B., . . . Wagner, H. (2015). vegan: Community Ecology Package. R package version 2.3-0. https://cran.r-project.org/package=vegan.

Paterson, J. R., & Brock, G. A. (2007). Early Cambrian trilobites from Angorichina, Flinders Ranges, South Australia, with a new assemblage from the Pararaia bunyerooensis Zone. *Journal of Paleontology, 81*, 116-142.

Paterson, J. R., Edgecombe, G. D., GarcÍa-Bellido, D. C., Jago, J. B., & Gehling, J. G. (2010). Nektaspid arthropods from the Lower Cambrian Emu Bay Shale Lagerstätte, South Australia, with a reassessment of lamellipedian relationships. *Palaeontology, 53*, 377-402.

Paterson, J. R., Edgecombe, G. D., & Jago, J. B. (2015). The ‘great appendage’ arthropod *Tanglangia*: Biogeographic connections between early Cambrian biotas of Australia and South China. *Gondwana Research, 27*, 1667-1672.

Paterson, J. R., García-Bellido, D. C., & Edgecombe, G. D. (2012). New Artiopodan arthropods from the Early Cambrian Emu Bay Shale Konservat-Lagerstätte of South Australia. *Journal of Palaeontology, 86*, 340-357.

Paterson, J. R., García-Bellido, D. C., Jago, J. B., Gehling, J. G., Lee, M. S. Y., & Edgecombe, G. D. (2016). The Emu Bay Shale Konservat-Lagerstätte: a view of Cambrian life from East Gondwana. *Journal of the Geological Society, London, 173*, 1-11.

Paterson, J. R., & Jago, J. B. (2006). New trilobites from the Lower Cambrian Emu Bay Shale Lagerstätte at Big Gully, Kangaroo Island, South Australia. *Memoirs of the Association of Australasian Palaeontologists, 32*, 43-57.

Paterson, J. R., Jago, J. B., Gehling, J. G., García-Bellido, D. C., Edgecombe, G. D., & Lee, M. S. Y. (2008). In I. Rábano, R. Gonzalo, & D. García-Bellido (Eds.), Early Cambrian arthropods from the Emu Bay Shale Lagerstätte, South Australia. *Advances in trilobite research* (pp. 319-325). Madrid: Instituto Geológico y Minero de España.

Peel, J. S., & Ineson, J. R. (2011). The Sirius Passet Lagerstätte (early Cambrian) of North Greenland. In P.A. Johnston, K. J. Johnston (Eds.), International Conference on the Cambrian Explosion, Proceedings. *Palaeontographica Canadiana, 31*, 109-118.

Peng, J., Zhao, Y. L., Wu, Y., Yuan, J. L., & Tai, T. S. (2005). The Balang Fauna—A new early Cambrian Fauna from Kaili City, Guizhou Province. *Chinese Science Bulletin, 50*, 1159-1162.

Peng, S. (2009). The newly-developed Cambrian biostratigraphic succession and chronostratigraphic scheme for South China. *Chinese Science Bulletin, 54*, 4161-4170.

Peng, S., Babcock, L. E., & Cooper, R. A. (2012). The Cambrian Period. In F. M. Gradstein, J. G. Ogg, M. D. Schmitz, & G. M. Ogg (Eds.), *The Geologic Time Scale 2012, Volume 2* (pp. 437-488). Oxford: Elsevier.

R Core Team. (2015). R: A language and environment for statistical computing. R Foundation for Statistical Computing, Vienna, Austria. URL https://www.r-project.org/.

Robison, R. A., & Babcock, L. E. (2011). Systematics, paleobiology, and taphonomy of some exceptionally preserved trilobites from Cambrian Lagerstätten of Utah. *The University of Kansas Paleontological Contributions, 5*, 1-47.

Robison, R. A., Babcock, L. E., & Gunther, V. G. (2015). *Exceptional Cambrian Fossils from Utah: A Window into the Age of Trilobites*. Salt Lake City: Utah Geological Society.

Rosen, B. R., & Smith, A. B. (1988). Tectonics from fossils? Analysis of reef-coral and sea-urchin distributions from late Cretaceous to Recent, using a new method. In M. G. Audley-Charles & A. Hallam (Eds.), Gondwana and Tethys. *Geological Society Special Publication, 37*, 275-306.

RStudio Team. (2015). RStudio: Integrated Development for R. RStudio, Inc., Boston, MA URL http://www.rstudio.com/.

Shi, G. R. (1993). Multivariate data analysis in palaeoecology and palaeobiogeography - a review. *Palaeogeography, Palaeoclimatology, Palaeoecology, 105*, 199-234.

Skinner, E. S. (2005). Taphonomy and depositional circumstances of exceptionally preserved fossils from the Kinzers Formation (Cambrian), southeastern

Pennsylvania. *Palaeogeography, Palaeoclimatology, Palaeoecology, 220*, 167-192.

Steiner, M., Li, G., Qian, Y., Zhu, M., & Erdtmann, B.-D. (2007). Neoproterozoic to Early Cambrian small shelly fossil assemblages and a revised biostratigraphic correlation of the Yangtze Platform (China). *Palaeogeography, Palaeoclimatology, Palaeoecology, 254*, 67-99.

Strang, K. M., Armstrong, H. A., Harper, D. A. T. & Trabucho-Alexandre, J. P. (2016). The Sirius Passet Lagerstätte: silica death masking opens the window on the earliest matground community of the Cambrian explosion. *Lethaia 49*, 631-643.

Swofford, D. L. (2001). PAUP*: Phylogenetic Analysis Using Parsimony (*and Other Methods), Version 4: Sinauer Associates, Sunderland, Massachusetts.

Torsvik, T. H., & Cocks, L. R. M. (2013). New global palaeogeographical reconstructions for the Early Palaeozoic and their generation. In D. A. T. Harper & T. Servais (Eds.), Early Palaeozoic Biogeography and Palaeogeography. *Geological Society, London, Memoirs, 38*, 5-24.

Yan, Q. J., Peng, J., Zhao, Y. L., Weng, R. Q., & Sun, H. J. (2014). Restudy of sedimentary and stratigraphy of the Qiandongian (Cambrian) Balang Formation at Jianhe, Guizhou, China - example for Jiaobang section of the Balang Formation. *Geological Review, 60*, 893-902 (in Chinese, with English abstract).

Zamora, S., Lefebvre, B., Álvaro, J. J., Clausen, S., Elicki, O., Fatka, O., Jell, P., . . . Smith, A. B. (2013). Cambrian echinoderm diversity and palaeobiogeography. In D. A. T. Harper & T. Servais (Eds.), Early Palaeozoic

Biogeography and Palaeogeography. *Geological Society, London, Memoirs, 38*, 157-171.

Zhao, F., Caron, J.-B., Bottjer, D. J., Hu, S., Yin, Z., & Zhu, M. (2014). Diversity and species abundance patterns of the Early Cambrian (Series 2, Stage 3) Chengjiang Biota from China. *Paleobiology, 40*, 50-69.

Zhao, F. C., Hu, S. X., Caron, J.-B., Zhu, M. Y., Yin, Z. J., & Lu, M. (2012). Spatial variation in the diversity and composition of the Lower Cambrian (Series 2, Stage 3) Chengjiang Biota, Southwest China. *Palaeogeography, Palaeoclimatology, Palaeoecology, 346-347*, 54-65.

Zhao, F. C., Zhu, M. Y., & Hu, S. X. (2010). Community structure and composition of the Cambrian Chengjiang biota. *Science China Earth Sciences, 53*, 1784-1799.

Zhao, Y. L., Zhu, M. Y., Babcock, L. E., & Peng, J. (2011). *The Kaili biota: marine organisms from 508 million years ago*. Guiyang: Guizhou Science and Technology Press.

Zhao, Y. L., Zhu, M. Y., Babcock, L. E., Yuan, J. L., Parsley, R. L., Peng, J., . . . Wang, Y. (2005). Kaili Biota: A Taphonomic Window on the Diversification of Metazoans from the Basal Middle Cambrian: Guizhou, China. *Acta Geologica Sinica, 79*, 751-765.

Chapter 4 – Variable trilobite moulting behaviour preserved in the Emu Bay Shale, South Australia

J. D. Holmes, H. B. Drage, A. C. Daley and D. C. García-Bellido

4.1 Abstract

The Cambrian Series 2 Emu Bay Shale (EBS) from Kangaroo Island, South Australia, preserves a diverse Burgess Shale-type (BST) biota with over 50 species now recognised. Trilobites dominate the assemblage in terms of density, with *Estaingia bilobata* Pocock, 1964 in particular being extremely abundant, with specimens of the larger *Redlichia takooensis* Lu, 1950 also common. Many trilobite specimens within the EBS appear to represent complete moulted exoskeletons, a situation that is apparently unusual for Cambrian fossil deposits, within which disturbance, probably resulting from decay and/or water movement, has generally resulted in the dismemberment and scattering of exuviae. The abundance of specimens within the EBS, as well as the high incidence of complete moults, provides an excellent sample record that has allowed the recognition of various moult 'configurations' for both species, which in turn has allowed the inference of sequences of movement required to produce such arrangements. Moult configurations of *E. bilobata* are characterised by detachment and slight displacement of the rostral plate and librigenae, with or without detachment of the cranidium, suggesting ecdysis was achieved by anterior withdrawal via opening of the facial and rostral sutures (the 'Sutural Gape' mode). Moulting in *R. takooensis* generally occurred via the same method, however, configurations for this species generally show greater displacement of cephalic sclerites, suggesting more vigorous movement during ecdysis. Both species also show rare examples of Salterian configurations, with the entire cephalon inverted by being 'flipped' forward. These results suggest that moulting in trilobites was perhaps a more variable process than

first thought. In contrast to the EBS, other Cambrian Lagerstätten with an abundance of trilobites (such as the Wheeler Shale and the Mount Stephen Trilobite Beds) tend to show larger numbers of ‘axial shields’ and isolated sclerites, often interpreted to represent disarticulated exuviae. This suggests higher levels of disturbance due to factors such as animal activity, depositional processes, or water movement due to currents or wave action (or a combination of these), compared to that suggested for the EBS, where quiescent conditions, intermittent anoxia on the seafloor, and presumed rapid burial (i.e. a high background sedimentation rate) have resulted in an unparalleled trilobite moulting record.

4.2 Introduction

In 1952, South Australian Geological Survey geologist R. C. Sprigg discovered the first fossils (including trilobites) from the early Cambrian (Series 2) Emu Bay Shale in the shoreline outcrops northwest of the Emu Bay jetty (Jago & Cooper, 2011; Sprigg, 1955). To the east of Emu Bay at "Big Gully", the formation is now known to house a diverse Konservat-Lagerstätte containing over 50 species, including sponges, brachiopods, hyoliths, polychaetes, priapulids, lobopodians, anomalocaridids, other non-mineralised arthropods (e.g. nektaspids, artiopodans and megacheirans), trilobites, vetulicolians, and several problematic forms (García-Bellido et al., 2009; Paterson et al., 2008; 2016). Like the majority of Cambrian Lagerstätten, the assemblage is dominated by arthropods; unusually however, trilobites, and in particular *Estaingia bilobata*, overwhelmingly dominate in terms of numerical abundance. *E. bilobata* approaches densities of up to 300 individuals per square metre within the Emu Bay Shale (up to 80% of individuals on each slab), and it is suggested that this species may have been an exaerobic specialist, occupying a niche between oxic and anoxic sections of the seafloor (Paterson et al., 2016). Specimens of the larger *Redlichia takooensis* are also very common. In contrast, the three other known species of trilobite from the Emu Bay Shale, *Balcoracania dailyi*, *Megapharanaspis nedini* and *Holyoakia simpsoni*, are all extremely rare.

The majority of trilobite specimens (>90%; Gehling et al., 2011) from the Emu Bay Shale Lagerstätte probably represent carcasses, although a substantial proportion appear to be moulted exoskeletons (exuviae). Many of these were preserved with little to no disturbance prior to burial, and therefore provide a unique

opportunity to infer moulting behaviours by reconstructing sequences of movement and disarticulation. This is unlike the vast majority of Cambrian fossil deposits, where even small amounts of disturbance have resulted in the movement and separation of disarticulated sclerites, and from which moult configurations therefore become difficult to interpret. The lack of disturbance and the sheer abundance of specimens within the Emu Bay Shale provide the perfect opportunity for a case study of moulting behaviour in Cambrian trilobites. Here we describe and interpret moult configurations of *E. bilobata* and *R. takooensis*, and compare these with moulting in other Cambrian trilobites as represented in the published literature.

4.3 Location, geological setting and age

Big Gully is situated on the north coast of Kangaroo Island, South Australia, approximately 7 km east of the Emu Bay township, and 1.5 km west of White Point (see Chapter 2, Fig. 2.1). Early collections from this locality were sourced from the wave-cut platform and cliff exposures immediately to the east of the mouth of Big Gully, however, in 2007 a new excavation was commenced at 'Buck Quarry' approximately 400 m inland that has yielded a richer assemblage and better quality preservation than previously encountered (García-Bellido et al., 2009). More recently, 'Daily Quarry' has been opened slightly closer to shore and is also yielding high quality material.

The Emu Bay Shale (EBS) forms part of the early Cambrian (Series 2) Kangaroo Island Group, a largely clastic shelf succession that outcrops on the

central northern coast of the island. Conglomerate facies within the EBS, as well as within the older White Point Conglomerate (that thin towards the south), suggest that the sequence was deposited adjacent to an active tectonic margin, with the source area immediately to the north of the present coastline (Daily et al., 1980; Gehling et al., 2011). It has been suggested that syndepositional faulting south of this margin resulted in the formation of isolated oxic-to-anoxic sections of the seafloor within which the Lagerstätte was rapidly deposited (Gehling et al., 2011). This near-shore depositional environment is very different from that observed for other Cambrian Lagerstätten, that are generally deposited in outer shelf settings (Gaines, 2014). This seems to be reflected in an unusual mode of preservation differing from that of other Burgess Shale-type (BST) localities. Preservation of non-mineralised material within Cambrian Lagerstätten is usually represented by two-dimensional compression fossils composed of primary carbonaceous remains, a pathway termed “Burgess Shale-type preservation” (Gaines, 2014). In contrast, preservation within the EBS seems to be somewhat different, with fossils exhibiting some three-dimensionality due to early-stage diagenetic mineralisation, including the phosphatisation of certain soft muscle and gut tissues, as well as phosphatisation and pyritisation of cuticular structures such as eyes, and late diagenetic replication of fossils by fibrous calcite (see Paterson et al., 2016 and references therein). Soft-bodied preservation occurs predominantly within the lowest 10 metres of the EBS at Big Gully, within dark grey, micaceous, finely laminated mudstone, interspersed with siltstone and fine sandstone horizons interpreted as gravity flow or storm deposits (Gehling et al., 2011). Geochemical analysis conducted by McKirdy et al. (2011) suggests that the EBS mudstones were deposited beneath an oxic water column, as is also suggested

by the diverse nekto-benthic and pelagic elements of the biota (Paterson et al., 2016). The original presence of pyrite within the sediment (McKirdy et al., 2011), little evidence of predation (although see Conway Morris & Jenkins, 1985; Nedin, 1999), scavenging or bioturbation (e.g. the high proportion of complete trilobite specimens), absence of trace fossils, as well as an impoverished representation of fixosessile taxa, suggest that pore water below the sediment-water interface was anoxic, with low-oxygen conditions likely also prevailing above the seafloor (Gehling et al., 2011). Evidence of predation or scavenging on *E. bilobata* by the chelicerate *Wisangacaris*, however, suggests that at times the substrate was at least partially oxygenated (Jago et al., 2016). It is possible that mat-forming cyanobacteria helped in maintaining a sharp redox boundary between water column and sediment, and in doing so facilitated the exceptional preservation seen in the EBS Lagerstätte by inhibiting the decay of soft tissues (McKirdy et al., 2011). The presence of cyanobacteria also provides evidence that the Lagerstätte was preserved within the photic zone. A lack of sedimentological evidence for water movement (Gehling et al., 2011), as well as complete moult configurations, suggests that within the mudstones certain taxa are found not only *in situ*, but with essentially no disturbance at all prior to burial.

Based on the presence of *E. bilobata*, *R. takooensis* and *B. dailyi*, the EBS has been correlated with the early Cambrian (Series 2, Stage 4) *Pararaia janeae* trilobite zone of mainland South Australia (Jell in Bengtson et al., 1990; Jago et al., 2006; Paterson & Brock, 2007), which is equivalent to the mid-late Botoman Stage of Siberia, the upper Nangaoan/lower Duyunian of South China, and the Dyeran of North America (Paterson & Brock, 2007; Peng et al., 2012). Absolute age is

estimated at 514 Ma based on correlation with the Cambrian timescale presented in Fig. 19.3 of Peng et al. (2012).

4.4 Material and methods

All figured material from the EBS Lagerstätte was collected from Buck and Daily Quarries and is housed in the palaeontological collections of the South Australian Museum, Adelaide (prefix SAM-P). Specimens were photographed dry using a Canon EOS 500D and 50D Digital SLR, with a Canon EF-S 60mm 1:2.8 Macro Lens under low-angle lighting. Particularly small specimens were photographed using a Canon MP-E 65mm 1:2.8 1–5x Macro Photo Lens. The camera was remotely controlled using the Canon EOS Utility 2.8.1.0 program. Photographs were adjusted and edited, and figures produced in Adobe Photoshop and Illustrator CS6.

The problem of distinguishing between exuviae and carcasses has been discussed by a number of authors and a range of criteria for distinguishing between these two types proposed (e.g. Daley & Drage, 2016; Henningsmoen, 1975; Whittington, 1990). In their review of the fossil record of ecdysis, Daley and Drage (2016) considered that the major requirements for the recognition of exuviae for trilobites were, (1) evidence for the opening of suture lines, and (2) repeated configurations of exoskeletal units, coupled with consideration of the preservational environment; these criteria were therefore used to identify moult configurations from

the collections of the South Australian Museum, following which the behavior leading to these arrangements was inferred.

When interpreting moulted exuviae it is important to remember that the entire exoskeleton of the trilobite was shed during moulting, including the non-mineralised cuticle that covered parts of the ventral side, such as the appendages. One must therefore take into account the fact that 'isolated' mineralised ecdysial units in configurations may in fact have been connected during and after moulting by integument, and that this may have an important effect on the configurations seen. Following ecdysis it is likely that unmineralised cuticle and connective membranes would have decayed rapidly, resulting in disarticulation except under conditions of rapid burial (Whittington, 1990), as is suggested for the EBS.

4.5 Results

4.5.1 Descriptions of recognised moult configurations

Minor variations on seven general types of moult configurations were recognised for the EBS specimens, three of which have been named in the literature for other trilobite species (see Henningsmoen, 1975). The existing configurations are presented here for clarity, and the four new configurations described and named for ease of use in future studies of trilobite moulting. They are as follows:

1. *Axial shield* (Fig. 4.1B; named in Henningsmoen, 1957). The cranidium, thorax, and pygidium joined as a single unit (i.e. entire dorsal exoskeleton minus the librigenae). May be used to designate part of an articulated trilobite, but often found in isolation and usually inferred to represent instances of moulting via disarticulation and subsequent transportation of the librigenae.
2. *Harrington's configuration* (Fig. 4.1C; named in Henningsmoen, 1975). Moult configuration comprising complete axial shield and displaced 'lower cephalic unit' (LCU; all parts of the cephalon, minus the cranidium, joined by soft cuticle, *sensu* Henningsmoen, 1975). The joined LCU (librigenae, rostral plate, hypostome and articulating cuticle) may be displaced posteriorly below the axial shield, or singular parts of the LCU may be disrupted presumably by decay of the connective integument.
3. *Henningsmoen's configuration* (Fig. 4.1D; named here). Similar to Harrington's configuration, but with little or no displacement of the LCU, and showing displacement of the cranidium with respect to the thoracopygon (thorax + pygidium, *sensu* Henningsmoen, 1975). Named such because Henningsmoen (1975, p.194) notes this possibility in addition to his Harrington's configuration.
4. *Nutcracker configuration* (Fig. 4.1E; named here). Librigenae disarticulated and usually displaced outwards from the axial shield. The ventral cephalic sclerites (rostral plate, hypostome) may remain relatively *in situ* or also be displaced outwards from the axial shield. So named for the outwards displacement of most cephalic sclerites.

5. *Lamborghini configuration* (Fig. 4.1F; named here). Moult configuration with one or both librigenae disarticulated from the cranidium and flipped forwards, leaving the genal spine pointing anteriorly. The rostral plate is often visibly displaced, and may remain articulated with the librigenae as a completely inverted and flipped LCU. Named for the similar forward movement of the side doors of the iconic sports car.
6. *McNamara's configuration* (Fig. 4.1G; named here). Moult configuration where one or both librigenae are disarticulated and laterally inverted. Suggested by McNamara and Rudkin (1984, Fig. 5) and McNamara (1986) to occur in *Encrinurus mitchelli, Asaphiscus wheeleri, Redlichia forresti* and *Redlichia micrograpta* through a decreasing water pressure gradient created underneath the cranidium through rising of the cephalic region. This presumably created laterally flowing water currents that dragged the librigenae inwards and caused them to be inverted.
7. *Salter's configuration* (or Salterian configuration (Fig. 4.1H); named in Henningsmoen, 1975; Richter, 1937). The cephalon is disarticulated from the thoracopygon and anteriorly inverted, usually resulting in the anterior margin becoming oriented posteriorly and often underlapping the thoracopygon.

All of these configurations (with the exception of Salter's) involve the 'Sutural Gape' mode of moulting as described by Henningsmoen (1975), i.e. requiring an anterior exuvial gape produced by the opening of the cephalic sutures (in this case the rostral and facial sutures). The cranidium and the LCU form the upper and lower "jaws" of the exuvial gape respectively, with variations in the final positioning of

sclerites resulting in the above configurations preserved at the EBS. Other rarer modes of moulting, resulting in more unusual configurations, were also described by Henningsmoen (1975), such as the *Harpes* mode using the marginal-intermellar suture (p. 189), or *Ductina* mode using the marginal cephalic suture sometimes resulting in 'Maksimova's configuration' (p. 190), as well as 'Hupe's configuration' with a displaced rostral plate (p. 192), although due to their anatomy, these are not observed for *E. bilobata* or *R. takooensis*. The definitions above are used below to describe the moult configurations of *E. bilobata* (Section 4.5.2) and *R. takooensis* (Section 4.5.3), and thus to interpret their ecdysial behaviour and movements (Section 4.6).

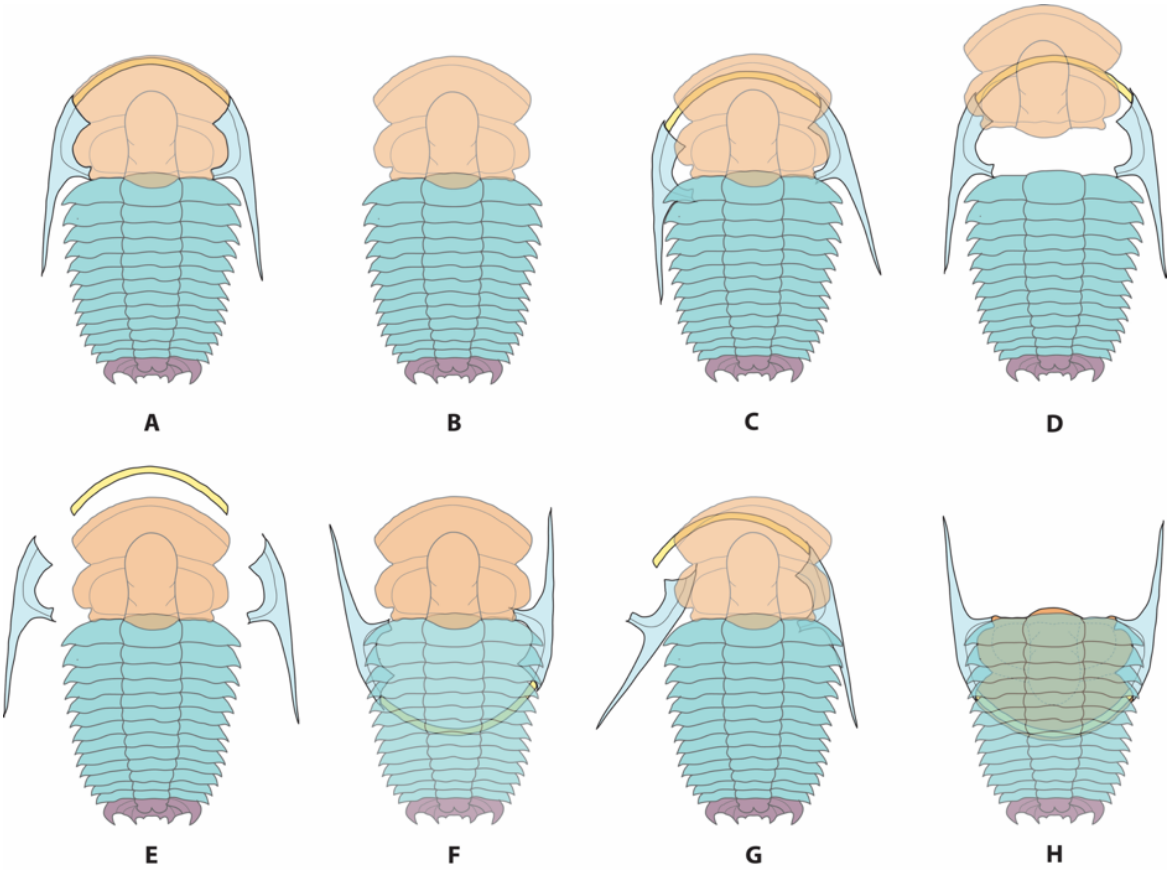

Figure 4.1: Moult configurations discussed in the text (based on *Estaingia bilobata* Pocock, 1964). A. complete trilobite; B, axial shield; C, Harrington's configuration; D. Henningsmoen's config.; E, Nutcracker config.(not seen in *E. bilobata* but pictured here for illustrative purposes); F, Lamborghini config.; G, McNamara's config.; H, Salterian config.

4.5.2 Description of moulting in *Estaingia bilobata* Pocock, 1964

E. bilobata is a small trilobite (up to c. 30mm in length) exhibiting 13 thoracic segments, narrow librigenae bearing long genal spines, and a small pygidium; the (opisthoparian) facial and rostral sutures are operative, with the detached rostral plate slightly shorter than the anterior border of the cranidium (Pocock, 1964). *Estaingia* is restricted to early Cambrian sediments of Australia, Antarctica and South China (e.g. Dai & Zhang, 2012; Palmer & Rowell, 1995; Paterson, 2005; Jell in Bengston et al., 1990; Paterson & Brock, 2007).

Pocock (1964; p.461) noted that: "Many specimens of *Estaingia* show that the cephalon has rolled forward over the detached rostral plate, and that the librigenae are free, but only slightly displaced; this appears to have been the characteristic mode of moulting in this trilobite". Our observations support this interpretation, although the moult configurations of *E. bilobata* exhibit considerable variation. Detachment and posterior displacement of the rostral plate, as well as displacement of one or both librigenae relative to the cranidium (i.e. Harrington's configuration, Fig. 4.1C) is common. The rostral plate normally appears joined to the librigenae (as part of the LCU), but the placement of this unit relative to the thoracopygon varies, and occasionally displays slight disassociation or rotation of some LCU elements. Although Pocock (1964) suggested the hypostomal suture was operative, we rarely observed the hypostome in specimens considered exuviae, suggesting it is either hard to discern or was potentially shed elsewhere. Henningsmoen's configuration (Fig. 4.1D) is also very common, with the cranidium displaced in addition to the LCU. In specimens interpreted to be moults,

disarticulation between the thorax and pygidium or thoracic segments is very rare. The majority of *E. bilobata* moult ensembles found at the EBS are represented by variations on Henningsmoen's and Harrington's configurations as illustrated in the following examples.

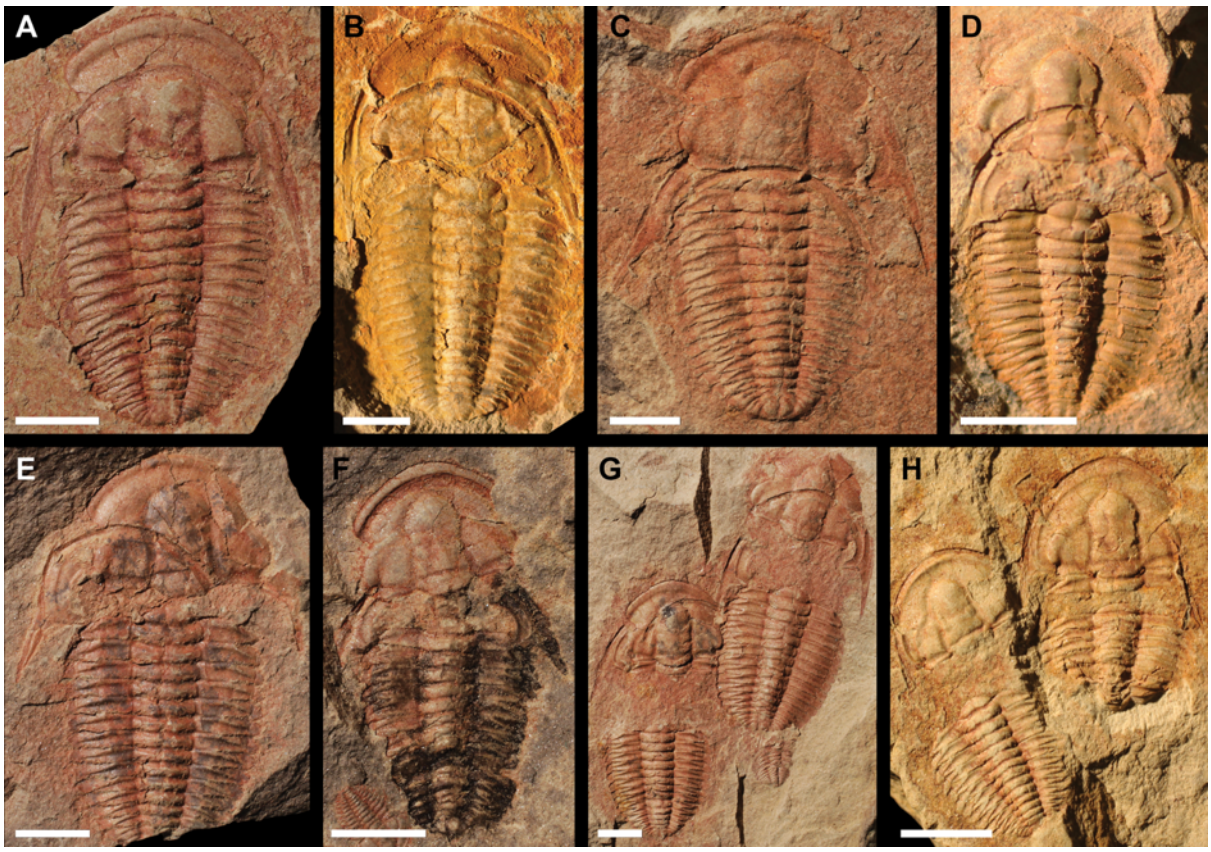

Figure 4.2: Example moult configurations of *Estaingia bilobata* Pocock, 1964 from the Emu Bay Shale collections of the South Australian Museum, referred to in the text. A, SAM-P 43837; B, SAM-P 43974; C, SAM-P 43402; D, SAM-P 45519; E, SAM-P 46933; F, SAM-P 46362; G, SAM-P 46956; H, SAM-P 45697. All specimens show variations of Henningsmoen's configuration. Scale bars 5 mm.

SAM-P 43837 (Fig. 4.2A) is an example of Henningsmoen's configuration in *E. bilobata*, showing slight displacement of the librigenae and posterior movement (2–3mm) of the rostral plate relative to the cranidium, with very slight separation (~1mm) of the cranidium from the thorax. SAM-P 43974 (Fig. 4.2B), 43402 (Fig. 4.2C), and 46933 (Fig. 4.2E) also display variations of Henningsmoen's

configuration. Fig. 4.2B displays separation (~2mm) and anti-clockwise rotation of the cranidium, lateral displacement of the left librigena, and conjoined right librigena with rostral plate. In Fig. 4.2C the cranidium is only slightly anteriorly displaced, and the rostral plate and left librigena have been pushed backwards to underlie the occipital ring and anterior of the thoracopygon. The right facial suture is open. In Fig. 4.2E the rostral plate and left librigena appear connected and are slightly displaced outwards and rotated. The cranidium and poorly preserved right librigena are anteriorly displaced, with some anti-clockwise rotation. SAM-P 45519 and 46362 (Fig. 4.2D, F) differ as their cranidia are anteriorly displaced (so that in Fig. 4.2D the middle of the glabella overlies the rostral plate) but the joined LCU remains largely *in situ* with almost negligible displacement. However, the rostral plate may remain in place for Fig. 4.2F based on the unusually deep anterior cephalic border furrow.

SAM-P 46956 (Fig. 4.2G) consists of a moulting pair of *E. bilobata*. The right-hand specimen in Fig. 4.2G shows a variant of Henningsmoen's configuration, with the left librigena remaining joined to the thoracopygon, the joined right librigena and rostral plate carried ~3mm forwards, and the cranidium deposited a further 2mm in front. Interestingly, the left specimen (Fig. 4.2G) has disarticulated between the first and second thoracic segments, rather than at the joint between cephalon and thorax. The cephalic region with associated first thoracic segment is displaced forwards ~6mm and laterally offset. The rostral plate and joined right librigena are marginally displaced to the right and rotated anti-clockwise. Other specimens, e.g. SAM-P 45697 (Fig. 4.2H), show similar moult ensembles to this paired example.

SAM-P 15339 (Fig. 4.3A) characterises Harrington's configuration in *E. bilobata.* This specimen shows left-lateral displacement and minor anti-clockwise

rotation of the LCU more-or-less as a joined structure. The axial shield is otherwise preserved intact. Moult ensembles similar to this are very common for this species. Moult configurations with inversion of the librigenae were also observed for *E. bilobata*, but were generally much rarer than Henningsmoen's or Harrington's configuration. Two specimens in the collection, including SAM-P 54204 (Fig. 4.3D) clearly exhibit the Lamborghini configuration, consisting of an intact axial shield and the librigenae anteriorly inverted. A further four specimens, including SAM-P 54207 (Fig. 4.3B), display laterally inverted librigenae, a variation of McNamara's configuration.

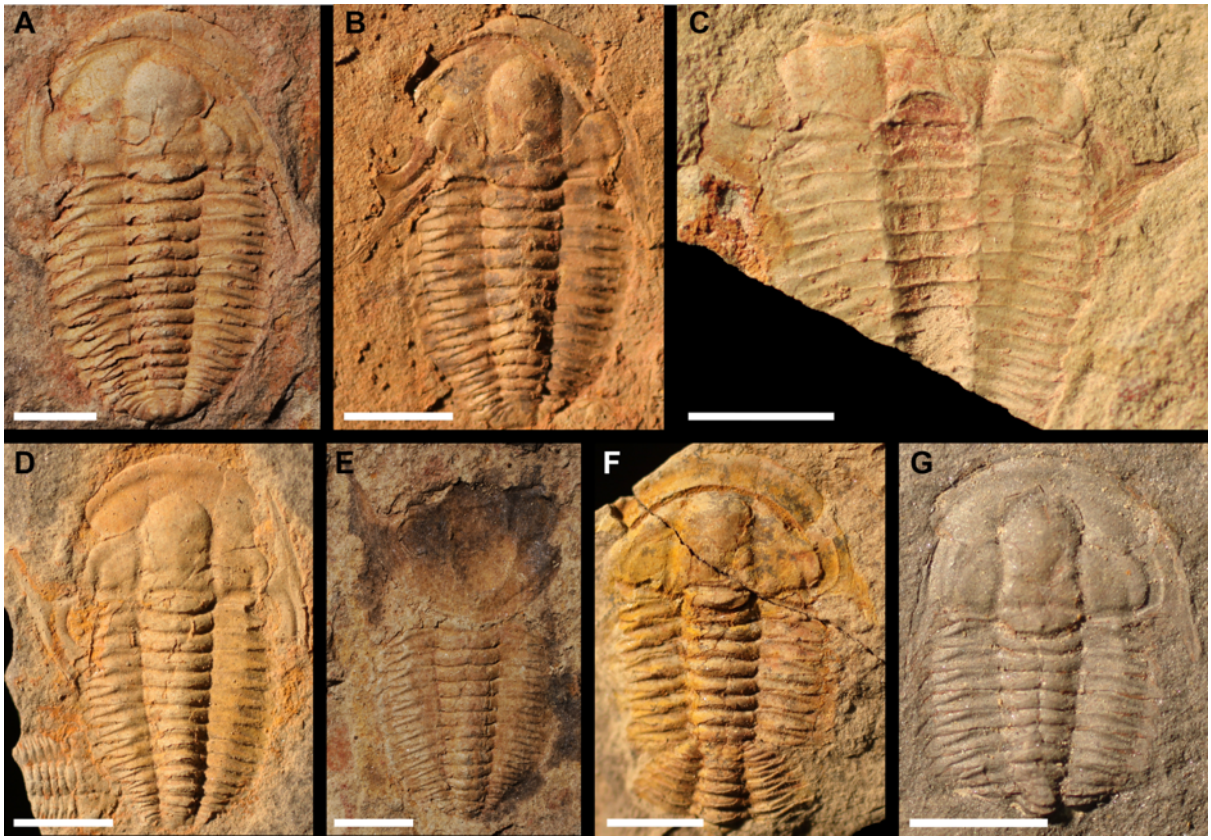

Figure 4.3: Example moult configurations of *Estaingia bilobata* Pocock, 1964 from the Emu Bay Shale collections of the South Australian Museum, referred to in the text. A, SAM-P 15339 (Harrington's configuration); B, SAM-P 54207 (McNamara's conf.); C, SAM-P 54206 (Salterian conf.); D, SAM-P 54204 (Lamborghini conf.); E, SAM-P 15459 (Salterian conf.); F, SAM-P 54205 (rotated pygidium and posteriormost five segments); G, SAM-P 54208 (carcass with curled lower thorax and pygidium). Scale bars 5 mm.

SAM-P 54206 and 15459 (Fig. 4.3C, E) show *E. bilobata* moults in Salterian configuration, the former with the thoracopygon resting on the inverted cephalon, and the latter with the cephalon inverted anteriorly, such that the anterior border lies adjacent to the anterior of the thorax. In the second specimen, the left librigena remains in place relative to the cranidium and the right is detached and missing. Interestingly, a single specimen (SAM-P 54205, Fig. 4.3F) had the final five thoracic segments and pygidium rotated 180^{o}, the rostral plate displaced backwards, and is possibly missing the left librigena. This may reflect a more unusual moult ensemble for *E. bilobata*.

4.5.3 Description of moulting in *Redlichia takooensis* Lu, 1950

Redlichia takooensis is a large redlichiid trilobite known from Lower Cambrian (late Botoman) sediments in Australia and South China (Jell in Bengtson et al., 1990; Zhang, 1980). The cephalic shield is semi-circular, with large librigenae bearing long genal spines that form a continuous curved border with the anterior of the cranidium, which in turn bears a long occipital spine. As in *E. bilobata*, the (opisthoparian) facial and rostral sutures are operative, with the rostral plate slightly narrower than the anterior of the cranidium (Jell in Bengtson et al., 1990). The hypostomal suture is present and functional. The thorax has 15 segments, each bearing a medial spine that is elongated in the 6th and particularly the 11th, and is relatively narrow compared to the width of the head shield, especially in smaller specimens (Paterson & Jago, 2006). The pygidium is small. Articulated specimens up to 25 cm long are

known from the vicinity of Big Gully (Paterson et al., 2016), although most specimens from Buck and Daily Quarries are between 5-7 cm in length.

As with *E. bilobata*, arrangements considered to be moults of *R. takooensis* exhibit considerable variation. *R. takooensis* also employed a 'Sutural Gape' mode of moulting, but produced different moult configurations. Outwards displacement of individual cephalic sclerites, rather than a joined LCU, was more common, as was thoracic disarticulation. The latter was often associated with segments 6 and 11, which support extended medial spines. Hypostome displacement is also apparent in *R. takooensis*, but rarely observed for *E. bilobata*.

SAM-P 48085 (Fig. 4.4A), 44214 (Fig. 4.4B), and 44544 (Fig. 4.4D) illustrate the Nutcracker configuration for *R. takooensis*. In these moult ensembles the librigenae are displaced outwards from the cranidium (by ~1–10mm), and show some rotation. Fig. 4.4A and D have the rostral plate displaced forwards, although this part is truncated and not preserved for Fig. 4.4B. In Fig. 4.4A the thorax is disarticulated between segments 11 and 12, with the posterior thoracopygon disrupted and rotated slightly clockwise. Fig. 4.4D displays disarticulation between thoracic segments 3 and 4 (~2mm), and 9 and 10 (~5mm), and displacement of the hypostome to lie beneath the anterior cephalic border. SAM-P 45440 (Fig. 4.4C) is a small specimen of *R. takooensis* that also shows moulting involving disarticulation of the librigenae, slight posterior displacement of the hypostome, and thoracic breakage. The thoracopygon posterior to segment 8 is missing, and segments 4-6 are clearly imbricated. The hypostome is much more visibly displaced in SAM-P 46207 (Fig. 4.4E), being adjacent to the right of segments 4 through 6. This specimen may also represent the Nutcracker configuration, as the librigenae seem

disarticulated, although the anterior and anterior right of the specimen has been truncated by rock fracture.

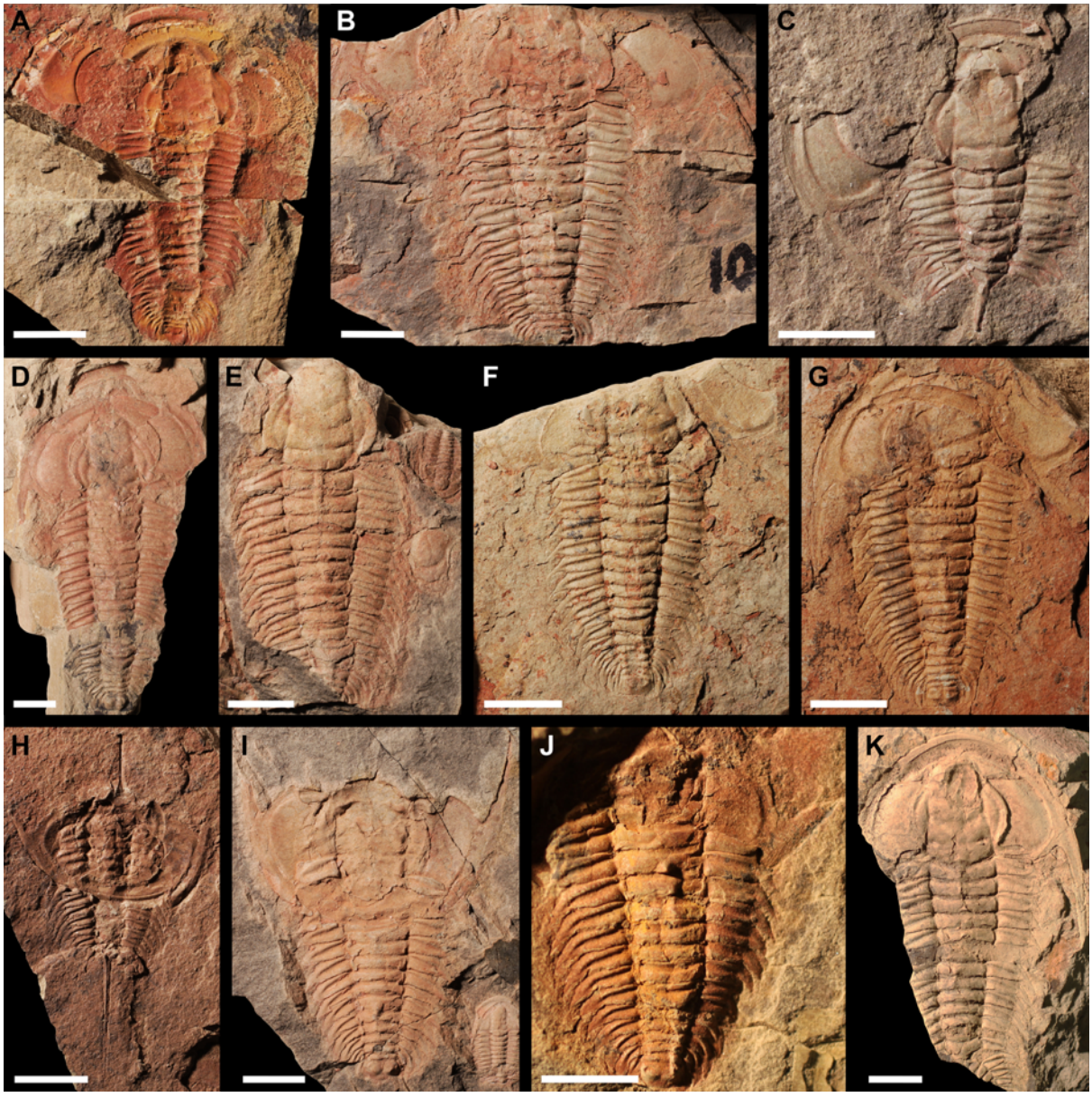

Figure 4.4: Example moult configurations of *Redlichia takooensis* Lu, 1950 from the Emu Bay Shale collections of the South Australian Museum, referred to in the text. A, SAM-P 48085 (Nutcracker configuration); B, SAM-P 44214 (Nutcracker config.); C, SAM-P 45440 (Nutcracker config.?); D, SAM-P 44544 (Uncertain – see text); E, SAM-P 46207 (Nutcracker config.? – note displaced hypostome); F, SAM-P 48062 (McNamara's config.); G, SAM-P 46047 (McNamara's config.); H, SAM-P 45368 (Salterian config.); I, SAM-P 43593 (Salterian config.); J, unregistered (Salterian config); K, SAM-P 54209 (Carcass with thoracic break). Scale bars 10 mm.

Moult ensemble SAM-P 48062 (Fig. 4.4F) also shows the left librigena displaced outwards (~5mm), however the right is laterally inverted so that the medial edge is facing away from the axial shield in the uncommon McNamara's configuration. The cranidium is also slightly disrupted, and the rostral plate is not preserved in this truncated specimen. SAM-P 46047 (Fig. 4.4G) displays a similar configuration, with the right librigena laterally inverted, and the cranidium (plus left librigena) rotated anti-clockwise (~20 degrees). The rostral plate is displaced from its *in situ* position.

SAM-P 45368, 43593 and an as yet unregistered specimen (Fig. 4.4H, I, J) show Salterian moult configurations. The first is broken posterior to the 11th segment, revealing the long medial thoracic spine, with the thoracopygon below this missing. The occipital spine extending from the cranidial base is also preserved for this specimen, indicating that the cephalon must have been inverted anteriorly during moulting, and that these are internal moulds (causing the underlapping cephalon to be impressed upon the overlying thoracopygon). Due to the impression of the cephalon upon the thorax it is likely that this is also the case for Fig. 4.4I.

A small number of moult ensembles are not complete, although this is a very rare case for *E. bilobata* and *R. takooensis* in the EBS. These usually consist of all disarticulated cephalic sclerites (for example, rostral plate with attached hypostome, and the individual librigenae), presumably from the same individual (i.e. are size compatible), but without a proximal axial shield. The corresponding axial shield may however have been preserved closeby, but broken from the moult specimen during collecting. In addition, isolated axial shields (i.e. missing the librigenae) are rare for moult ensembles of both *E. bilobata* and *R. takooensis*.

4.6 Discussion

4.6.1 Inferred moulting behaviour of *Estaingia bilobata*

The prevalence of librigenal and rostral plate displacement in moult configurations of *E. bilobata* suggests that the operation of the facial and rostral sutures, producing an ecdysial gape in the manner described by Henningsmoen (1975), was the standard mode of ecdysis in this trilobite. This, coupled with the high proportion of specimens exhibiting anterior displacement of the cranidium, suggests that *E. bilobata* moulted in a manner similar to that described for a number of other Cambrian trilobite genera, e.g. *Ogygopsis* and *Paradoxides* (McNamara & Rudkin, 1984; Whittington, 1990), *Balcoracania* (Paterson et al., 2007) and *Redlichia* (McNamara, 1986). This method involved an initial downward (towards the sediment) angling of the cephalon and upwards flexure of the dorsum (referred to as 'dorsal flexure'), followed by the opening of the facial sutures, allowing anterior egression of the trilobite from the old exoskeleton. This was possibly accomplished by a relaxation and extension of the moulting trilobite from the partially enrolled exuviae (Whittington, 1990). In the case of *E. bilobata*, the LCU (that formed the lower jaw of the ecdysial gape) was often preserved relatively intact, while the cranidium often became detached from the thoracopygon. Anterior inversion of the librigenae (Lamborghini configuration), and Salterian configurations (Richter, 1937), where the entire cephalon is anteriorly inverted, are rare. Moult configurations showing this type of inversion would require a relatively severe degree of dorsal flexure, with the cephalon at a high angle to the sediment. In some rare cases, the anterior

withdrawal of the animal may then have resulted in the dragging forward of the thoracopygon and causing the librigenae or LCU to hinge forwards (see Whittington, 1990, Figs. 2-6; McNamara & Rudkin, 1984, Fig. 11); however, the rarity of these configurations, compared to the prevalence of the standard Henningsmoen's and Harrington's configurations, suggest that this was an unusual and chance occurrence in this species.

It appears that the opening of the facial and rostral sutures in *E. bilobata* and the resulting ecdysial gape was generally sufficient for anterior withdrawal from the old exoskeleton, most often producing variations of Harrington's configuration (e.g Fig. 4.3A). After the opening of the facial and rostral sutures, the LCU would have been completely free of the cranidium, but seems to have generally remained articulated and connected to the thorax by ventral cuticle. This is consistent with the common observation of the rostral plate and/or librigenae remaining relatively *in situ* or only slightly displaced relative to the thoracopygon (e.g. Fig. 4.2A, B, D). Millimeter-scale displacements are possibly due to some degree of flexibility in the unmineralised cuticle connecting these sclerites, disturbance caused by the exuviating animal, and/or decay of these connections. The LCU is often found displaced slightly posteriorly of the life-position, presumably having been pushed backwards by the forwards movement of the individual (e.g. Fig. 4.2D). Disarticulation of the LCU from the cranidium as a complete unit was not always necessary for successful exuviation, with a number of specimens exhibiting rostral plates with one associated librigena, and the other attached to the displaced cranidium (Fig. 4.2C, E, possibly B). SAM-P 46956 (Fig. 4.2G) is particularly interesting in this regard as it seems to show a moulting progression. Initially the

thoracopygon and left librigena were shed, the trilobite then moving forward and discarding the rostral plate and right librigena, before leaving behind the cranidium. This implies multiple progressive breakages of the unmineralised cuticle connecting the various mineralised exoskeletal units.

Henningsmoen's configuration (with displacement of the LCU and cranidia; Fig. 4.2) is also very common in *E. bilobata*, and suggests that the cephalothoracic joint may have been relatively weak, easily becoming disarticulated during moulting and in doing so enlarging the ecdysial gape. Whittington (1990), however, noted that the weakest link of a cast exuviae would have been the flexible membranes attaching the cranidium to the thorax, decay of which could easily result in disarticulation and transport; he therefore suggested caution in interpreting cranidium detachment as an aid in moulting. Nevertheless, the frequency of occurrence within the EBS, and general scarcity of other disarticulations attributed to decay and transport, suggest this is a legitimate pattern. Cranidial displacement was usually to the anterior, presumably due to being carried forward by the post-ecdysial trilobite. The apparent weakness in the cephalothoracic joint may also help to explain the Salterian configurations preserved for this species (Fig. 4.3C, E). This may have provided an alternative method of exuviation following the failed opening of the facial and/or rostral sutures, with the trilobite extracting itself through the gap opened by the separation and hinging forward of the cephalon.

The majority of moult configurations preserved for *E. bilobata* within the EBS can be explained by the Sutural Gape mode, with the opening of the cephalic sutures, and common dislocation at the cephalothoracic joint, resulting in a range of configurations, probably largely due to the movements of the moulting trilobite. The

majority of configurations for *E. bilobata* show minor displacement of the LCU in Harrington's configuration (e.g. Fig. 4.3A), while Henningsmoen's configuration was also common (Fig. 4.2). Inversions of the librigenae (Lamborghini and McNamara's configurations; the latter possibly created by a pressure gradient as described in McNamara & Rudkin, 1984, Fig. 5) were very rare, as were Salterian configurations and instances of thoracic disarticulation in specimens considered to be exuviae.

4.6.2 Inferred moulting behaviour of *Redlichia takooensis*

In general, *Redlichia takooensis* also used the Sutural Gape mode of moulting via opening of the facial and rostral sutures. In contrast to *E. bilobata*, however, specimens considered to represent exuviae tend to show greater displacement of cephalic sclerites in variations of the Nutcracker configuration, exhibiting displacement of the librigenae, rostral plate and hypostome, rather than the more subtle Harrington's and Henningsmoen's configurations. This implies that breakage of the connective integument between sclerites prior to burial was common in the larger *R. takooensis* but rare in *E. bilobata*, which in turn suggests that exuvial movements in *R. takooensis* were perhaps more vigorous, resulting in "messier" exuviae. It is also possible that the articulating integument between sclerites was less robust in the larger species, and that this displacement may be a result of decay and subsequent disarticulation and movement (although we consider this less likely). Assuming disarticulation occurred during ecdysis, the disarticulated cephalic sclerites would then have fallen back to the sediment and been displaced by the movements of the moulting trilobite, pushing them away from the emptied axial

shield (e.g. Fig 4.4A, B). The apparent breakage of integument between the librigenae and rostral plate (compared to the generally articulated LCU of *E. bilobata*) and greater outwards displacement of these sclerites may also indicate more lateral body movement during moulting for *R. takooensis* compared to *E. bilobata*.

As has been suggested for other species of *Redlichia* (McNamara, 1986), it is probable that dorsal flexure played an important role in the standard mode of moulting in *R. takooensis*. The absence of anterior librigenal inversion (i.e. the Lamborghini configuration), however, suggests that enrolment may have been less acute prior to opening of the facial sutures, causing the librigenae to settle back down to the sediment following ecdysis in their relatively normal orientations. This also implies less pressure on the cephalothoracic joint, possibly explaining the relative rarity of cranidial displacement in moult ensembles of *R. takooensis*, although this may have also resulted from stronger articulation in this larger species. However, as Salterian moult configurations were more common for *R. takooensis* than *E. bilobata* (although still rare), the facial sutures may have failed to open more frequently (if this is taken to be an alternative method of ecdysis). In these scenarios, the individual may have employed a greater amount of dorsal flexure to enable the cephalothoracic joint to break. McNamara (1986, Figs. 1, 2) observed pygidial inversion for *Redlichia forresti*, which he inferred to have resulted due to posterior movement during moulting to allow extraction from the cephalic region following failure of the sutures, increasing the angle of dorsal flexure at the pygidium. He also noted thoracic segment inversions for both *R. forresti* and *R. idonea* that he interpreted to have resulted from dorsal flexure, as well as a specimen of each with an inverted right librigena in variations of McNamara's configuration (McNamara,

1986, Figs. 1B, C, E, 3). Whittington (1990), however, rejected the idea of posterior movement, and suggested such patterns of displacement and movement may simply be a result of transport and disturbance of partially decayed exuviae, or even carcasses (a possibility given the lack of evidence for the opening of facial sutures in certain specimens). We agree that specimens that do not show evidence of opened cephalic sutures, other than possible Salterian configurations, are unlikely to be moults; however, the fact that multiple specimens of *R. takooensis* within the EBS collections also exhibit McNamara's configuration, suggest that this arrangement is likely a repeated ecdysial configuration. McNamara (1986) also considered imbrication of thoracic segments to result from posterior movement, however, the imbrication seen in the EBS specimens could also result from the extraction of the thorax from the exoskeleton during anterior exuviation. Inversions, other than of cephalic structures, were not observed for *R. takooensis* or *E. bilobata*.

It is possible that the posterior-most pleural spines of *R. takooensis* were pushed into the sediment as an anchor for dorsal flexure, as suggested by Whittington (1990) for *Paradoxides*. Assuming the specimens exhibiting pygidial inversion figured by McNamara (1986) *do* represent moults, an alternative explanation to posterior movement during moulting could be that in these species the pygidium was used as anchor for dorsal flexure in a similar way; this could explain why pygidial and thoracic segment inversions are not seen in *R. takooensis*. The inverted pygidium and posteriormost thoracic segments observed in *E. bilobata* (Fig. 4.3F) might also be explained by use as an anchor for dorsal flexure, particularly given the spinose nature of the pygidium in this species (Pocock, 1964). Recurring presence of thoracic disarticulation in putative moult ensembles immediately below

segments 6 and 11, both of which support extended dorsal spines (Paterson & Jago, 2006), is unlikely to have occurred during moulting, and is probably the result of physical processes acting on the larger surface area of these segments prior to or during burial.

The normal sequence of moulting in *R. takooensis* likely began with dorsal flexure away from the sediment, followed by the opening of the cephalic sutures, with the trilobite exiting the exoskeleton through the resulting anterior gape suture, possibly using vigorous lateral and forward movements, causing the disarticulated librigenae to be displaced sideways and outwards from their usual position or, very occasionally, to become laterally inverted (Fig. 4.4F, G). Salterian configurations, although rare, are more common than in *E. bilobata*, suggesting that this was potentially an important alternative strategy following the failure of the cephalic sutures to open.

4.6.3 Comparisons with other Cambrian trilobites and localities

As discussed above, it is likely that *R. takooensis* and *E. bilobata* moulted in a similar manner to that proposed for a number of other Cambrian trilobites, namely *Ogygopsis* and *Paradoxides* (McNamara & Rudkin, 1984; Whittington, 1990), *Balcoracania* (also present within the EBS: Paterson & Jago, 2006; Paterson et al., 2007), as well as other species of *Redlichia* (McNamara, 1986). McNamara and Rudkin (1984) described two moults of *Ogygopsis klotzi* (as well as a partial possible failed moult), and a specimen of *Paradoxides davidis* from the Mount Stephen Trilobite Beds, all in a modified version of the Lamborghini configuration, possibly

with the entire LCU inverted to lie beneath the cranidium, and used this to argue for a sharp (greater than 90°) flexure of the cephalothoracic joint (and the first few thoracic segments) aimed to dislocate the cranidium from the thorax. Whittington (1990) suggested this was unlikely given that the standard mode of moulting appears to have been by opening of the ecdysial gape by removal of the LCU, based on the prevalence of complete axial shields within the deposit, as well as the fact that the facial sutures had operated in these specimens and, therefore, cranidium removal was not necessary. He suggested that such a sharp angle would have dislocated all joints between the cephalon and the first 3 thoracic segments and suggested a more continuous enrolment as an initial exuvial movement, and used these specimens as evidence to suggest that *O. klotzi* moulted in a manner similar to which he described for *Paradoxides* (i.e. via the Sutural Gape mode with dorsal flexure facilitated by posterior thoracic pleural spines). We propose that the EBS trilobites discussed in this paper moulted in a similar way.

The preservation of such detailed evidence relating to moulting behaviour in Cambrian trilobites seems to be unique to the EBS. Even exceptionally preserved deposits with very high trilobite abundances such as the Mount Stephen Trilobite Beds and the Wheeler Shale, seemingly do not preserve such a complete and diverse record. The greater prevalence of isolated axial shields within these deposits, as well as evidence for accumulations of disarticulated sclerites (Rudkin, 2009), indicate a higher level of transportation and thus disturbance of moult configurations prior to preservation (very minor currents may have been sufficient to transport disarticulated sclerites such as the librigenae, etc.). The presence of intact moult configurations within these deposits (Gaines & Droser, 2003; McNamara &

Rudkin, 1984; Rudkin, 2009), however, suggest a range of conditions. These deposits likely represent a combination of census and time-averaged assemblages as suggested by (Caron & Jackson, 2006) for the Greater Phyllopod Bed (Burgess Shale). While this is likely true for the EBS as well, conditions in general suggest extremely low levels of disturbance, with isolated axial shields and accumulations of sclerites extremely rare. It has been suggested that a fluctuating oxycline may have resulted in episodic mass kill events that excluded scavengers and inhibited decay (Paterson et al., 2016), with carcasses (and exuviae) then smothered in a steady accumulation of fine sediment. This could explain how such an exceptional *in situ* record of moulting could be preserved within the EBS.

4.6.4 Recognising moult configurations

The sedimentological context and depositional environment must be considered when distinguishing moults and carcasses in the fossil record (Daley & Drage, 2016), and moulting interpretations should be based upon a carefully reasoned identification of moult configurations. Determining the significance of thoracic segment disarticulation in ecdysis is particularly problematic. We must distinguish whether thoracic breakages are produced during moulting, and thus may be used as an indicator of a moult configuration, or if these are produced through disarticulation during decay of the soft tissue articulating the segments in exuviae or carcasses. The tendency towards systematic breaks below segments bearing long medial spines in *R. takooensis* may support the former proposition. However, for specimens of *R. takooensis* such as Fig. 4.4D, with relatively small amounts of

cephalic displacement and thoracic breaks, or of *E. bilobata* with multiple thoracic dislocations as is common in EBS specimens, it is more difficult to distinguish moults from carcasses. SAM-P 54209 (Fig. 4.4K) shows a thoracic break in a specimen we consider a carcass, note the fused cephalic units. Whittington (1990) mentioned this problem when reviewing some of the *Redlichia* specimens interpreted by McNamara (1986) to be moults, suggesting these could easily represent carcasses following decay and disturbance. We suggest that the presence of thoracic intersegmental dislocation alone (i.e. without disruption of the cephalic sutures suggesting an ecdysial gape) is likely to represent decay rather than evidence of ecdysis, although some uncertainty remains. This uncertainty, which is also true of specimens that show very minor disarticulation of cephalic sutures, can make the identification of trilobite moults problematic.

Ventral cephalic structures can be important for identifying moult configurations in groups of trilobites with hypostomal and rostral sutures. For trilobites that moulted in a similar manner to *E. bilobata* and *R. takooensis*, disarticulation of the rostral plate from the cranidium was integral to the opening of the anterior gape suture (except perhaps for Salterian configurations). The hypostome was also frequently observed displaced for *R. takooensis* (e.g. Fig 4.4E); however, several specimens otherwise considered to be moult ensembles due to their obvious anterior gape sutures seem to have the hypostome (Fig. 4.4B) and occasionally rostral plate (Fig. 4.4C) seemingly close to life position, possibly held in place by ventral unmineralised cuticle. Hypostomes both isolated and attached to disarticulated rostral plates are also known from the EBS, suggesting that dislocation of the hypostome from the rostral plate was not necessary for successful ecdysis.

Preservation at other localities (e.g. the Wheeler Shale) does not necessarily allow for identification of the ventral structures (HBD, pers. obs. 2016), presumably either due to these structures not being preserved, or obscured by the dorsal cuticle of the specimen. The preservational mode of internal/external moulds at the EBS, however, means observations and subsequent interpretations are greatly assisted by the impressions left of ventral structures. Displacement of the ventral cephalic structures, if observed, may therefore be useful in positive identification of a moult given their importance to the opening of an anterior gape suture, however, observed amounts of displacement may be minimal, and does not not necessarily preclude specimens from being exuviae if not seen.

The pygidium and final few thoracic segments of *E. bilobata* often appear curled under the thorax, presumably due to muscle contraction during death and/or decay. This occurs in complete, intact exoskeletons, considered putative carcasses. Exuviae of *E. bilobata* do not appear to display this pygidial enrolment, presumably due to the lack of required musculature. This may assist in moult identification for specimens of *E. bilobata* with only slight displacement of sclerites, and has the potential to be of broader use if identified in other trilobite species.

Interestingly, a large proportion of trilobite specimens within the EBS are preserved “dorsum-down”; previous sampling of a number of different surfaces have suggested greater than 75% of specimens are orientated in this manner (Gehling et al., 2011). A recent field sample of 100 specimens of *E. bilobata* taken from adjacent mudstone beds revealed 90 “dorsum-down” specimens, 6 “upright” specimens, and 4 small and/or partial specimens either enrolled, or (less likely) representing moulted exoskeletons in Salter’s configuration (JDH pers. obs. 2015). It has been suggested

previously that carcasses may be turned dorsum-down due to the escape of decay gases (Gehling et al., 2011). It is therefore possible that the majority of upright specimens in this sample represent moults. The 6 “upright” specimens from the field study were examined in this light, with at least two specimens likely representing moults. Unfortunately, the remaining specimens were difficult to analyse due to poor/partial preservation. If this is indeed the case, it may provide additional evidence in identifying moults from carcasses in the EBS, and potentially at other sites as well.

It is important to note that more unusual moult configurations are likely to be preferentially collected rather than those displaying more subtle patterns (McNamara & Rudkin, 1984). For *E. bilobata* this is particularly important, as most putative moult ensembles observed *in situ* show only minor displacement of the LCU, as originally suggested by Pocock (1964). The examples illustrated here show a relatively wide range of moult configurations and we have invariably overemphasised the importance of some relative to others in terms of overall numerical abundance, in the interest of describing the majority of scenarios. We stress that in the case of *E. bilobata* the majority of moult configurations probably resemble Figs. 4.2A and 4.3A, but that a quantitative study of the relative proportions of configurations (for both species) would be invaluable for greater understanding of their moulting behaviour (see Section 5.2).

4.7 Conclusions

The uniquely abundant moult configurations of two trilobite species from the early Cambrian EBS Lagerstätte, *Estaingia bilobata* and *Redlichia takooensis*, have allowed for detailed interpretations of moulting behaviour to be made. The moult configurations figured and discussed suggest that these trilobites used a 'Sutural Gape' mode of moulting (Henningsmoen, 1975), with disarticulation of the facial and rostral sutures creating an anterior exuvial gape. Dorsal flexure (i.e. partial enrolment) of the exoskeleton away from the sediment is implicated in producing a number of the configurations described for both species, suggesting that *E. bilobata* and *R. takooensis* moulted in a manner consistent with that described for certain other Cambrian trilobites (McNamara, 1986; McNamara & Rudkin, 1984; Paterson et al., 2007; Whittington, 1990).

Despite these similarities, *E. bilobata* and *R. takooensis* tend to exhibit different patterns of variation within the Sutural Gape mode. For example, *E. bilobata* usually produced arrangements in Harrington's or Henningsmoen's configurations, with an articulated 'lower cephalic unit' (*sensu* Henningsmoen, 1975), whereas in *R. takooensis* these sclerites usually became separated and displaced laterally outwards from the axial shield (i.e. the Nutcracker configuration). This suggests that *R. takooensis* may have used more vigorous or spasmodic movements to withdraw from the old exoskeleton than *E. bilobata*, similar to some modern marine arthropods. Both species also show rare instances of McNamara's and Salter's configurations, with the latter more common in *R. takooensis*.

The preservation of detailed moulting information in the EBS trilobites seems to be a result of a unique depositional environment, with an almost complete lack of water movement, anoxic conditions on the seafloor, and a high sedimentation rate likely contributing factors to the minimal disturbance observed. This is in contrast to other sites with an abundance of trilobites, where there is often evidence for greater levels of exoskeletal disturbance resulting from transport and disarticulation. It is likely that the more limited preservation at other sites has masked some of the variation in trilobite moulting behaviour.

4.8 Acknowledgements

Mary-Anne Binnie (SAM) and Claire Mellish (NHMUK) are thanked for access to specimens. John Paterson provided extremely helpful discussions on this paper. Emu Bay Shale research has been possible thanks to the Buck family for allowing continued access to the fossil sites and by funding from the Australian Research Council (grant LP0774959), a National Geographic Society Research and Exploration Grant (#8991-11) and Spanish Ministry of Economy and Competitiveness (CGL2009-07073 and CGL2013-48877-P), with financial assistance from Beach Energy Ltd and the South Australian Museum. H. B. Drage is supported by Natural Environment Research Council doctoral training grant number NE/L002612/1, J. D. Holmes by a Masters (No Honours) scholarship from the University of Adelaide and D. C. García-Bellido by Australian Research Council Future Fellowship FT130101329.

4.9 References

Bengtson, S., Conway Morris, S., Cooper, B. J., Jell, P. A., & Runnegar, B. N. (1990). Early Cambrian fossils from South Australia. *Memoirs of the Association of Australasian Palaeontologists, 9*, 1-364.

Caron, J. B., & Jackson, D. A. (2006). Taphonomy of the Greater Phyllopod Bed Community, Burgess Shale. *Palaios, 21*, 451-465.

Conway Morris, S., & Jenkins, R. J. F. (1985). Healed injuries in Early Cambrian trilobites from South Australia. *Alcheringa, 9*, 167-177.

Dai, T., & Zhang, X. L. (2012). Ontogeny of the trilobite *Estaingia sinensis* (Chang) from the Lower Cambrian of South China. *Bulletin of Geosciences, 87*, 151-158.

Daily, B., Moore, P. S., & Rust, B. R. (1980). Terrestrial-marine transition in the Cambrian rocks of Kangaroo Island, South Australia. *Sedimentology, 27*, 379-399.

Daley, A. C., & Drage, H. B. (2016). The fossil record of ecdysis, and trends in the moulting behaviour of trilobites. *Arthropod Structure & Development, 45*, 71-96.

Gaines, R. R. (2014). Burgess Shale-type preservation and its distribution in space and time. In M. Laflamme, J. D. Schiffbauer (Eds.), Reading and Writing of the Fossil Record: Preservational Pathways to Exceptional Fossilization. *The Paleontological Society Papers, 20*, 123-146.

Gaines, R. R., & Droser, M. L. (2003). Paleoecology of the familiar trilobite *Elrathia kingii*: An early exaerobic zone inhabitant. *Geology, 31*, 941-944.

García-Bellido, D. C., Paterson, J. R., Edgecombe, G. D., Jago, J. B., Gehling, J. G., & Lee, M. S. Y. (2009). The bivalved arthropods *Isoxys* and *Tuzoia* with soft-part preservation from the Lower Cambrian Emu Bay Shale Lagerstätte (Kangaroo Island, Australia). *Palaeontology, 52*, 1221-1241.

Gehling, J. G., Jago, J. B., Paterson, J. R., García-Bellido, D. C., & Edgecombe, G. D. (2011). The geological context of the Lower Cambrian (Series 2) Emu Bay Shale Lagerstätte and adjacent stratigraphic units, Kangaroo Island, South Australia. *Australian Journal of Earth Sciences, 58*, 243-257.

Henningsmoen, G. (1957). The trilobite Family Olenidae. *Skrifter utgitt av det Norske Videnskaps-Akademi i Oslo. 1 Matematisk-naturvidenskapelig klasse, 1957, 1*, 1-303.

Henningsmoen, G. (1975). Moulting in trilobites. *Fossils and Strata, 4*, 179-200.

Jago, J. B., & Cooper, B. J. (2011). The Emu Bay Shale Lagerstätte: a history of investigations. *Australian Journal of Earth Sciences, 58*, 235-241.

Jago, J. B., García-Bellido, D. C., & Gehling, J. G. (2016). An early Cambrian chelicerate from the Emu Bay Shale, South Australia. *Palaeontology, 59*, 549-562.

Jago, J. B., Zang, W.-L., Sun, X., Brock, G. A., Paterson, J. R., & Skovsted, C. B. (2006). A review of the Cambrian biostratigraphy of South Australia. *Palaeoworld, 15*, 406-423.

Lu, Y. H. (1950). On the genus *Redlichia* with description of its new species. *Geological Review, 15*, 157-170.

McKirdy, D. M., Hall, P. A., Nedin, C., Halverson, G. P., Michaelsen, B. H., Jago, J. B., . . . Jenkins, R. J. F. (2011). Paleoredox status and thermal alteration of

the lower Cambrian (Series 2) Emu Bay Shale Lagerstätte, South Australia. *Australian Journal of Earth Sciences, 58*, 259-272.

McNamara, K. J. (1986). Techniques of exuviation in Australian species of the Cambrian trilobite *Redlichia*. *Alcheringa, 10*, 403-412.

McNamara, K. J., & Rudkin, D. M. (1984). Techniques of trilobite exuviation. *Lethaia, 17*, 153-173.

Nedin, C. (1999). *Anomalocaris* predation of nonmineralized and mineralized trilobites. *Geology, 27*, 987-990.

Palmer, A. R., & Rowell, A. J. (1995). Early Cambrian Trilobites from the Shackleton Limestone of the Central Transantarctic Mountains. *Palaeontological Society Memoir, 45*.

Paterson, J. R. (2005). Revision of *Discomesites* and *Estaingia* (Trilobita) from the Lower Cambrian Cymbric Vale Formation, Western New South Wales: Taxonomic, Biostratigraphic and Biogeographic Implications. *Proceedings of the Linnean Society of New South Wales, 126*, 89-93.

Paterson, J. R., & Brock, G. A. (2007). Early Cambrian trilobites from Angorichina, Flinders Ranges, South Australia, with a new assemblage from the Pararaia bunyerooensis Zone. *Journal of Paleontology, 81*, 116-142.

Paterson, J. R., García-Bellido, D. C., Jago, J. B., Gehling, J. G., Lee, M. S. Y., & Edgecombe, G. D. (2016). The Emu Bay Shale Konservat-Lagerstätte: a view of Cambrian life from East Gondwana. *Journal of the Geological Society, London, 173*, 1-11.

Paterson, J. R., & Jago, J. B. (2006). New trilobites from the Lower Cambrian Emu Bay Shale Lagerstätte at Big Gully, Kangaroo Island, South Australia. *Memoirs of the Association of Australasian Palaeontologists, 32*, 43-57.

Paterson, J. R., Jago, J. B., Brock, G. A., & Gehling, J. G. (2007). Taphonomy and palaeoecology of the emuellid trilobite *Balcoracania dailyi* (early Cambrian, South Australia). *Palaeogeography, Palaeoclimatology, Palaeoecology, 249*, 302-321.

Paterson, J. R., Jago, J. B., Gehling, J. G., García-Bellido, D. C., Edgecombe, G. D., & Lee, M. S. Y. (2008). Early Cambrian arthropods from the Emu Bay Shale Lagerstätte, South Australia. In I. Rábano, R. Gonzalo, & D. García-Bellido (Eds.), *Advances in trilobite research* (pp. 319-325). Madrid: Instituto Geológico y Minero de España.

Peng, S., Babcock, L. E., & Cooper, R. A. (2012). The Cambrian Period. In F. M. Gradstein, J. G. Ogg, M. D. Schmitz, & G. M. Ogg (Eds.), *The Geologic Time Scale 2012, Volume 2* (pp. 437-488). Oxford: Elsevier.

Pocock, K. J. (1964). *Estaingia*, a new trilobite genus from the Lower Cambrian of South Australia. *Palaeontology, 7*, 458-471.

Richter, R. (1937). Von Bau und Leben der Trilobiten. 8. Die "Salter'sche Einbettung" als Folge und Kennzeichen des Häutungs-Vorgangs. *Senckenbergiana, 19*, 413-431.

Rudkin, D. M. (2009). The Mount Stephen Trilobite Beds. In J.-B. Caron and D. Rudkin (Eds.), A Burgess Shale Primer: History, Geology, and Research Highlights. The Burgess Shale Consortium, Toronto, Canada, p. 91–102.

Sprigg, R. C. (1955). The Point Marsden Cambrian beds, Kangaroo Island, South Australia. *Transactions of the Royal Society of South Australia, 78*, 165-168.

Whittington, H. B. (1990). Articulation and exuviation in Cambrian trilobites. *Philosophical Transactions of the Royal Society B: Biological Sciences, 329*, 27-46.

Zhang, W.-T., Lu, Y.-H., Zhu, Z.-L., Qian, Y.-Y., Lin, H.-L., Zhou, Z.-Y., Zhang, S.-G. & Yuan, J.-L. (1980). Cambrian trilobite faunas of southwestern China. *Palaeontologia Sinica, new series B, 159*, 1-497.

Chapter 5 – Conclusions

5.1 Summary

The papers presented in this thesis examine two major aspects of the Emu Bay Shale (EBS) biota, and how these compare to other Burgess Shale-type (BST) assemblages, initially in a broad sense by analysing the biogeographic relationships between these sites from a global perspective, and then at a more focused level by examining and comparing the preservation of trilobite moulting characteristics within the EBS and other similar deposits.

BST biotas from around the world have been the subject of much scientific investigation, and similarities and links between these exceptionally preserved assemblages have been proposed by numerous studies, however, no quantitative analysis between sites has previously been undertaken. The analyses conducted in Chapter 2 therefore provide the first quantitative study examining the biogeographic links between BST assemblages. Findings suggest that similarity between assemblages increases from Cambrian Series 2 through Series 3, driven largely by an increase in shared biomineralised taxa that are subject to frequent turnover, against a background of cosmopolitan taxa that are characteristic of BST biotas, many of which persist across long periods – in some cases the entire period under question (e.g. *Anomalocaris*, *Tuzoia*, *Isoxys*). There are also clear trends in the proportional dominance of groups within these communities (based on numbers of genera), suggesting systematic change in the structure of these communities across the period. This is consistent with the idea that these were some of the earliest modern-type ecosystems, within which lineages (and therefore communities) were likely evolving rapidly.

As expected, the EBS exhibits similarities with other Gondwanan sites from South China, likely reflecting a regional relationship, although given the importance of age demonstrated in assemblage similarity (albeit mostly in younger sites), and the similarity in age between the South Chinese and EBS assemblages, it is stressed that age is likely to be an important factor as well. In contrast, the decreasing level of assemblage similarity between the EBS and assemblages further to the west in the continental reconstructions implies a geographic signal, and also suggests that the appearance and dispersal of constituent taxa occurred between Gondwana to the east and Laurentia to the west, with little evidence for dispersal across the Iapetus Ocean.

The findings discussed in Chapter 3 suggest that the EBS preserves a record of trilobite moulting behaviour unparalleled in other fossil assemblages. An abundance of specimens, coupled with little-to-no disturbance prior to burial, has allowed the detailed description of the moult configurations for two species of trilobite, *Estaingia bilobata* and *Redlichia takooensis*, from which moulting behaviours were inferred. This has shown that both species used a "sutural gape" method of moulting, however, analysis also revealed a level of plasticity in the moulting behaviours within this mode, and suggests that methods described for trilobites from deposits exhibiting lower quality preservation most likely reflect "normal" modes of ecdysis, rather than the range of possibilities. In the Mount Stephen Trilobite Beds and the Wheeler Shale, both of which house BST biotas, specimens are mostly present as axial shields and provide little information on the movements made by *Elrathia kingii* and *Ogygopsis klotzi*, other than that they likely

also employed a “sutural gape” method. Rarer complete specimens described in the literature suggest they moulted in a similar way to the EBS trilobites.

The results presented in this thesis lend support to the idea that the EBS assemblage is a typical BST biota, preserved in an abnormal fashion. The unusual depositional setting of the EBS appears to have little effect on the taxa present within the assemblage, while allowing preservation of certain aspects of the biota that are not preserved at other sites, e.g. moulting behaviours and unique preservation of structures such as eyes. As such, it is of great importance to our understanding of early life and the evolution of some of the earliest animals and communities on Earth.

5.2 Future directions

There is still much to be learnt from the EBS and other BST biotas despite over a century of investigation into the latter. One of the major reasons behind the importance of these assemblages is the ability to gain enough information for complex ecological analyses, something that is much more limited for other sites. Broad assemblage comparisons from an ecological perspective using abundance data for individual localities would provide a greater understanding of the relationships between sites, particularly from an environmental perspective. This is no small undertaking and would require detailed classification of individual species into various ‘life history’ groupings common across all localities. Ecological analysis of this kind has been undertaken for a number of sites, such as the Phyllopod Bed

(Burgess Shale) and various locations of the Chengjiang Biota, although it is yet to be conducted on the EBS material. The abundance of trilobite exuviae within the EBS also invites a quantitative study to determine the frequency of certain configurations, and hence behaviours, for this very successful and long-ranging group of arthropods.

No significant problems were encountered during the course of this project.

Chapter 6 – Appendices

6.1 Electronic Supplementary Material

PDF file of thesis (identical to this version)

Chapter 3

- Data matrices for R and PAST analyses
- R script files for all analyses conducted
- MrBayes (Bayesian) and PAUP* (PAE) executable files
- Matrix of presence/absence of genera and high level taxonomic classification

6.2 Supplementary Material for Chapter 3

Supplementary Table 6.1: Presence/absence matrix of genera at 12 Cambrian Lagerstätten analysed in Chapter 3. Uncertain assignations (e.g. c.f., aff. ?) were coded as "?". Phylum/Type was used to conduct the phyla diversity analysis (with additional taxa from sites not identified to genus level – see Supp. Tab. 6.3 for a list of references).

	Genus	Phylum/Type	Chengjiang	Sirius Passet	Sinsk	Guanshan	Balang	Emu Bay Shale	Kinzers	Kaili	Spence	Burgess Shale	Wheeler	Marjum
1	Aldanophyton	Algae/Cyanobacteria	0	0	1	0	0	0	0	0	0	0	0	0
2	Bosworthia	Algae/Cyanobacteria	0	0	0	0	0	0	0	1	0	1	0	0
3	Chuaria	Algae/Cyanobacteria	0	0	0	0	0	0	0	1	0	0	0	0
4	Dalyia	Algae/Cyanobacteria	0	0	0	0	0	0	1	0	0	1	0	0
5	Dictyophycus	Algae/Cyanobacteria	0	0	0	0	0	0	0	0	0	1	0	0
6	Doushantuophyton	Algae/Cyanobacteria	0	0	0	0	0	0	0	1	0	0	0	0
7	Enteromophites	Algae/Cyanobacteria	1	0	0	0	0	0	0	1	0	0	0	0
8	Eosargassum	Algae/Cyanobacteria	0	0	0	0	0	0	0	1	0	0	0	0
9	Epiphyton	Algae/Cyanobacteria	0	0	0	0	0	0	0	0	0	0	1	0
10	Fractibeltia	Algae/Cyanobacteria	0	0	0	0	0	0	0	1	0	0	0	0
11	Fuxianospira	Algae/Cyanobacteria	1	0	0	0	0	0	0	0	0	0	0	0
12	Girvanella	Algae/Cyanobacteria	0	0	0	0	0	0	0	0	0	0	1	0
13	Laenigma	Algae/Cyanobacteria	0	0	1	0	0	0	0	0	0	1	0	0
14	Leafiophyton	Algae/Cyanobacteria	0	0	0	0	0	0	0	1	0	0	0	0
15	Lechampia	Algae/Cyanobacteria	0	0	1	0	0	0	0	0	0	0	0	0
16	Lenocladium	Algae/Cyanobacteria	0	0	1	0	0	0	0	0	0	0	0	0
17	Lenodesmia	Algae/Cyanobacteria	0	0	1	0	0	0	0	0	0	0	0	0
18	Margaretia	Algae/Cyanobacteria	0	0	0	1	0	0	1	0	1	1	1	1
19	Marpolia	Algae/Cyanobacteria	0	0	1	0	0	0	1	1	1	1	1	0
20	Megaspinella	Algae/Cyanobacteria	0	0	0	0	0	0	0	1	0	0	0	0
21	Megaspirellus	Algae/Cyanobacteria	1	0	0	0	0	0	0	0	0	0	0	0
22	Morania	Algae/Cyanobacteria	0	0	0	0	0	0	1	1	1	1	1	1
23	Palaeodictyota	Algae/Cyanobacteria	0	0	0	0	0	0	0	1	0	0	0	0
24	Parafunaria	Algae/Cyanobacteria	0	0	0	0	0	0	0	1	0	0	0	0
25	Parallelphyton	Algae/Cyanobacteria	0	0	0	0	0	0	0	1	0	0	0	0
26	Renalcis	Algae/Cyanobacteria	0	0	0	0	0	0	0	0	0	0	1	0
27	Sinocylindra	Algae/Cyanobacteria	1	0	0	0	0	0	0	1	0	0	1	1
28	Sphaerocodium	Algae/Cyanobacteria	0	0	0	0	0	0	0	0	0	?	0	0
29	Thamnophyton	Algae/Cyanobacteria	0	0	0	0	0	0	0	1	0	0	0	0
30	Wahpia	Algae/Cyanobacteria	0	0	0	0	0	0	0	0	0	1	0	0
31	Waputikia	Algae/Cyanobacteria	0	0	0	0	0	0	0	0	0	1	0	0
32	Burgessochaeta	Annelida	0	0	0	0	0	0	0	0	0	1	0	0
33	Canadia	Annelida	0	0	0	0	0	0	0	0	1	1	0	0
34	Guanshanchaeta	Annelida	0	0	0	1	0	0	0	0	0	0	0	0
35	Hyolithellus	Annelida	0	1	0	0	0	0	0	0	0	0	1	1
36	Insolicorypha	Annelida	0	0	0	0	0	0	0	0	0	1	0	0
37	Maotianchaeta	Annelida	?	0	0	0	0	0	0	0	0	0	0	0
38	Peronochaeta	Annelida	0	0	0	0	0	0	0	0	0	1	0	0
39	Phragmochaeta	Annelida	0	1	0	0	0	0	0	0	0	0	0	0
40	Pygocirrus	Annelida	0	1	0	0	0	0	0	0	0	0	0	0

41	Selkirkia	Annelida	1	0	0	0	0	0	1	1	1	1	1	1
42	Stephenoscolex	Annelida	0	0	0	0	0	0	0	0	0	1	0	0
43	Aaveqaspis	Arthropoda	0	1	0	0	0	0	0	0	0	0	0	0
44	Acanthomeridion	Arthropoda	1	0	0	0	0	0	0	1	0	0	0	0
45	Actaeus	Arthropoda	0	0	0	0	0	0	0	0	0	1	0	0
46	Alalcomenaeus	Arthropoda	0	0	0	0	0	0	0	0	0	1	0	0
47	Alicaris	Arthropoda	0	0	0	0	0	0	0	1	0	0	0	0
48	Aluta	Arthropoda	0	0	0	0	1	0	0	0	0	0	0	0
49	Alutella	Arthropoda	0	0	0	0	1	0	0	0	0	0	0	0
50	Amplectobelua	Arthropoda	1	0	0	0	0	0	0	1	0	1	0	0
51	Anabarochilina	Arthropoda	0	0	0	0	0	0	0	0	0	0	0	1
52	Anomalocaris	Arthropoda	1	0	0	1	1	1	1	1	1	1	1	1
53	Arthroaspis	Arthropoda	0	1	0	0	0	0	0	0	0	0	0	0
54	Auriculatella	Arthropoda	1	0	0	0	0	0	0	0	0	0	0	0
55	Australimicola	Arthropoda	0	0	0	0	0	1	0	0	0	0	0	0
56	Branchiocaris	Arthropoda	?	0	0	1	0	0	0	0	?	1	?	?
57	Buenaspis	Arthropoda	0	1	0	0	0	0	0	0	0	0	0	0
58	Burgessia	Arthropoda	0	0	0	0	0	0	0	0	0	1	0	0
59	Cambropodus	Arthropoda	0	0	0	0	0	0	0	0	0	0	1	0
60	Campanamuta	Arthropoda	0	1	0	0	0	0	0	0	0	0	0	0
61	Canadaspis	Arthropoda	1	0	0	0	0	0	0	1	1	1	1	0
62	Carnarvonia	Arthropoda	0	0	0	0	0	0	0	0	0	1	0	0
63	Caryosyntrips	Arthropoda	0	0	0	0	0	0	0	0	0	1	0	0
64	Chengjiangocaris	Arthropoda	1	0	0	0	0	0	0	0	0	0	0	0
65	Cindarella	Arthropoda	1	0	0	0	0	0	0	0	0	0	0	0
66	Combinivalvula	Arthropoda	1	0	0	0	0	0	0	1	0	0	0	0
67	Comptaluta	Arthropoda	1	0	0	0	1	0	0	0	0	0	0	0
68	Cucumericrus	Arthropoda	1	0	0	0	0	0	0	0	0	0	0	0
69	Cyathocephalus	Arthropoda	1	0	0	0	0	0	0	0	0	0	0	0
70	Dabashanella	Arthropoda	1	0	0	0	0	0	0	0	0	0	0	0
71	Dicerocaris	Arthropoda	0	0	0	0	0	0	0	0	0	0	1	0
72	Dicranocaris	Arthropoda	0	0	0	0	0	0	0	0	0	0	1	1
73	Dioxycaris	Arthropoda	0	0	0	0	0	0	0	0	1	0	0	0
74	Diplopyge	Arthropoda	1	0	0	0	0	0	0	0	0	0	0	0
75	Dongshanocaris	Arthropoda	1	0	0	0	0	0	0	0	0	0	0	0
76	Duibianella	Arthropoda	0	0	1	0	0	0	0	0	0	0	0	0
77	Dytikosicula	Arthropoda	0	0	0	0	0	0	0	0	0	0	0	1
78	Ecnomocaris	Arthropoda	0	0	0	0	0	0	0	0	0	0	1	0
79	Emeiella	Arthropoda	1	0	0	0	0	0	0	0	0	0	0	0
80	Emeraldella	Arthropoda	0	0	0	0	0	0	0	0	0	1	1	0
81	Emucaris	Arthropoda	0	0	0	0	0	1	0	0	0	0	0	0
82	Ercaia	Arthropoda	1	0	0	0	0	0	0	0	0	0	0	0
83	Ercaicunia	Arthropoda	1	0	0	0	0	0	0	0	0	0	0	0
84	Erjiecaris	Arthropoda	1	0	0	0	0	0	0	0	0	0	0	0
85	Forfexicaris	Arthropoda	1	0	0	0	0	0	0	1	0	0	0	0
86	Fortiforceps	Arthropoda	1	0	0	0	0	0	0	0	0	0	0	0
87	Fuxianhuia	Arthropoda	1	0	0	0	0	0	0	0	0	0	0	0
88	Glossocaris	Arthropoda	1	0	0	0	0	0	0	0	0	0	0	0
89	Guangweicaris	Arthropoda	0	0	0	1	0	0	0	0	0	0	0	0
90	Habelia	Arthropoda	0	0	0	0	0	0	0	0	0	1	0	0
91	Haifengella	Arthropoda	1	0	0	0	0	0	0	0	0	0	0	0
92	Haikoucaris	Arthropoda	1	0	0	0	0	0	0	0	0	0	0	0
93	Hanchiangella	Arthropoda	1	0	0	0	0	0	0	0	0	0	0	0

94	Helmetia	Arthropoda	0	0	0	0	0	0	0	0	0	1	0	0
95	Houlongdongella	Arthropoda	0	0	0	1	0	0	0	0	0	0	0	0
96	Hurdia	Arthropoda	0	0	0	0	0	0	0	0	1	1	1	0
97	Isoxys	Arthropoda	1	1	0	1	1	1	0	1	1	1	0	0
98	Jianfengia	Arthropoda	1	0	0	0	0	0	0	0	0	0	0	0
99	Jiucunella	Arthropoda	1	0	0	0	0	0	0	0	0	0	0	0
100	Jugatacaris	Arthropoda	1	0	0	0	0	0	0	0	0	0	0	0
101	Kangacaris	Arthropoda	1	0	0	0	0	1	0	0	0	0	0	0
102	Kerygmachela	Arthropoda	0	1	0	0	0	0	0	0	0	0	0	0
103	Kiisortoqia	Arthropoda	0	1	0	0	0	0	0	0	0	0	0	0
104	Kleptothule	Arthropoda	0	1	0	0	0	0	0	0	0	0	0	0
105	Kuamaia	Arthropoda	1	0	0	0	0	0	0	1	0	0	0	0
106	Kunmingella	Arthropoda	1	0	0	0	0	0	0	1	0	0	0	0
107	Kunmingocaris	Arthropoda	1	0	0	0	0	0	0	0	0	0	0	0
108	Kunyangella	Arthropoda	1	0	0	0	0	0	0	0	0	0	0	0
109	Kwanyinaspis	Arthropoda	1	0	0	0	0	0	0	0	0	0	0	0
110	Leanchoilia	Arthropoda	1	0	0	1	0	0	0	1	1	1	0	1
111	Liangshanella	Arthropoda	1	0	0	1	0	0	0	1	0	1	1	0
112	Liangwangshania	Arthropoda	1	0	0	0	0	0	0	0	0	0	0	0
113	Longquania	Arthropoda	0	0	0	1	0	0	0	0	0	0	0	0
114	Loricicaris	Arthropoda	0	0	0	0	0	0	0	0	0	1	0	0
115	Luohuilinella	Arthropoda	1	0	0	0	0	0	0	0	0	0	0	0
116	Mafangia	Arthropoda	1	0	0	0	0	0	0	0	0	0	0	0
117	Mafangocaris	Arthropoda	1	0	0	0	0	0	0	0	0	0	0	0
118	Malongella	Arthropoda	1	0	0	0	0	0	0	0	0	0	0	0
119	Marrella	Arthropoda	0	0	0	0	1	0	0	1	0	1	0	0
120	Meishucunella	Arthropoda	1	0	0	0	0	0	0	0	0	0	0	0
121	Meristosoma	Arthropoda	0	0	0	0	0	0	0	0	1	0	0	1
122	Misszhouia	Arthropoda	0	0	0	0	0	0	0	0	0	1	0	0
123	Molaria	Arthropoda	0	0	0	0	0	0	0	0	0	1	0	0
124	Mollisonia	Arthropoda	0	0	0	0	0	0	0	1	1	1	1	0
125	Nanchengella	Arthropoda	1	0	0	0	0	0	0	0	0	0	0	0
126	Naraoia	Arthropoda	1	0	0	0	1	0	0	1	0	1	1	1
127	Neokunmingella	Arthropoda	1	0	0	1	0	0	0	0	0	0	0	0
128	Nereocaris	Arthropoda	0	0	0	0	0	0	0	0	0	1	0	0
129	Nettapezoura	Arthropoda	0	0	0	0	0	0	0	0	0	0	0	1
130	Occacaris	Arthropoda	1	0	0	0	0	0	0	?	0	0	0	0
131	Odaraia	Arthropoda	?	0	0	0	0	0	0	0	0	1	0	0
132	Oestokerkus	Arthropoda	0	0	0	0	0	1	0	0	0	0	0	0
133	Opabinia	Arthropoda	0	0	0	0	0	0	0	0	0	1	0	0
134	Ovalicephalus	Arthropoda	1	0	0	0	0	0	0	0	0	0	0	0
135	Pahvantia	Arthropoda	0	0	0	0	0	0	0	0	0	0	1	0
136	Pambdelurion	Arthropoda	0	1	0	0	0	0	0	0	0	0	0	0
137	Panlongia	Arthropoda	0	0	0	1	0	0	0	0	0	0	0	0
138	Paranomalocaris	Arthropoda	0	0	0	1	0	0	0	0	0	0	0	0
139	Parapaleomerus	Arthropoda	1	0	0	0	0	0	0	0	0	0	0	0
140	Parapeytoia	Arthropoda	1	0	0	1	0	0	0	?	0	0	0	0
141	Pauloterminus	Arthropoda	0	1	0	0	0	0	0	0	0	0	0	0
142	Pectocaris	Arthropoda	1	0	0	0	0	0	0	0	0	0	0	0
143	Perspicaris	Arthropoda	0	0	0	0	0	0	0	1	0	1	?	?
144	Peytoia	Arthropoda	0	0	0	0	1	0	0	0	0	1	0	0
145	Phasoia	Arthropoda	1	0	0	0	0	0	0	0	0	0	0	0
146	Phytophilaspis	Arthropoda	0	0	1	0	0	0	0	0	0	0	0	0

147	Pisinnocaris	Arthropoda	1	0	0	0	0	0	0	0	0	0	0	0
148	Plenocaris	Arthropoda	0	0	0	0	0	0	0	0	0	1	0	0
149	Primicaris	Arthropoda	1	0	0	0	0	0	0	0	0	1	0	0
150	Proboscicaris	Arthropoda	0	0	0	0	0	0	0	0	0	0	1	0
151	Pseudoarctolepis	Arthropoda	0	0	0	0	0	0	0	1	0	0	1	0
152	Pseudoiulia	Arthropoda	1	0	0	0	0	0	0	0	0	0	0	0
153	Pterofrum	Arthropoda	1	0	0	0	0	0	0	0	0	0	0	0
154	Pygmaclypeatus	Arthropoda	1	0	0	0	0	0	0	0	0	0	0	0
155	Retifacies	Arthropoda	1	0	0	0	0	0	0	0	0	0	0	0
156	Rhombicalvaria	Arthropoda	1	0	0	0	0	0	0	0	0	0	0	0
157	Sanctacaris	Arthropoda	0	0	0	0	0	0	0	0	0	1	0	0
158	Saperion	Arthropoda	1	0	0	0	0	0	0	0	0	0	0	0
159	Sarotrocercus	Arthropoda	0	0	0	0	0	0	0	0	0	1	0	0
160	Serracaris	Arthropoda	0	0	0	0	0	0	1	0	0	0	0	0
161	Shangsiella	Arthropoda	1	0	0	0	0	0	0	0	0	0	0	0
162	Shankouia	Arthropoda	1	0	0	0	0	0	0	0	0	0	0	0
163	Sidneyia	Arthropoda	1	0	0	0	0	0	0	0	1	1	?	0
164	Sinoburius	Arthropoda	1	0	0	1	0	0	0	0	0	0	0	0
165	Sinskolutella	Arthropoda	0	0	1	0	0	0	0	0	0	0	0	0
166	Siriocaris	Arthropoda	0	1	0	0	0	0	0	0	0	0	0	0
167	Skania	Arthropoda	0	0	0	0	0	0	0	1	0	1	0	0
168	Skioldia	Arthropoda	1	0	0	0	0	0	0	0	0	0	0	0
169	Spinokunmingella	Arthropoda	1	0	0	0	0	0	0	0	0	0	0	0
170	Squamacula	Arthropoda	1	0	0	0	0	1	0	0	0	0	0	0
171	Stanleycaris	Arthropoda	0	0	0	0	0	0	0	0	0	1	0	0
172	Sunella	Arthropoda	1	0	0	0	0	0	0	0	0	0	0	0
173	Surusicaris	Arthropoda	0	0	0	0	0	0	0	0	0	1	0	0
174	Synophalos	Arthropoda	1	0	0	0	0	0	0	0	0	0	0	0
175	Syrrhaptis	Arthropoda	1	0	0	0	0	0	0	0	0	0	0	0
176	Tamisiocaris	Arthropoda	0	1	0	0	0	0	0	0	0	0	0	0
177	Tanglangia	Arthropoda	1	0	0	0	0	1	0	0	0	0	0	0
178	Tegopelte	Arthropoda	0	0	0	0	0	0	0	0	0	1	0	0
179	Thelxiope	Arthropoda	0	0	0	0	0	0	0	0	0	1	0	0
180	Tsunyiella	Arthropoda	1	0	0	0	0	0	0	0	0	0	0	0
181	Tubuterium	Arthropoda	0	0	1	0	0	0	0	0	0	0	0	0
182	Tuzoia	Arthropoda	1	0	1	1	1	1	1	1	1	1	?	1
183	Urokodia	Arthropoda	1	0	0	0	0	0	0	1	0	0	0	0
184	Utahcaris	Arthropoda	0	0	0	0	0	0	0	0	1	0	0	0
185	Waptia	Arthropoda	1	0	0	1	0	0	0	?	1	1	0	0
186	Wisangocaris	Arthropoda	0	0	0	0	0	1	0	0	0	0	0	0
187	Worthenella	Arthropoda	0	0	0	0	0	0	0	0	0	1	0	0
188	Wutingella	Arthropoda	1	0	0	0	0	0	0	0	0	0	0	0
189	Xandarella	Arthropoda	1	0	0	0	0	0	0	1	0	0	0	0
190	Yakutingella	Arthropoda	0	0	1	0	0	0	0	0	0	0	0	0
191	Yawunik	Arthropoda	0	0	0	0	0	0	0	0	0	1	0	0
192	Yohoia	Arthropoda	0	0	0	0	0	0	0	0	1	1	0	0
193	Yunnanocaris	Arthropoda	1	0	0	0	0	0	0	0	0	0	0	0
194	Acanthotretella	Brachiopoda	0	0	0	1	0	0	0	0	0	1	0	0
195	Acrothele	Brachiopoda	0	0	0	0	0	0	0	1	1	0	1	1
196	Acrothyra	Brachiopoda	0	0	0	0	0	0	0	0	0	1	1	0
197	Alisina	Brachiopoda	1	0	0	0	0	0	0	0	0	0	0	0
198	Askepasma	Brachiopoda	0	0	0	0	1	0	0	0	0	0	0	0
199	Botsfordia	Brachiopoda	0	0	1	0	0	0	0	0	0	0	0	0

200	Canthylotreta	Brachiopoda	0	0	0	0	0	0	0	0	0	0	0	1
201	Diandongia	Brachiopoda	1	0	0	1	?	1	0	0	0	0	0	0
202	Dictyonina	Brachiopoda	0	0	0	0	0	0	0	1	1	1	1	0
203	Diraphora	Brachiopoda	0	0	0	0	0	0	0	0	?	1	0	0
204	Eoconcha	Brachiopoda	0	0	0	0	0	0	0	1	0	0	0	0
205	Eoobolus	Brachiopoda	0	0	1	0	0	0	0	0	0	0	0	0
206	Glyptacrothele	Brachiopoda	0	0	0	0	1	0	0	0	0	0	0	0
207	Heliomedusa	Brachiopoda	1	0	0	1	0	0	0	0	0	0	0	0
208	Kuangshanotreta	Brachiopoda	1	0	0	0	0	0	0	0	0	0	0	0
209	Kutorgina	Brachiopoda	1	0	0	1	0	0	0	1	0	0	0	0
210	Linarssonia	Brachiopoda	0	0	0	0	0	0	0	0	0	0	0	1
211	Lingulella	Brachiopoda	1	0	0	0	0	0	0	1	1	1	1	1
212	Lingulellotreta	Brachiopoda	1	0	0	1	1	0	0	0	0	0	0	0
213	Lingulepis	Brachiopoda	0	0	0	0	0	0	0	1	0	0	0	0
214	Linnarssonia	Brachiopoda	0	0	1	0	0	0	0	1	0	1	1	0
215	Longtancunella	Brachiopoda	1	0	0	0	0	0	0	0	0	0	0	0
216	Micromitra	Brachiopoda	0	0	0	0	0	0	0	1	0	1	1	1
217	Nisusia	Brachiopoda	0	0	?	1	1	0	0	1	0	1	1	1
218	Palaeobolus	Brachiopoda	0	0	0	1	0	0	0	1	0	0	0	0
219	Paterina	Brachiopoda	0	0	0	0	0	0	1	1	0	1	0	0
220	Prototreta	Brachiopoda	0	0	0	0	0	0	0	0	0	0	1	1
221	Wangyuia	Brachiopoda	1	0	0	0	0	0	0	0	0	0	0	0
222	Wimanella	Brachiopoda	0	0	0	0	0	0	0	0	1	0	0	0
223	Xianshanella	Brachiopoda	1	0	0	0	0	0	0	0	0	0	0	0
224	Beidazoon	Chordata	1	0	0	0	0	0	0	0	0	0	0	0
225	Cathaymyrus	Chordata	1	0	0	0	0	0	0	0	0	0	0	0
226	Cheungkongella	Chordata	1	0	0	0	0	0	0	0	0	0	0	0
227	Didazoon	Chordata	1	0	0	0	0	0	0	0	0	0	0	0
228	Haikouichthys	Chordata	1	0	0	0	0	0	0	0	0	0	0	0
229	Heteromorphus	Chordata	1	0	0	0	0	0	0	0	0	0	0	0
230	Metaspriggina	Chordata	0	0	0	0	0	0	1	0	0	1	0	0
231	Myllokunmingia	Chordata	1	0	0	0	0	0	0	0	0	0	0	0
232	Nesonektris	Chordata	0	0	0	0	0	1	0	0	0	0	0	0
233	Ooedigera	Chordata	0	1	0	0	0	0	0	0	0	0	0	0
234	Pikaia	Chordata	0	0	0	0	0	0	0	0	0	1	0	0
235	Pomatrum	Chordata	1	0	0	0	0	0	0	0	0	0	0	0
236	Shankouclava	Chordata	1	0	0	0	0	0	0	0	0	0	0	0
237	Vetulicola	Chordata	1	0	0	1	0	0	0	0	0	0	0	0
238	Yunnanozoon	Chordata	1	0	0	0	0	0	0	0	0	0	0	0
239	Yuyuanozoon	Chordata	1	0	0	0	0	0	0	0	0	0	0	0
240	Zhongjianichthys	Chordata	1	0	0	0	0	0	0	0	0	0	0	0
241	Zhongxiniscus	Chordata	1	0	0	0	0	0	0	0	0	0	0	0
242	Archisaccophyllia	Cnidaria	1	0	0	0	0	0	0	0	0	0	0	0
243	Byronia	Cnidaria	0	0	0	?	1	0	0	1	0	1	1	0
244	Cambrohydra	Cnidaria	1	0	0	0	0	0	0	0	0	0	0	0
245	Cambromedusa	Cnidaria	0	0	0	0	0	0	0	0	0	0	1	0
246	Cambrorhytium	Cnidaria	0	0	1	0	0	0	0	0	0	1	1	1
247	Cambrovitus	Cnidaria	0	0	0	0	0	0	0	1	0	0	0	0
248	Conicula	Cnidaria	1	0	0	0	0	0	0	0	0	0	0	0
249	Mackenzia	Cnidaria	0	0	0	0	0	0	0	0	0	1	0	0
250	Priscapennamarina	Cnidaria	1	0	0	0	0	0	0	0	0	0	0	0
251	Sphenothallus	Cnidaria	0	0	0	1	0	0	0	1	0	1	0	0
252	Xianguangia	Cnidaria	1	0	0	0	0	0	0	0	0	0	0	0

253	Ctenorhabdotus	Ctenophora	0	0	0	0	0	0	0	0	0	1	0	0
254	Fasciculus	Ctenophora	0	0	0	0	0	0	0	0	0	1	?	0
255	Maotianoascus	Ctenophora	1	0	0	0	0	0	0	0	0	0	0	0
256	Sinoascus	Ctenophora	1	0	0	0	0	0	0	0	0	0	0	0
257	Trigoides	Ctenophora	1	0	0	0	0	0	0	0	0	0	0	0
258	Xanioascus	Ctenophora	0	0	0	0	0	0	0	0	0	1	0	0
259	Yunnanoascus	Ctenophora	1	0	0	0	0	0	0	0	0	0	0	0
260	Archaeocothurnus	Echinodermata	0	0	0	0	0	0	0	0	0	0	1	0
261	Balangicystis	Echinodermata	0	0	0	0	0	0	0	1	0	0	0	0
262	Camptostroma	Echinodermata	0	0	0	0	0	0	1	0	0	0	0	0
263	Castericystis	Echinodermata	0	0	0	0	0	0	0	0	0	0	0	1
264	Coleicarpus	Echinodermata	0	0	0	0	0	0	0	0	0	0	1	0
265	Ctenocystis	Echinodermata	0	0	0	0	0	0	0	0	1	0	1	0
266	Curtoeocrinus	Echinodermata	0	0	0	0	0	0	0	1	0	0	0	0
267	Dianchicystis	Echinodermata	1	0	0	0	0	0	0	0	0	0	0	0
268	Echmatocrinus	Echinodermata	0	0	0	0	0	0	0	0	0	1	0	0
269	Globoeocrinus	Echinodermata	0	0	0	0	0	0	0	1	0	0	0	0
270	Gogia	Echinodermata	0	0	0	0	0	0	0	0	1	1	1	1
271	Guizhoueocrinus	Echinodermata	0	0	0	0	1	0	0	0	0	0	0	0
272	Kailidiscus	Echinodermata	0	0	0	0	0	0	0	1	0	0	0	0
273	Kinzercystis	Echinodermata	0	0	0	0	0	0	1	0	0	0	0	0
274	Lepidocystis	Echinodermata	0	0	0	0	0	0	1	0	0	0	0	0
275	Lyracystis	Echinodermata	0	0	0	0	0	0	0	0	1	1	0	0
276	Marjumicystis	Echinodermata	0	0	0	0	0	0	0	0	0	0	0	1
277	Ponticulocarpus	Echinodermata	0	0	0	0	0	0	0	0	1	0	0	0
278	Sinoeocrinus	Echinodermata	0	0	0	0	0	0	0	1	0	0	0	0
279	Totiglobus	Echinodermata	0	0	0	0	0	0	0	0	0	0	0	?
280	Turbanicystis	Echinodermata	0	0	0	0	0	0	0	1	0	0	0	0
281	Ubaghsicystis	Echinodermata	0	0	0	0	0	0	0	0	0	?	0	0
282	Vetulocystis	Echinodermata	1	0	0	0	0	0	0	0	0	0	0	0
283	Walcottidiscus	Echinodermata	0	0	0	0	0	0	0	0	0	1	0	0
284	Wudingeocrinus	Echinodermata	0	0	0	1	0	0	0	0	0	0	0	0
285	Archaeolafoea	Hemichordata	0	0	0	0	0	0	0	0	0	0	1	0
286	Chaunograptus	Hemichordata	0	0	0	0	0	0	0	0	0	1	0	0
287	Galeaplumosus	Hemichordata	1	0	0	0	0	0	0	0	0	0	0	0
288	Mastograptus	Hemichordata	0	0	0	0	0	0	0	0	0	0	0	1
289	Spartobranchus	Hemichordata	0	0	0	0	0	0	0	0	0	1	0	0
290	Sphenoecium	Hemichordata	0	0	0	0	0	0	0	0	1	0	1	1
291	Tarnagraptus	Hemichordata	0	0	0	0	0	0	0	0	0	0	1	0
292	Yuknessia	Hemichordata	1	0	0	0	0	0	1	1	1	1	1	1
293	Acinocricus	Lobopoda	0	0	0	0	0	0	0	0	1	0	0	0
294	Antennacanthopodia	Lobopoda	1	0	0	0	0	0	0	0	0	0	0	0
295	Aysheaia	Lobopoda	1	0	0	0	0	0	0	0	0	1	1	0
296	Cardiodictyon	Lobopoda	1	0	0	0	0	0	0	0	0	0	0	0
297	Diania	Lobopoda	1	0	0	0	0	0	0	0	0	0	0	0
298	Facivermis	Lobopoda	1	0	0	0	0	0	0	0	0	0	0	0
299	Hadranax	Lobopoda	0	1	0	0	0	0	0	0	0	0	0	0
300	Hallucigenia	Lobopoda	1	0	0	1	0	0	0	0	0	1	0	0
301	Jianshanopodia	Lobopoda	1	0	0	0	0	0	0	0	0	0	0	0
302	Luolishania	Lobopoda	1	0	0	0	0	0	0	0	0	0	0	0
303	Magadictyon	Lobopoda	1	0	0	0	0	0	0	0	0	0	0	0
304	Microdictyon	Lobopoda	1	0	1	0	0	0	0	1	0	0	0	0
305	Miraluolishania	Lobopoda	1	0	0	0	0	0	0	0	0	0	0	0

306	Onychodictyon	Lobopoda	1	0	0	0	0	0	0	0	0	0	0	0
307	Paucipodia	Lobopoda	1	0	0	0	0	0	0	0	0	0	0	0
308	Ambrolinevitus	Mollusca	1	0	0	0	1	0	0	1	0	0	0	0
309	Burithes	Mollusca	1	0	0	0	0	0	0	0	0	0	0	0
310	Coreospira	Mollusca	0	0	0	0	0	0	0	1	0	0	0	0
311	Fordilla	Mollusca	0	0	0	0	0	0	0	?	0	0	0	0
312	Glossolites	Mollusca	1	0	0	0	0	0	0	0	0	0	0	0
313	Haplophrentis	Mollusca	0	0	0	0	1	0	?	1	1	1	0	0
314	Halkieria	Mollusca	0	1	0	0	0	0	0	0	0	0	0	0
315	Helcionella	Mollusca	1	0	0	0	0	0	0	0	0	1	0	0
316	Hyolithes	Mollusca	0	0	0	0	0	0	0	?	?	0	?	?
317	Latouchella	Mollusca	0	0	0	0	0	0	0	1	1	0	1	0
318	Linevitus	Mollusca	1	0	0	1	1	0	0	1	0	0	0	0
319	Melopegma	Mollusca	0	0	0	0	0	0	0	0	0	0	1	0
320	Nectocaris	Mollusca	0	0	0	0	0	0	0	0	0	1	0	0
321	Odontogriphus	Mollusca	0	0	0	0	0	0	0	0	0	1	0	0
322	Oikozetetes	Mollusca	0	0	0	0	0	0	0	0	0	1	0	0
323	Orthrozanclus	Mollusca	0	0	0	0	0	0	0	0	0	1	0	0
324	Pelagiella	Mollusca	0	0	0	0	0	0	1	0	0	0	1	0
325	Petalilium	Mollusca	1	0	0	0	0	0	0	0	0	0	0	0
326	Scenella	Mollusca	0	0	0	0	0	0	0	1	1	1	0	0
327	Stenothecoides	Mollusca	0	0	0	0	0	0	0	0	0	0	1	0
328	Totoralia	Mollusca	0	0	0	0	0	0	0	0	0	1	0	0
329	Trapezovitus	Mollusca	0	1	0	0	0	0	0	0	0	0	0	0
330	Wiwaxia	Mollusca	1	0	1	0	0	0	0	1	1	1	0	0
331	Archaeogolfingia	Other	1	0	0	0	0	0	0	0	0	0	0	0
332	Cambrosiphunculus	Other	1	0	0	0	0	0	0	0	0	0	0	0
333	Eophoronis	Other	1	0	0	0	0	0	0	0	0	0	0	0
334	Protosagita	Other	1	0	0	0	0	0	0	0	0	0	0	0
335	Allantospongia	Porifera	1	0	0	0	0	0	0	0	0	0	0	0
336	Brooksella	Porifera	0	0	0	0	0	0	0	0	?	0	0	0
337	Capsospongia	Porifera	0	0	0	0	0	0	0	0	0	1	0	0
338	Choia	Porifera	1	1	1	1	1	0	0	0	0	1	1	1
339	Choiaella	Porifera	1	0	0	0	0	0	0	1	0	0	0	0
340	Cjulanciella	Porifera	0	0	1	0	0	0	0	0	0	0	0	0
341	Crumillospongia	Porifera	1	0	0	1	0	0	0	0	0	1	0	0
342	Cystospongia	Porifera	1	0	0	0	0	0	0	0	0	0	0	0
343	Diagoniella	Porifera	0	0	1	0	0	0	0	0	0	1	1	1
344	Dodecaactinella	Porifera	0	0	1	0	0	0	0	0	0	0	0	0
345	Eiffelia	Porifera	0	0	0	0	0	0	0	0	0	1	0	0
346	Eiffelospongia	Porifera	0	0	0	0	0	0	0	0	0	1	0	0
347	Falospongia	Porifera	0	0	0	0	0	0	0	0	0	1	0	0
348	Fieldospongia	Porifera	0	0	0	0	0	0	0	0	0	1	0	0
349	Halichondrites	Porifera	1	0	0	0	0	0	0	1	0	1	0	0
350	Hamptonia	Porifera	1	0	0	0	0	0	0	0	0	1	1	1
351	Hamptoniella	Porifera	0	0	0	0	0	0	0	0	0	1	0	0
352	Hazelia	Porifera	1	0	0	0	0	0	1	1	0	1	0	1
353	Hintzespongia	Porifera	0	0	0	0	0	0	0	0	0	1	1	1
354	Hyalosinica	Porifera	1	0	0	0	0	0	0	0	0	0	0	0
355	Ischnspongia	Porifera	1	0	0	0	0	0	0	0	0	0	0	0
356	Ivantsovia	Porifera	0	0	1	0	0	0	0	0	0	0	0	0
357	Kiwetinokia	Porifera	0	0	0	0	0	0	0	0	0	0	1	0
358	Lenica	Porifera	0	0	1	0	0	0	0	0	0	0	0	0

359	Leptomitella	Porifera	1	0	0	1	0	0	0	0	0	1	0	1
360	Leptomitus	Porifera	1	0	0	0	1	0	0	1	0	1	0	1
361	Moleculospina	Porifera	0	0	0	0	0	0	0	0	0	1	0	0
362	Nabaviella	Porifera	0	0	1	0	0	0	0	0	0	0	0	0
363	Paradiagoniella	Porifera	1	0	0	0	0	0	0	0	0	0	0	0
364	Paraleptomitella	Porifera	1	0	0	0	0	0	0	0	0	0	0	0
365	Petaloptyon	Porifera	0	0	0	0	0	0	0	0	0	1	0	0
366	Pirania	Porifera	0	0	0	0	0	0	0	0	0	1	0	0
367	Protoprisma	Porifera	0	0	0	0	0	0	0	0	0	1	0	0
368	Protospongia	Porifera	1	0	0	0	0	0	0	1	1	1	0	1
369	Ptilispongia	Porifera	1	0	0	0	0	0	0	0	0	0	0	0
370	Quadrolaminiella	Porifera	1	0	0	0	0	0	0	0	0	0	0	0
371	Ratcliffespongia	Porifera	0	0	0	0	0	0	0	0	0	0	1	1
372	Saetaspongia	Porifera	1	0	0	0	0	0	0	0	0	0	0	0
373	Sanshapentella	Porifera	0	0	0	0	0	0	0	0	0	?	0	0
374	Sentinella	Porifera	0	0	0	0	0	0	0	0	0	0	1	0
375	Stephenospongia	Porifera	0	0	0	0	0	0	0	0	0	1	0	0
376	Styloleptomitus	Porifera	1	0	0	0	0	0	0	0	0	0	0	0
377	Takakkawia	Porifera	1	0	0	0	0	0	0	0	0	1	0	0
378	Triticispongia	Porifera	1	0	0	0	0	0	0	0	0	0	0	0
379	Ulospongiella	Porifera	0	0	0	0	0	0	0	0	0	1	0	0
380	Valospongia	Porifera	1	0	0	0	0	0	0	0	0	0	0	1
381	Vauxia	Porifera	0	0	0	0	0	0	0	1	1	1	1	0
382	Wapkia	Porifera	1	0	1	0	0	0	0	0	0	1	0	0
383	Acosmia	Priapulida	1	0	0	0	0	0	0	0	0	0	0	0
384	Ancalagon	Priapulida	0	0	0	0	0	0	0	0	0	1	0	0
385	Anningvermis	Priapulida	1	0	0	0	0	0	0	0	0	0	0	0
386	Chalazoscolex	Priapulida	0	1	0	0	0	0	0	0	0	0	0	0
387	Corralioscolex	Priapulida	0	0	1	0	0	0	0	0	0	0	0	0
388	Corynetis	Priapulida	1	0	0	1	0	0	0	0	0	0	0	0
389	Cricocosmia	Priapulida	1	0	0	0	0	0	0	1	0	0	0	0
390	Eximipriapulus	Priapulida	1	0	0	0	0	0	0	0	0	0	0	0
391	Fieldia	Priapulida	0	0	0	0	0	0	0	0	0	1	0	0
392	Guanduscolex	Priapulida	0	0	0	1	0	0	0	0	0	0	0	0
393	Hadimopanella	Priapulida	0	0	0	0	1	0	0	0	0	0	0	0
394	Lagenula	Priapulida	1	0	0	0	0	0	0	0	0	0	0	0
395	Laojieella	Priapulida	1	0	0	0	0	0	0	0	0	0	0	0
396	Louisella	Priapulida	0	0	0	0	0	0	0	0	0	1	0	0
397	Mafangscolex	Priapulida	1	0	0	0	0	0	0	0	0	0	0	0
398	Maotianshania	Priapulida	1	0	0	0	0	0	0	0	0	0	0	0
399	Omnidens	Priapulida	1	0	0	0	0	0	0	0	0	0	0	0
400	Ottoia	Priapulida	0	0	0	0	0	0	0	1	1	1	0	1
401	Palaeopriapulites	Priapulida	1	0	0	0	0	0	0	0	0	0	0	0
402	Paramaotianshania	Priapulida	0	0	0	1	0	0	0	0	0	0	0	0
403	Paraselkirkia	Priapulida	1	0	0	0	0	0	0	0	0	0	0	0
404	Paratubiluchus	Priapulida	1	0	0	0	0	0	0	0	0	0	0	0
405	Piloscolex	Priapulida	0	0	1	0	0	0	0	0	0	0	0	0
406	Sandaokania	Priapulida	1	0	0	0	0	0	0	0	0	0	0	0
407	Scathascolex	Priapulida	0	0	0	0	0	0	0	0	0	1	0	0
408	Scolecofurca	Priapulida	0	0	0	0	0	0	0	0	0	1	0	0
409	Sicyophorus	Priapulida	1	0	0	0	0	0	0	1	0	0	0	0
410	Sirilorica	Priapulida	0	1	0	0	0	0	0	0	0	0	0	0
411	Tabelliscolex	Priapulida	1	0	0	0	0	0	0	0	0	0	0	0

412	Tylotites	Priapulida	1	0	0	0	0	0	0	0	0	0	0	0
413	Vladipriapulus	Priapulida	0	0	1	0	0	0	0	0	0	0	0	0
414	Wronascolex	Priapulida	1	0	1	1	1	1	0	0	?	0	0	?
415	Wudingscolex	Priapulida	0	0	0	1	0	0	0	0	0	0	0	0
416	Xiaoheiqingella	Priapulida	1	0	0	0	0	0	0	0	0	0	0	0
417	Xishania	Priapulida	1	0	0	0	0	0	0	0	0	0	0	0
418	Xystoscolex	Priapulida	0	1	0	0	0	0	0	0	0	0	0	0
419	Yunnanoscolex	Priapulida	0	0	0	1	0	0	0	0	0	0	0	0
420	Yunnanpriapulus	Priapulida	1	0	0	0	0	0	0	0	0	0	0	0
421	Achlysopsis	Trilobita	0	0	0	0	0	0	0	0	1	0	0	0
422	Agnostus	Trilobita	0	0	0	0	0	0	0	0	0	0	0	1
423	Aldonaia	Trilobita	0	0	1	0	0	0	0	0	0	0	0	0
424	Alokistocare	Trilobita	0	0	0	0	0	0	0	0	1	1	1	0
425	Alokistocarella	Trilobita	0	0	0	0	0	0	0	0	1	0	0	0
426	Altiocculus	Trilobita	0	0	0	0	0	0	0	0	0	0	1	?
427	Amecephalus	Trilobita	0	0	0	0	0	0	0	0	1	0	0	0
428	Ammagnostus	Trilobita	0	0	0	0	0	0	0	0	0	0	0	1
429	Anoria	Trilobita	0	0	0	0	0	0	0	0	0	?	0	0
430	Arthricocephalites	Trilobita	0	0	0	0	1	0	0	0	0	0	0	0
431	Arthricocephalus	Trilobita	0	0	0	0	1	0	0	0	0	0	0	0
432	Asaphiscus	Trilobita	0	0	0	0	0	0	0	0	0	0	1	1
433	Athabaskia	Trilobita	0	0	0	0	0	0	0	0	1	0	0	0
434	Athabaskiella	Trilobita	0	0	0	0	0	0	0	0	0	0	0	1
435	Balangcunaspis	Trilobita	0	0	0	0	0	0	0	1	0	0	0	0
436	Balangia	Trilobita	0	0	0	0	1	0	0	0	0	0	0	0
437	Balcoracania	Trilobita	0	0	0	0	0	1	0	0	0	0	0	0
438	Baltagnostus	Trilobita	0	0	0	0	0	0	0	0	0	0	1	0
439	Bathyuriscellus	Trilobita	0	0	1	0	0	0	0	0	0	0	0	0
440	Bathyuriscidella	Trilobita	0	0	0	0	0	0	0	0	0	0	0	1
441	Bathyuriscus	Trilobita	0	0	0	0	0	0	0	0	1	1	1	1
442	Bergeroniaspis	Trilobita	0	0	1	0	0	0	0	0	0	0	0	0
443	Bergeroniellus	Trilobita	0	0	1	0	0	0	0	0	0	0	0	0
444	Binodaspis	Trilobita	0	0	1	0	0	0	0	0	0	0	0	0
445	Bolaspidella	Trilobita	0	0	0	0	0	0	0	0	0	0	1	1
446	Bonnia	Trilobita	0	0	0	0	0	0	1	0	0	0	0	0
447	Brachyaspidion	Trilobita	0	0	0	0	0	0	0	0	0	0	1	0
448	Breviredlichia	Trilobita	0	0	0	1	0	0	0	0	0	0	0	0
449	Buenellus	Trilobita	0	1	0	0	0	0	0	0	0	0	0	0
450	Burlingia	Trilobita	0	0	0	0	0	0	0	1	0	1	0	1
451	Bythicheilus	Trilobita	0	0	0	0	0	0	0	0	1	0	0	0
452	Chancia	Trilobita	0	0	0	0	0	0	0	0	1	1	0	0
453	Changaspis	Trilobita	0	0	0	0	1	0	0	0	0	0	0	0
454	Chengjiangaspis	Trilobita	1	0	0	0	0	0	0	0	0	0	0	0
455	Clavagnostus	Trilobita	0	0	0	0	0	0	0	0	0	0	0	1
456	Cotalagnostus	Trilobita	0	0	0	0	0	0	0	0	0	0	0	1
457	Curvoryctocephalus	Trilobita	0	0	0	0	0	0	0	1	0	0	0	0
458	Danzhaiaspis	Trilobita	0	0	0	0	0	0	0	1	0	0	0	0
459	Delgadella	Trilobita	0	0	1	0	0	0	0	0	0	0	0	0
460	Diplagnostus	Trilobita	0	0	0	0	0	0	0	0	0	0	0	1
461	Doryagnostus	Trilobita	0	0	0	0	0	0	0	0	0	0	0	?
462	Dorypyge	Trilobita	0	0	0	0	0	0	0	0	1	0	0	0
463	Douposiella	Trilobita	0	0	0	0	0	0	0	1	0	0	0	0
464	Duyunaspis	Trilobita	0	0	0	0	1	0	0	0	0	0	0	0

465	Edelsteinaspis	Trilobita	0	0	1	0	0	0	0	0	0	0	0	0	0
466	Ehmaniella	Trilobita	0	0	0	0	0	0	0	0	1	1	1	0	
467	Elrathia	Trilobita	0	0	0	0	0	0	0	0	0	1	1	1	
468	Elrathina	Trilobita	0	0	0	0	0	0	0	0	0	1	0	0	
469	Eoredlichia	Trilobita	1	0	0	0	0	0	0	0	0	0	0	0	
470	Eosoptychoparia	Trilobita	0	0	0	0	0	0	0	1	0	0	0	0	
471	Estaingia	Trilobita	0	0	0	0	0	1	0	0	0	0	0	0	
472	Euarthricocephalus	Trilobita	0	0	0	0	0	0	0	1	0	0	0	0	
473	Gaotanaspis	Trilobita	0	0	0	0	0	0	0	1	0	0	0	0	
474	Gedongaspis	Trilobita	0	0	0	0	0	0	0	1	0	0	0	0	
475	Glossopleura	Trilobita	0	0	0	0	0	0	0	0	1	1	0	0	
476	Hanburia	Trilobita	0	0	0	0	0	0	0	0	0	1	0	0	
477	Hemirhodon	Trilobita	0	0	0	0	0	0	0	0	0	0	1	1	
478	Holteria	Trilobita	0	0	0	0	0	0	0	0	0	0	0	1	
479	Holyoakia	Trilobita	0	0	0	0	0	1	0	0	0	0	0	0	
480	Hypagnostus	Trilobita	0	0	0	0	0	0	0	0	0	0	1	1	
481	Iniospheniscus	Trilobita	0	0	0	0	0	0	0	0	0	0	0	1	
482	Jakutus	Trilobita	0	0	1	0	0	0	0	0	0	0	0	0	
483	Jenkinsonia	Trilobita	0	0	0	0	0	0	0	0	0	0	1	0	
484	Judomia	Trilobita	0	0	1	0	0	0	0	0	0	0	0	0	
485	Kailiella	Trilobita	0	0	0	0	0	0	0	1	0	0	0	0	
486	Kaotaia	Trilobita	0	0	0	0	0	0	0	1	0	0	0	0	
487	Kermanella	Trilobita	0	0	0	0	0	0	0	1	0	0	0	0	
488	Kochina	Trilobita	0	0	0	0	0	0	0	0	1	0	0	0	
489	Kootenia	Trilobita	0	0	0	1	0	0	1	1	1	1	1	0	
490	Kuanyangia	Trilobita	1	0	0	0	0	0	0	0	0	0	0	0	
491	Kunmingaspis	Trilobita	0	0	0	0	0	0	0	1	0	0	0	0	
492	Kutsingocephalus	Trilobita	0	0	0	0	0	0	0	1	0	0	0	0	
493	Lancastria	Trilobita	0	0	0	0	0	0	1	0	0	0	0	0	
494	Lejopyge	Trilobita	0	0	0	0	0	0	0	0	0	0	1	1	
495	Linguagnostus	Trilobita	0	0	0	0	0	0	0	0	0	0	0	1	
496	Majiangia	Trilobita	0	0	0	0	0	0	0	1	0	0	0	0	
497	Malungia	Trilobita	1	0	0	0	0	0	0	0	0	0	0	0	
498	Marjumia	Trilobita	0	0	0	0	0	0	0	0	0	0	0	1	
499	Megapalaeolenus	Trilobita	0	0	0	1	0	0	0	0	0	0	0	0	
500	Megapharanaspis	Trilobita	0	0	0	0	0	1	0	0	0	0	0	0	
501	Metabalangia	Trilobita	0	0	0	0	0	0	0	1	0	0	0	0	
502	Metarthricocephalus	Trilobita	0	0	0	0	0	0	0	1	0	0	0	0	
503	Miaobanpoia	Trilobita	0	0	0	0	0	0	0	1	0	0	0	0	
504	Modocia	Trilobita	0	0	0	0	0	0	0	0	0	0	1	1	
505	Nangaoia	Trilobita	0	0	0	0	0	0	0	1	0	0	0	0	
506	Oedorhachis	Trilobita	0	0	0	0	0	0	0	0	0	0	0	1	
507	Ogygopsis	Trilobita	0	0	0	0	0	0	0	0	1	1	0	0	
508	Olenellus	Trilobita	0	0	0	0	0	0	1	0	0	0	0	0	
509	Olenoides	Trilobita	0	0	0	0	0	0	0	1	1	1	1	1	
510	Oryctocara	Trilobita	0	0	0	0	0	0	0	0	1	1	0	0	
511	Oryctocephalina	Trilobita	0	0	0	0	0	0	0	1	0	0	0	0	
512	Oryctocephalites	Trilobita	0	0	0	0	0	0	0	1	0	0	0	0	
513	Oryctocephaloides	Trilobita	0	0	0	0	0	0	0	1	0	0	0	0	
514	Oryctocephalus	Trilobita	0	0	0	0	0	0	0	1	1	1	0	0	
515	Pagetia	Trilobita	0	0	0	0	0	0	0	1	1	1	0	0	
516	Palaeolenus	Trilobita	0	0	0	1	0	0	0	0	0	0	0	0	
517	Panzhaiaspis	Trilobita	0	0	0	0	0	0	0	1	0	0	0	0	

518	Paramgaspis	Trilobita	0	0	0	0	0	0	0	1	0	0	0	0
519	Parashuiyuella	Trilobita	0	0	0	0	0	0	0	1	0	0	0	0
520	Parkaspis	Trilobita	0	0	0	0	0	0	0	0	0	1	0	0
521	Peronopsis	Trilobita	0	0	0	0	0	0	0	1	1	0	1	1
522	Pianaspis	Trilobita	0	0	0	0	0	0	0	1	0	0	0	0
523	Piochaspis	Trilobita	0	0	0	0	0	0	0	0	1	0	0	0
524	Poliella	Trilobita	0	0	0	0	0	0	0	0	0	1	0	0
525	Polypleuraspis	Trilobita	0	0	0	0	0	0	0	0	1	1	0	0
526	Probowmania	Trilobita	0	0	0	0	1	0	0	1	0	0	0	0
527	Probowmaniella	Trilobita	0	0	0	0	0	0	0	1	0	0	0	0
528	Pseudophalacroma	Trilobita	0	0	0	0	0	0	0	0	0	0	0	1
529	Ptychagnostus	Trilobita	0	0	0	0	0	0	0	0	0	1	1	1
530	Ptychoparella	Trilobita	0	0	0	0	0	0	0	0	1	0	1	0
531	Redlichia	Trilobita	0	0	0	1	1	1	0	0	0	0	0	0
532	Sanhuangshania	Trilobita	0	0	0	0	0	0	0	1	0	0	0	0
533	Sanwania	Trilobita	0	0	0	0	0	0	0	1	0	0	0	0
534	Schmalenseeia	Trilobita	0	0	0	0	0	0	0	1	0	0	0	0
535	Semisphaerocephalus	Trilobita	0	0	0	0	0	0	0	0	0	0	1	0
536	Sinoschistometopus	Trilobita	0	0	0	0	0	0	0	1	0	0	0	0
537	Solenopleura	Trilobita	0	0	0	0	0	0	0	0	1	0	0	0
538	Spencella	Trilobita	0	0	0	0	0	0	0	0	0	1	1	0
539	Stoecklinia	Trilobita	0	0	0	0	0	0	0	1	0	0	0	0
540	Taijiangocephalus	Trilobita	0	0	0	0	0	0	0	1	0	0	0	0
541	Temnoura	Trilobita	0	0	0	0	0	0	0	1	0	0	0	0
542	Thoracocare	Trilobita	0	0	0	0	0	0	0	0	1	0	0	0
543	Tomagnostella	Trilobita	0	0	0	0	0	0	0	0	0	0	0	1
544	Tonkinella	Trilobita	0	0	0	0	0	0	0	0	0	0	1	0
545	Trymataspis	Trilobita	0	0	0	0	0	0	0	0	0	0	0	1
546	Tsunyidiscus	Trilobita	1	0	0	0	0	0	0	0	0	0	0	0
547	Utagnostus	Trilobita	0	0	0	0	0	0	0	0	0	0	0	1
548	Utaspis	Trilobita	0	0	0	0	0	0	0	0	0	0	0	1
549	Utia	Trilobita	0	0	0	0	0	0	0	0	1	0	0	0
550	Wanneria	Trilobita	0	0	0	0	0	0	1	0	0	0	0	0
551	Wutingaspis	Trilobita	1	0	0	0	0	0	0	0	0	0	0	0
552	Xingrenaspis	Trilobita	0	0	0	0	0	0	0	1	0	0	0	0
553	Yuehsienszella	Trilobita	0	0	0	1	0	0	0	0	0	0	0	0
554	Yunnanocephalus	Trilobita	1	0	0	0	0	0	0	0	0	0	0	0
555	Zacanthoides	Trilobita	0	0	0	0	0	0	0	0	1	1	1	1
556	Allonnia	uncertain	1	0	0	1	0	0	1	0	0	1	0	0
557	Amiskwia	uncertain	1	0	0	0	0	0	0	0	0	1	0	0
558	Anthotrum	uncertain	1	0	0	0	0	0	0	0	0	0	0	0
559	Archiasterella	uncertain	0	0	1	1	0	0	0	1	0	1	0	0
560	Archotuba	uncertain	1	0	0	0	1	0	0	0	0	0	0	0
561	Atalotaenia	uncertain	0	0	0	0	0	0	1	0	0	0	0	0
562	Banffia	uncertain	1	0	0	0	0	0	0	0	1	1	0	0
563	Batofasciculus	uncertain	1	0	0	0	0	0	0	0	0	0	0	0
564	Calathites	uncertain	1	0	0	0	0	0	0	0	0	0	0	0
565	Cambrocornulitus	uncertain	1	0	0	0	0	0	0	0	0	0	0	0
566	Chancelloria	uncertain	0	0	0	0	1	?	0	1	0	1	1	0
567	Cotyledion	uncertain	1	0	0	0	0	0	0	0	0	0	0	0
568	Dinomischus	uncertain	1	0	0	0	0	0	0	1	0	1	0	0
569	Discoides	uncertain	1	0	0	0	0	0	0	0	0	0	0	0
570	Eldonia	uncertain	1	0	1	0	0	0	0	0	1	1	1	1

571	Gangtoucunia	uncertain	0	0	0	1	0	0	0	0	0	0	0	0
572	Herpetogaster	uncertain	0	0	0	0	0	0	0	0	0	1	0	0
573	Hippotrum	uncertain	1	0	0	0	0	0	0	0	0	0	0	0
574	Jiucunia	uncertain	1	0	0	0	0	0	0	0	0	0	0	0
575	Kinzeria	uncertain	0	0	0	0	0	0	1	0	0	0	0	0
576	Maanshania	uncertain	1	0	0	0	0	0	0	0	0	0	0	0
577	Macrocephalus	uncertain	1	0	0	0	0	0	0	0	0	0	0	0
578	Malongitubes	uncertain	1	0	0	0	0	0	0	0	0	0	0	0
579	Myoscolex	uncertain	0	0	0	0	0	1	0	0	0	0	0	0
580	Nidelric	uncertain	1	0	0	0	0	0	0	0	0	0	0	0
581	Oesia	uncertain	0	0	0	0	0	0	0	0	0	1	0	0
582	Oligonodus	uncertain	1	0	0	0	0	0	0	0	0	0	0	0
583	Pararotadiscus	uncertain	0	0	0	0	0	0	0	1	0	0	0	0
584	Parvulonoda	uncertain	1	0	0	0	0	0	0	0	0	0	0	0
585	Phacatrum	uncertain	1	0	0	0	0	0	0	0	0	0	0	0
586	Phasganula	uncertain	1	0	0	0	0	0	0	0	0	0	0	0
587	Phlogites	uncertain	1	0	0	1	0	0	0	0	0	0	0	0
588	Pollingeria	uncertain	0	0	0	0	0	0	0	0	0	1	0	0
589	Portalia	uncertain	0	0	0	0	0	0	0	0	0	1	0	0
590	Priscansermarinus	uncertain	0	0	0	1	0	0	0	0	0	1	0	0
591	Pristioites	uncertain	1	0	0	0	0	0	0	0	0	0	0	0
592	Pseudoperipatus	uncertain	0	0	0	0	0	0	0	0	0	1	0	0
593	Rhipitrus	uncertain	1	0	0	0	0	0	0	0	0	0	0	0
594	Rotadiscus	uncertain	1	0	0	0	0	0	0	1	0	0	0	0
595	Salterella	uncertain	0	0	0	0	0	0	1	0	0	0	0	0
596	Sinoflabrum	uncertain	1	0	0	1	0	0	0	0	0	0	0	0
597	Siphusauctum	uncertain	0	0	0	0	0	0	0	0	0	1	0	0
598	Skeemella	uncertain	0	0	0	0	0	0	0	0	0	0	1	0
599	Stellostomites	uncertain	1	0	0	0	0	0	0	0	0	0	0	0
600	Stromatoveris	uncertain	1	0	0	0	0	0	0	0	0	0	0	0
601	Thaumaptilon	uncertain	0	0	0	0	0	0	0	0	0	1	0	0
602	Tripexia	uncertain	0	0	0	0	0	0	0	1	0	0	0	0
603	Tubulella	uncertain	0	0	0	0	0	0	1	0	0	1	0	0
604	Vetustovermis	uncertain	1	0	0	0	0	1	0	0	0	0	0	0
605	Yuganotheca	uncertain	1	0	0	0	0	0	0	0	0	0	0	0

Supplementary Table 6.2: Mantel test results for the analysis of geographic, assemblage and age distances referred to in Chapter 3.

Mantel Tests		**Ochiai, Singletons**		**Ochiai, No Singletons**		**Jaccard, Singletons**		**Jaccard, No Singletons**	
Recontruction	**Model**	**r**	**p-value**	**r**	**p-value**	**r**	**p-value**	**r**	**p-value**
Torsvik & Cocks	geo ~ age	0.32	0.026						
(2013)	ass ~ geo	0.39	0.003	0.44	0.004	0.37	0.006	0.38	0.009
	ass ~ log(geo)	0.58	0.001	0.56	0.002	0.58	0.001	0.56	0.001
	ass ~ age	0.37	0.008	0.36	0.011	0.38	0.006	0.36	0.013
	ass ~ log(age)	0.37	0.010	0.36	0.012	0.39	0.010	0.36	0.006
Alvaro et al.	geo ~ age	0.29	0.037						
(2013)	ass ~ geo	0.37	0.007	0.40	0.008	0.35	0.006	0.35	0.005
	ass ~ log(geo)	0.58	0.001	0.56	0.001	0.58	0.001	0.56	0.001
McKerrow et a.l	geo ~ age	0.22	0.060						
(1992)	ass ~ geo	0.35	0.012	0.37	0.008	0.33	0.012	0.33	0.014
	ass ~ log(geo)	0.57	0.001	0.54	0.002	0.56	0.001	0.55	0.001

r = Mantel r statistic

Supplementary Table 6.2: MRM results for the analysis of geographic, assemblage and age distances referred to in Chapter 3, using the continental reconstruction of Torsvik and Cocks (2013), the Ochiai coefficient, with singleton taxa included. All combinations of the three continental reconstructions under consideration, the Ochiai or Jaccard coefficients, or including or excluding singleton taxa, produced similar results. The R script files for analysis of all combinations are provided in the electronic Supplementary Material.

```
> MRM(ass.dist ~ geo.dist)
$coef
                        ass.dist        pval
Int                     8.026866e-01    0.267
geo.dist                6.065031e-06    0.005

$r.squared
R2              pval
0.1519028       0.0050000

$F.test
F               F.pval
11.46305        0.00500
```

```
> MRM(ass.dist ~ age.dist)
$coef
                        ass.dist        pval
Int                     0.803361684     0.394
age.dist                0.008607366     0.007

$r.squared
R2              pval
0.1398442       0.0070000

$F.test
F               F.pval
10.40513        0.00700
```

```
> MRM(ass.dist ~ geo.dist + age.dist)
$coef
                        ass.dist        pval
Int                     7.746377e-01    0.366
geo.dist                4.670075e-06    0.017
age.dist                6.369970e-03    0.046

$r.squared
R2              pval
0.2204583       0.0050000

$F.test
F               F.pval
8.90836         0.00500
```

```
> MRM(ass.dist ~ log(geo.dist+1) + age.dist)
$coef
                        ass.dist        pval
Int                     0.659787263     0.762
log(geo.dist + 1)       0.020049004     0.001
age.dist                0.005352882     0.059

$r.squared
R2              pval
0.3895444       0.0010000

$F.test
F               F.pval
20.1008         0.0010


> MRM(ass.dist ~ log(geo.dist+1) + log(age.dist+1))
$coef
                        ass.dist        pval
Int                     0.62962885      0.956
log(geo.dist + 1)       0.02029107      0.001
log(age.dist + 1)       0.03493218      0.030

$r.squared
R2              pval
0.4015224       0.0010000

$F.test
F               F.pval
21.13355        0.00100


> MRM(log(ass.dist+1) ~ log(geo.dist+1) + log(age.dist+1))
$coef
                        log(ass.dist + 1) pval
Int                     0.48950346      0.328
log(geo.dist + 1)       0.01142984      0.001
log(age.dist + 1)       0.01961380      0.030

$r.squared
R2              pval
0.4103633       0.0010000

$F.test
F               F.pval
21.92273        0.00100
```

Supplementary Table 6.3: Table of references used in construction of the presence/absence matrix analysed in Chapter 3.

Locality	References
Chengjiang	Chen (2005); Chen et al. (2015); Cong et al. (2015); Fu et al. (2014); Hou et al. (2004; 2014); Jiao and Han (2013); Luo et al. (1999); Ma et al. (2014); Wang et al. (2012); Xu (2000); Yang et al. (2013); X. L. Zhang et al. (2012a, 2012b); Z. F. Zhang et al. (2011, 2014); Zhao et al. (2012, 2014a, 2014b)
Sirius Passet	Peel and Ineson (2011a, 2011b); Stein et al. (2013); Vinther et al. (2011)
Sinsk	Ivantsov et al. (2005); Pomorenko (2005)
Guanshan	Hu et al. (2013; 2010)
Balang	Liu (2013a, 2013b); Liu and Lei (2013); McNamara et al. (2010); Peng et al. (2005, 2010, 2012, 2015); Sun et al (2014); Zhao et al (2007)
Emu Bay Shale	Edgecombe et al. (2011); García-Bellido et al. (2009, 2013a, 2013b, 2014); Paterson et al. (2010; 2012; 2015; 2016); Paterson and Jago (2006)
Kinzers	Conway Morris and Caron (2014); Skinner (2005)
Kaili	Zhao et al. (2011)
Spence, Wheeler, Marjum	Briggs et al. (2008); Conway Morris et al. (2015); Gunther and Gunther (1981); Maletz and Steiner (2015); Robison and Babcock (2011); Robison et al. (2015); Robison and Richards (1981)
Burgess Shale	Aria et al. (2015); Aria and Caron (2015); Bengtson and Collins (2015); Caron et al. (2010; 2013; 2014); Caron and Jackson (2006); Conway Morris and Peel (2013); Devereux (2001); Haug and Haug (2014); Legg and Caron (2014); O'Brien et al. (2014); Rigby (1986); Smith (2015); Sumrall and Zamora (2015); The Burgess Shale – Royal Ontario Museum (2015)

6.3 References

Aria, C., Caron, J.-B., & Gaines, R. (2015). A large new leanchoiliid from the Burgess Shale and the influence of inapplicable states on stem arthropod phylogeny. *Palaeontology, 58*, 629-660.

Aria, C., & Caron, J. B. (2015). Cephalic and Limb Anatomy of a New Isoxyid from the Burgess Shale and the Role of "Stem Bivalved Arthropods" in the Disparity of the Frontalmost Appendage. *PLoS ONE, 10*, e0124979.

Bengtson, S., & Collins, D. (2015). Chancelloriids of the Cambrian Burgess Shale. *Palaeontologia Electronica, 18.1.6A*, 1-67.

Briggs, D. E. G., Lieberman, B. S., Hendricks, J. R., Halgedahl, S. L., & Jarrard, R. D. (2008). Middle Cambrian arthropods from Utah. *Journal of Paleontology, 82*, 238-254.

Caron, J.-B., Gaines, R. R., Mangano, M. G., Streng, M., & Daley, A. C. (2010). A new Burgess Shale-type assemblage from the "thin" Stephen Formation of the southern Canadian Rockies. *Geology, 38*, 811-814.

Caron, J. B., Conway Morris, S., & Cameron, C. B. (2013). Tubicolous enteropneusts from the Cambrian period. *Nature, 495*, 503-506.

Caron, J. B., Gaines, R. R., Aria, C., Mangano, M. G., & Streng, M. (2014). A new phyllopod bed-like assemblage from the Burgess Shale of the Canadian Rockies. *Nature Communications, 5*, 3210.

Caron, J. B., & Jackson, D. A. (2006). Taphonomy of the Greater Phyllopod Bed Community, Burgess Shale. *Palaios, 21*, 451-465.

Chen, A. L. (2005). A new Fuxianhula-like arthropod of the early Cambrian Chengjiang Fauna in Yunnan. *Yunnan Geology, 24*, 108-113.

Chen, A. L., Müller, W. E. G., Hou, X. G., & Xiao, S. H. (2015). New articulated protospongiid sponges from the early Cambrian Chengjiang biota. *Palaeoworld, 24*, 46-54.

Cong, P. Y., Hou, X. G., Aldridge, R. J., Purnell, M. A., & Li, Y. Z. (2015). New data on the palaeobiology of the enigmatic yunnanozoans from the Chengjiang Biota, Lower Cambrian, China. *Palaeontology, 58*, 45-70.

Conway Morris, S., & Caron, J. B. (2014). A primitive fish from the Cambrian of North America. *Nature, 512*, 419-422.

Conway Morris, S., & Peel, J. S. (2013). A New Helcionelloid Mollusk from the Middle Cambrian Burgess Shale, Canada. *Journal of Paleontology, 87*, 1067-1070.

Conway Morris, S., Selden, P. A., Gunther, G., Jamison, P. G., & Robison, R. A. (2015). New records of Burgess Shale-type taxa from the middle Cambrian of Utah. *Journal of Paleontology, 89*, 411-423.

Devereux, M. G. (2001). *Palaeoecology of the Middle Cambrian Raymond Quarry Fauna, Burgess Shale, British Columbia.* (M.Sc), University of Western Ontario, London.

Edgecombe, G. D., García-Bellido, D. C., & Paterson, J. R. (2011). A New Leanchoiliid Megacheiran Arthropod from the lower Cambrian Emu Bay Shale, South Australia. *Acta Palaeontologica Polonica, 56*, 385-400.

Fu, D. J., Zhang, X. L., & Budd, G. E. (2014). The first dorsal-eyed bivalved arthropod and its significance for early arthropod evolution. *GFF, 136*, 80-84.

García-Bellido, D. C., Edgecombe, G. D., Paterson, J. R., & Ma, X. (2013). A 'Collins' monster'-type lobopodian from the Emu Bay Shale Konservat-Lagerstätte (Cambrian), South Australia. *Alcheringa, 37*, 474-478.

García-Bellido, D. C., Lee, M. S. Y., Edgecombe, G. D., Jago, J. B., Gehling, J. G., & Paterson, J. R. (2014). A new vetulicolian from Australia and its bearing on the chordate affinities of an enigmatic Cambrian group. *BMC Evolutionary Biology, 14*, 214.

García-Bellido, D. C., Paterson, J. R., & Edgecombe, G. D. (2013). Cambrian palaeoscolecids (Cycloneuralia) from Gondwana and reappraisal of species assigned to *Palaeoscolex*. *Gondwana Research, 24*, 780-795.

García-Bellido, D. C., Paterson, J. R., Edgecombe, G. D., Jago, J. B., Gehling, J. G., & Lee, M. S. Y. (2009). The bivalved arthropods *Isoxys* and *Tuzoia* with soft-part preservation from the Lower Cambrian Emu Bay Shale Lagerstätte (Kangaroo Island, Australia). *Palaeontology, 52*, 1221-1241.

Gunther, L. F., & Gunther, V. G. (1981). *Some Middle Cambrian Fossils of Utah*. Department of Geology, Brigham Young University.

Haug, J. T., & Haug, C. (2014). A new cycloneuralian from the Burgess Shale with a palaeoscolecid-type terminal end. *Neues Jahrbuch für Geologie und Paläontologie - Abhandlungen, 274*, 73-79.

Hou, X. G., Aldridge, R. J., Bergström, J., Siveter, D. J., Siveter, D. J., & Feng, X. H. (2004). *The Cambrian Fossils of Chengjiang, China: The Flowering of Early Animal Life*. Oxford: Blackwell.

Hou, X. G., Williams, M., Siveter, D. J., Siveter, D. J., Gabbott, S., Holwell, D., & Harvey, T. H. P. (2014). A chancelloriid-like metazoan from the early Cambrian Chengjiang Lagerstätte, China. *Scientific Reports, 4*, 7340.

Hu, S. X., Zhu, M. Y., Luo, H. L., Steiner, M., Zhao, F. C., Li, G. X., . . . Zhang, Z. F. (2013). *The Guanshan Biota*. Kunming: Yunnan Science and Technology Press.

Hu, S. X., Zhu, M. Y., Steiner, M., Luo, H. L., Zhao, F. C., & Liu, Q. (2010). Biodiversity and taphonomy of the Early Cambrian Guanshan biota, eastern Yunnan. *Science China Earth Sciences, 53*, 1765-1773.

Ivantsov, A. Yu., Zhuravlev, A. Yu., Leguta, A. V., Krassilov, V. A., Melnikova, L. M., & Ushatinskaya, G. T. (2005). Palaeoecology of the Early Cambrian Sinsk biota from the Siberian Platform. *Palaeogeography, Palaeoclimatology, Palaeoecology, 220*, 69-88.

Jiao, G. X., & Han, J. (2013). A New Species of the Leptomitidae (Demospongea) from the Lower Cambrian Chengjiang Biota in Yunnan Province. *Ground Water, 35*, 176-179.

Legg, D. A., & Caron, J.-B. (2014). New Middle Cambrian bivalved arthropods from the Burgess Shale (British Columbia, Canada). *Palaeontology, 57*, 691-711.

Liu, Q. (2013a). The first discovery of anomalocaridid appendages from the Balang Formation (Cambrian Series 2) in Hunan, China. *Alcheringa, 37*, 338-343.

Liu, Q. (2013b). The first discovery of *Marrella* (Arthropoda, Marrellomorpha) from the Balang Formation (Cambrian Series 2) in Hunan, China. *Journal of Paleontology, 87*, 391-394.

Liu, Q., & Lei, Q. P. (2013). Discovery of an exceptionally preserved fossil assemblage in the Balang Formation (Cambrian Series 2, Stage 4) in Hunan, China. *Alcheringa, 37*, 269-271.

Luo, H. L., Hu, S. X., Chen, L. Z., Zhang, S. S., & Tao, Y. H. (1999). *Early Cambrian Chengjiang Fauna from Kunming region, China*. Kunming: Yunnan Science and Technology Press.

Ma, X. Y., Aldridge, R. J., Siveter, D. J., Siveter, D. J., Hou, X. G., & Edgecombe, G. D. (2014). A new exceptionally preserved Cambrian priapulid from the Chengjiang Lagerstätte. *Journal of Paleontology, 88*, 371-384.

Maletz, J., & Steiner, M. (2015). Graptolite (Hemichordata, Pterobranchia) preservation and identification in the Cambrian Series 3. *Palaeontology, 58*, 1073-1107.

McNamara, K. J. Ontogeny and heterochrony in the early Cambrian oryctocephalid trilobites *Changaspis*, *Duyunaspis* and *Balangia* from China. *Palaeontology, 49*, 1-19.

O'Brien, L. J., Caron, J. B., & Gaines, R. R. (2014). Taphonomy and Depositional Setting of the Burgess Shale Tulip Beds, Mount Stephen, British Columbia. *Palaios, 29*, 309-324.

Paterson, J. R., Edgecombe, G. D., GarcÍa-Bellido, D. C., Jago, J. B., & Gehling, J. G. (2010). Nektaspid arthropods from the Lower Cambrian Emu Bay Shale Lagerstätte, South Australia, with a reassessment of lamellipedian relationships. *Palaeontology, 53*, 377-402.

Paterson, J. R., Edgecombe, G. D., & Jago, J. B. (2015). The 'great appendage' arthropod *Tanglangia*: Biogeographic connections between early Cambrian biotas of Australia and South China. *Gondwana Research, 27*, 1667-1672.

Paterson, J. R., García-Bellido, D. C., & Edgecombe, G. D. (2012). New Artiopodan arthropods from the Early Cambrian Emu Bay Shale Konservat-Lagerstätte of South Australia. *Journal of Palaeontology, 86*, 340-357.

Paterson, J. R., García-Bellido, D. C., Jago, J. B., Gehling, J. G., Lee, M. S. Y., & Edgecombe, G. D. (2016). The Emu Bay Shale Konservat-Lagerstätte: a view of Cambrian life from East Gondwana. *Journal of the Geological Society, London, 173*, 1-11.

Paterson, J. R., & Jago, J. B. (2006). New trilobites from the Lower Cambrian Emu Bay Shale Lagerstätte at Big Gully, Kangaroo Island, South Australia. *Memoirs of the Association of Australasian Palaeontologists, 32*, 43-57.

Peel, J. S., & Ineson, J. R. (2011a). The extent of the Sirius Passet Lagerstätte (early Cambrian) of North Greenland. *Bulletin of Geosciences, 86*, 535-543.

Peel, J. S., & Ineson, J. R. (2011b). The Sirius Passet Lagerstätte (early Cambrian) of North Greenland. In P.A. Johnston, K. J. Johnston (Eds.), International Conference on the Cambrian Explosion, Proceedings. *Palaeontographica Canadiana, 31*, 109-118.

Peng, J., Feng, H. Z., Fu, X. P., Zhao, Y. L., & Yao, L. (2010). New Bradoriid Arthropods from the Early Cambrian Balang Formation of Eastern Guizhou, South China. *Acta Geologica Sinica, 84*, 56-68.

Peng, J., Huang, D. Y., Zhao, Y. L., & Sun, H. J. (2015). Palaeoscolecids from the Balang Fauna of the Qiandongian (Cambrian Series 2), Guizhou, China. *Geological Magazine*, 1-11.

Peng, J., Zhao, Y. L., Qin, Q., Yan, X., & Ma, H. T. (2010). New data on brachiopods from the Qiandongian (Lower Cambrian) Balang Formation, eastern Guizhou, South China. *Acta Palaeontologica Sinica, 49*, 365-379.

Peng, J., Zhao, Y. L., & Sun, H. J. (2012). Discovery and significance of *Naraoia* from the Qiandongian (lower Cambrian) Balang Formation, Eastern Guizhou, South China. *Bulletin of Geosciences, 87*, 143-150.

Peng, J., Zhao, Y. L., Wu, Y., Yuan, J. L., & Tai, T. S. (2005). The Balang Fauna—A new early Cambrian Fauna from Kaili City, Guizhou Province. *Chinese Science Bulletin, 50*, 1159-1162.

Pomorenko, A. G. (2005). *Unikal'nye sinskie mestonakhozhdeniya rannekembriskikh organizmov (Sibirskaya Platform) [Unique Sinsk localities of Early Cambrian organisms (Siberian Platform)]* (A. G. Pomorenko Ed. Vol. 284). Moscow: Rossiyskaya Akademiya Nauk.

Rigby, J. K. (1986). Sponges of the Burgess Shale (Middle Cambrian), British Columbia. *Palaeontographica Canadiana, 2*, 1-105.

Robison, R. A., & Babcock, L. E. (2011). Systematics, paleobiology, and taphonomy of some exceptionally preserved trilobites from Cambrian Lagerstätten of Utah. *The University of Kansas Paleontological Contributions, 5*, 1-47.

Robison, R. A., Babcock, L. E., & Gunther, V. G. (2015). *Exceptional Cambrian Fossils from Utah: A Window into the Age of Trilobites*. Salt Lake City: Utah Geological Society.

Robison, R. A., & Richards, B. C. (1981). Larger bivalve arthropods from the Middle Cambrian of Utah. *The University of Kansas Paleontological Contributions, 106*, 1-19.

Skinner, E. S. (2005). Taphonomy and depositional circumstances of exceptionally preserved fossils from the Kinzers Formation (Cambrian), southeastern Pennsylvania. *Palaeogeography, Palaeoclimatology, Palaeoecology, 220*, 167-192.

Smith, M. R. (2015). A palaeoscolecid worm from the Burgess Shale. *Palaeontology, 58*, 973-979.

Stein, M., Budd, G. E., Peel, J. S., & Harper, D. A. T. (2013). *Arthroaspis* n. gen., a common element of the Sirius Passet Lagerstatte (Cambrian, North Greenland), sheds light on trilobite ancestry. *BMC Evolutionary Biology, 13*, 99.

Sumrall, C. D., & Zamora, S. (2015). A columnal-bearing eocrinoid from the Cambrian Burgess Shale (British Columbia, Canada). *Journal of Paleontology, 89*, 366-368.

Sun, H. J., Babcock, L. E., Peng, J., & Zhao, Y. L. (2014). Hyolithids and associated trace fossils from the Balang Formation (Cambrian Stage 4), Guizhou, China. *Palaeoworld, 24*, 55-60.

The Burgess Shale – Royal Ontario Museum (2015, December 3). Retrieved from http://burgess-shale.rom.on.ca/en/

Vinther, J., Eibye-Jacobsen, D., & Harper, D. A. T. (2011). An Early Cambrian stem polychaete with pygidial cirri. *Biology Letters, 7*, 929-932.

Wang, H. Z., Zhang, Z. F., Holmer, L. E., Hu, S. X., Wang, X. G., & Li, G. X. (2012). Peduncular attached secondary tiering acrotretoid brachiopods from the Chengjiang fauna: Implications for the ecological expansion of brachiopods during the Cambrian explosion. *Palaeogeography, Palaeoclimatology, Palaeoecology, 323*, 60-67.

Xu, Z. L. (2000). Discovery of Enteromophites in the Chengjiang Biota and its ecological significance. *Acta Botanica Sinica, 43*, 863-867.

Yang, X. F., Vinn, O., Hou, X. G., & Tian, X. L. (2013). New tubicolous problematic fossil with some “lophophorate” affinities from the Early Cambrian Chengjiang biota in south China. *GFF, 135*, 184-190.

Zhang, X. L., Fu, D. J., & Dai, T. (2012a). A new species of Kangacaris (Arthropoda) from the Chengjiang lagerstätte, lower Cambrian, southwest China. *Alcheringa, 36*, 23-25.

Zhang, X. L., Fu, D. J., & Dai, T. (2012b). A new xandarellid arthropod from the Chengjiang Lagerstätte, Lower Cambrian of Southwest China. *Geobios, 45*, 335-338.

Zhang, Z. F., Holmer, L. E., Popov, L., & Shu, D. G. (2011). An obolellate brachiopod with soft-part preservation from the Early Cambrian Chengjiang Fauna of China. *Journal of Paleontology, 85*, 460-463.

Zhang, Z. F., Li, G. X., Holmer, L. E., Brock, G. A., Balthasar, U., Skovsted, C. B., . . . Shu, D. G. (2014). An early Cambrian agglutinated tubular lophophorate with brachiopod characters. *Scientific Reports, 4*, 4682.

Zhao, F. C., Hu, S. X., Caron, J.-B., Zhu, M. Y., Yin, Z. J., & Lu, M. (2012). Spatial variation in the diversity and composition of the Lower Cambrian (Series 2,

Stage 3) Chengjiang Biota, Southwest China. *Palaeogeography, Palaeoclimatology, Palaeoecology, 346-347*, 54-65.

Zhao, F. C., Hu, S. X., Zeng, H., & Zhu, M. Y. (2014a). A New Helmetiid Arthropod From The Early Cambrian Chengjiang Lagerstätte, Southwest China. *Journal of Paleontology, 88*, 367-370.

Zhao, F. C., Smith, M. R., Yin, Z. J., Zeng, H. A. N., Hu, S. X., Li, G. X., & Zhu, M. Y. (2014b). First report of *Wiwaxia* from the Cambrian Chengjiang Lagerstätte. *Geological Magazine, 152*, 378-382.

Zhao, Y. L., Parsley, R. L., & Peng, J. (2007). Early Cambrian eocrinoids from Guizhou Province, South China. *Palaeogeography, Palaeoclimatology, Palaeoecology, 254*, 317-327.

Zhao, Y. L., Zhu, M. Y., Babcock, L. E., & Peng, J. (2011). *The Kaili biota: marine organisms from 508 million years ago*. Guiyang: Guizhou Science and Technology Press.